SUPPRESSION OF COLD-SENSITIVE EXTRA-MICROTUBULE MUTANTS OF YEAST α-TUBULIN BY OVEREXPRESSION OF WILD-TYPE GENES

by

David Thomas Kirkpatrick

B.S. Carnegie-Mellon University, Pittsburgh, PA
(1987)

Submitted to the Department of Biology in partial fulfillment of the requirements for the degree of

Doctor of Philosophy /

at the

Massachusetts Institute of Technology

February, 1994

Signature of Author_____
Department of Biology
January 28, 1994

Certified by_____
Frank Solomon
Professor, Biology
Thesis Supervisor

Accepted by_____
Frank Solomon
Professor, Biology
Chair, Departmental Graduate Committee

SUPPRESSION OF COLD-SENSITIVE EXTRA-MICROTUBULE MUTANTS OF YEAST α-TUBULIN BY OVEREXPRESSION OF WILD-TYPE GENES

David T. Kirkpatrick

ABSTRACT

Microtubules in eukaryotic cells participate in a variety of nuclear and cytoplasmic structures, reflecting functional requirements and cell cycle position. We are studying the cellular regulation of microtubule assembly and organization in the yeast *Saccharomyces cerevisiae*. We screened for genes that when overexpressed suppress the growth phenotype of conditional mutants in α-tubulin that arrest with excess microtubules at the non-permissive temperature (Class 2 mutations). Here we describe one such suppressing element, called *ATS1* (for Alpha Tubulin Suppressor). Overexpression of this gene rescues both the growth and microtubule phenotypes of all Class 2 mutations, but not the cold-sensitive mutations that arrest with no microtubules (Class 1). Deletion of *ATS1* confers a modest slow growth phenotype which is slightly enhanced in strains containing both a deletion of *ATS1* and a Class 2 *tub1* mutation. The predicted *ATS1* protein contains 333 amino acids, and has considerable structural homology to the products of both the mammalian mitotic control gene RCC1 and to the *S. cerevisiae* gene *SRM1/PRP20*. Overexpression of *SRM1/PRP20* also suppresses Class 2 mutants. The results suggest that this family of genes may participate in regulatory interactions between microtubules and the cell cycle.

Thesis Supervisor: Dr. Frank Solomon
Title: Professor of Biology

Publications

Kirkpatrick, David and Frank Solomon. Overexpression of yeast homologs of the mammalian checkpoint gene RCC1 suppresses the class of α-tubulin mutations that arrest with excess microtubules. (submitted, December 1993 to Genetics).

Solomon, F., S. Guénette, D. Kirkpatrick, V. Praitis, B. Weinstein, and J. Archer. A Genetic Analysis of Microtubule Assembly and Function in Yeast. In *Chromosome Segregation and Aneuploidy*, NATO ASI Series H: Cell Biology, Vol. 72 (B.K. Vig, ed), Springer-Verlag, pp. 199-209 (1993).

Solomon, F., L. Connell, D. Kirkpatrick, V. Praitis, and B. Weinstein. Methods for Studying the Yeast Cytoskeleton. In *The Cytoskeleton: A Practical Approach* (K. Carraway and C. Carraway, eds.), Oxford University Press, Oxford, pp. 197-222 (1992).

Acknowledgements:

This thesis would not have been possible without the help and encouragement of a large number of people. At the earliest level, I was aided by many teachers. They continually pushed me to excel when I easily could have just coasted along. But more, I am forever in debt to my family - my parents and brother. To them I owe the fundamental part of who I am and how I see the world. It would be impossible to put into words how much I owe them all. Without them, I certainly would not be the person I am now.

At Carnegie-Mellon University, I was influenced by two of the teachers that I encountered. They were teachers in the best sense of the word - they opened my eyes to the world of possibilities both around and within me. I would not have gone on to do graduate work in biology if it hadn't been for Dr. Elizabeth Jones or Dr. Linda Kauffman. Dr. Jones gave me a work-study job in her lab my freshman year. Over the course of the next four years, the enthusiasm and energy that she showed for her work convinced me that there couldn't be a better choice for a life's path. While Dr. Jones and her lab demonstrated science at its best, Linda Kauffman showed me exactly how that science could, and should, be done, when I was lucky enough to take her year-long laboratory course in molecular biology, genetics and biochemistry. The combination of those two teachers determined my life's goals: to continue looking into intriguing problems, and to teach others the joy of that search.

This desire to do research was fueled by the members of Frank Solomon's lab at MIT. Frank and the members of his lab brought the science of biology into sharp focus, allowing me to see how to approach the rest of my life in science. To all the members of the Solomon lab, past and present, thank you for all the help, insight, and wonderful conversations (not to mention more chocolate than humans should be capable of consuming!)

Finally, MIT is the place I met my wife, Catherine. Everything that I have accomplished in many ways can be traced back to her. I owe her more than I can ever say, and count myself the luckiest person alive for having the privilege of having her share my life.

To all of the people who have shaped me over the years, I dedicate this thesis. It wouldn't exist without all of you, and I wouldn't be who I am without you also. Thank you.

Table of Contents:

List of Figures:

List of Tables:

INTRODUCTION

The Study of Microtubules in *Saccharomyces cerevisiae*

The microtubule cytoskeleton has been the subject of study for a number of decades. Microtubules in various eukaryotic cells form what appear to be vastly different structures from proteins (the α- and β-tubulins) that are relatively homologous. These differing structures can be found in the same cell at different stages in development or the cell cycle. For example, the dense web of cytoplasmic microtubules emanating from microtubule organizing centers near the nucleus stands in stark contrast to the single bundle of microtubules that form an elliptical band at the circumference of nonmammalian erythrocytes. However, during development of those erthrocytes, the former structure is converted into the latter (Kim et al., 1987). Understanding the mechanisms by which the various structures are specified, and how the timing of their appearance is regulated, is a major goal of research on the microtubule cytoskeleton.

The yeast *Saccharomyces cerevisiae*, by virtue of well-developed genetic, biochemical and cell biological techniques, can be instrumental in unraveling some of the intricacies of the regulation of microtubules. Information gathered through work on yeast microtubules is likely to be applicable to other eukaryotic systems, given that microtubules exhibit a range of structures and functions during the yeast life cycle that approximate those seen in most eukaryotes.

Microtubules in yeast are polymers composed of heterodimers of α- and β-tubulin. All of the β-tubulin in a cell is provided by the *TUB2* gene

(Neff et al., 1983) . The α-tubulin derives from two genes, *TUB1* and *TUB3* (Schatz et al., 1986a; Schatz et al., 1986b). Deletion of *TUB2* is lethal, as is deletion of *TUB1* (but see below).

Models for Regulation of Microtubule Function

Three different models have been proposed for regulating microtubule functioning. The first model proposes that microtubules are regulated by differences in the tubulin sequences themselves. Divergent sequences would specify different functions or microtubule structures. The second model is based on the hypothesis that quantitative changes in the level of tubulin proteins can alter the extent or regulation of microtubule assembly. Finally, the association of other proteins with the microtubule might be the regulating element in specifying diverse functions and structures.

The first model does not appear to be relevant in explaining microtubule functioning in *S. cerevisiae*. Approximately 85% of the α-tubulin in a yeast cell is produced by the *TUB1* locus; the remainder is from the *TUB3* locus (Schatz et al., 1986b). Elimination of *TUB3* results in a number of relatively minor phenotypes, including benomyl sensitivity. Loss of *TUB1* is normally a lethal event but overexpression of Tub3p, returning α-tubulin protein levels to wildtype, allows cells to tolerate this loss. In a similar manner, overexpression of Tub1p eliminates the phenotypes associated with *TUB3* deletion (Schatz et al., 1986b). Tub1p and Tub3p are approximately 10% divergent at the amino acid level (Schatz et al., 1986a).

In general, the carboxyl domain of β-tubulins is rather variable. This variability might exist because the region is important for microtubule

regulation (Cleveland and Sullivan, 1985). The yeast β-tubulin protein contains a unique carboxy terminal region when compared to other eukaryotic β-tubulin (Neff et al., 1983). This β-tubulin 'tail' consists of an extension of twelve amino acids beyond the normal carboxyl terminus of β-tubulins from most eukaryotes. However, deletion of the β-tubulin tail confers only a dominant hypersensitivity to the microtubule-depolymerizing drug benomyl (Katz and Solomon, 1988). Transfection into animal cells of a yeast-chicken chimera of β-tubulin, in which the carboxyl portion of the protein is derived from yeast, demonstrates that the chimeric β-tubulin is incorporated into microtubules in a manner identical to the endogenous β-tubulin (Bond et al., 1986). These data indicate that the yeast β-tubulin region does not contain sequences that could cause the protein to be excluded from certain microtubules. The above results, including the *TUB1* and *TUB3* interchangeability, demonstrate that control of the differing functions of yeast microtubules is not intrinsic to the residues of the tubulin proteins that directly comprise the microtubule.

Another mechanism for regulation of microtubule function could be regulation of the protein level. By this model, changes in the level of tubulin protein might act to alter the equilibrium between the polymerized and unassembled pools of αβ dimers. Work from the Solomon lab has demonstrated that alterations in the concentration of α- and β-tubulin do not have drastic effects on the functioning of the microtubules. Diploid cells containing a deletion of one of the two alleles of *TUB2* are viable. More importantly, they are phenotypically normal (Katz et al., 1990). Growth rates and microtubule morphologies of the hemizygote are indistinguishable from cells homozygous for *TUB2*. However, when tubulin protein levels are examined, the level of tubulin (both α- and β-tubulin), is 50% that of

wildtype diploids. As these cells have normal microtubule structures, the concentration of tubulin protein in these cells is not limiting for microtubule assembly.

The first two models for regulation of microtubules do not fit with experimental data. The primary sequence of the tubulins does not appear to allow for differential functioning, while changes in tubulin protein level do not affect microtubule structures. The available experiments suggest that associated proteins and structures may control the interactions, timing, and organization of microtubules.

Identifying Microtubule-Interacting Elements

There are a number of general approaches to the problem of identifying factors that might regulate microtubules. The first is to analyze cellular structures or processes, such as kinetochores or chromosome transmission, in which microtubules are intimately involved. The second approach is to examine mutations in the tubulins themselves through the use of methods such as suppression analysis. Such genetic analysis might identify elements that regulate microtubules; similar studies with actin have identified numerous microfilament-regulating proteins (see for example Drubin, 1990). Other methods, which I will not discuss here, include biochemistry and cell fractionation experiments.

Analysis of Cellular Structures & Processes to Identify Microtubule-Interacting Elements

-The cell cycle in yeast:

Microtubule regulation is intimately connected with the cell cycle in *Saccharomyces cerevisiae*, as microtubules are required to perform various functions depending on the specific phase of the cell cycle. The cell cycle can be divided into four distinct stages: G1, S, G2 and M (for an overview of the yeast cell cycle see Pringle and Hartwell, 1981). Cells in G1 (immediately following mitosis) pass through a point called START, beyond which the cell is committed to passage through another cell cycle. Cells at START may continue through the mitotic cell cycle, or differentiate for mating (if haploid) or meiosis (if diploid). After transit through the first growth phase, G1, cells enter S phase. S phase is the stage in which DNA synthesis occurs. Cells then go through G2, and enter mitosis (M phase). After mitosis and cytokinesis, cells return to G1. The position in the cell cycle of a particular cell can be determined by examination of the size of its bud. Buds emerge at the G1/S transition and grow continuously during the cell cycle, finally separating from the mother cell at the end of mitosis.

-Microtubules during the cell cycle:

Microtubule structures vary during the course of the cell cycle (see figure 1-1). During G1 microtubules are present as very short polymers at the spindle pole body (SPB). The SPB is a microtubule-organizing center that is embedded in the nuclear membrane. The SPB duplicates during G1, with the two SPBs remaining associated with each other. Microtubules lengthen from the SPBs, oriented toward the site of the

Figure 1-1:

The cell cycle in *Saccharomyces cerevisiae*, with emphasis on the microtubule stuctures visible at each stage. Very small microtubules emanate from a spindle pole body during G1. The spindle pole body duplicates, and microtubules orient toward the site of the emerging bud as the cell moves through G1 and into S phase. As cells transit through G2, the microtubules elongate and nuclear microtubules become visible as cells enter mitosis. The nuclear membrane does not break down during mitosis. The nucleus moves to the neck of the bud and elongates. The spindle microtubules are the predominant microtubules in the cell at this point. By the end of mitosis, the nucleus has divided, with each nucleus receiving one spindle pole body. This cycle applies to both haploid and diploid cells. When haploid cells mate, as depicted in the upper right series of images, mating cells form projections. Microtubules reorient in the direction of the projections. The mating 'shmoos' fuse, and the microtubules pull the nuclei together to allow them to fuse. The newly formed diploid resembles a dumbbell. A new bud forms from the "neck" of the dumbbell, with microtubules directed toward the new bud. The budding cell then continues through a normal cell cycle. This figure was modified from a figure in Pringle and Hartwell, 1981.

Microtubule Behaviour

During the

Cell Cycle in *S. cerevisiae*

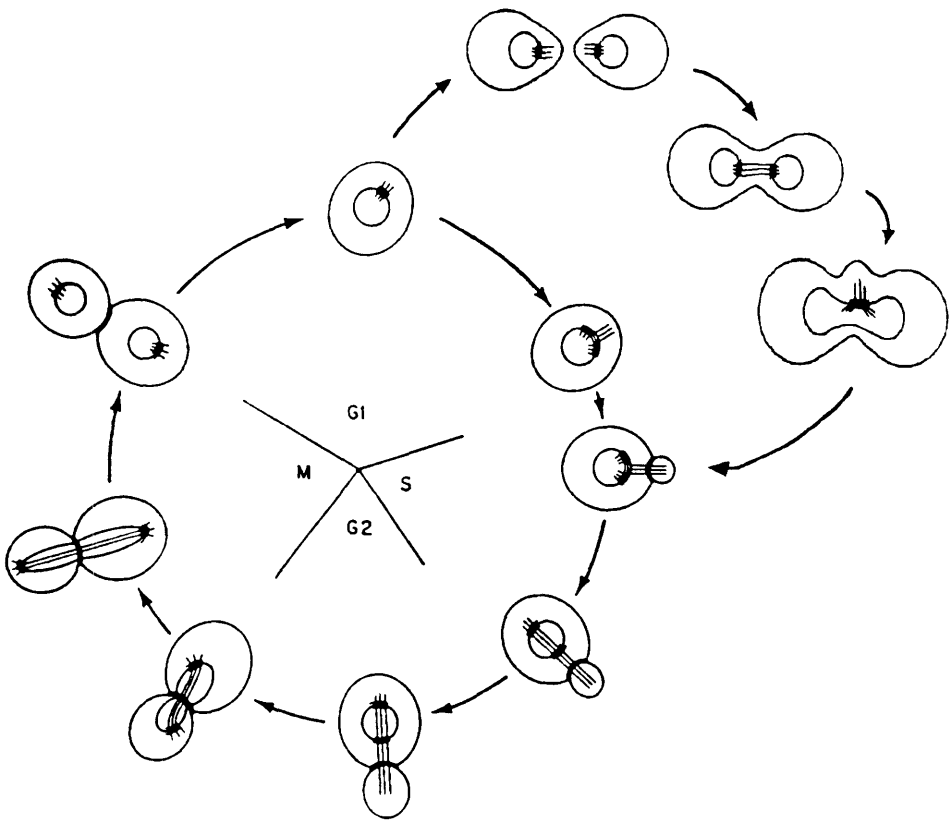

emerging bud. Near the end of S phase the SPBs separate and move away from each other, while still staying localized in the nuclear envelope. A short spindle forms between the two SPBs. This spindle lengthens during mitosis as the nucleus moves into the neck of the bud. The spindle microtubules associate with chromosomal kinetochores in order to segregate chromosomes between the mother and daughter cells. The spindle disassembles and the nucleus and cells divide.

During mating of two haploid yeast cells, microtubules serve another essential function. Cells prior to mating adopt a unique shape, the 'shmoo'. A projection, the shmoo tip, is oriented toward the mating partner. Microtubules from the SPB are oriented toward the tip of this projection. After fusion of the two mating cells, the cytoplasmic microtubules pull the nuclei toward one another to allow nuclear fusion to occur. Once karyogamy has taken place, microtubules are re-oriented toward the site of the next bud.

-Microtubules interact with various structures and processes:

Microtubules interact with a number of cellular structures and processes during the course of the cell cycle. These include, but are not limited to, the spindle pole body, centromeres of chromosomes, the nuclear envelope, and other microtubules (during mating for example). Cellular processes which involve microtubules include chromosome segregation, nuclear migration, and nuclear fusion.

-Spindle pole bodies:

Microtubules are intimately associated with the yeast microtubule-organizing center, the spindle pole body. Both nuclear and cytoplasmic

microtubules emanate from the SPB during the course of the cell cycle. Many genes have been isolated whose products are localized to the SPB or that exhibit mutant phenotypes indicating the gene functions at the SPB. Among these genes are *CDC31* (Spang et al., 1993), *KAR1* (Conde and Fink, 1976), *MPS1* and *2* (Winey et al., 1991), *ESP1* (Baum et al., 1988), *CIK1* (Page and Snyder, 1992), *NDC1* (Thomas and Botstein, 1986), and *CMD1* (calmodulin) (Sun et al., 1992). Mutations in many of these genes lead to defective microtubules, and have consequences in other microtubule-mediated functions. For example, *kar1* mutants were originally isolated as defective in karyogamy during mating (Conde and Fink, 1976), but they also exhibit defects in SPBs and cytoplasmic microtubules (Rose and Fink, 1987). Recent work localizes a Karlp fusion protein to the newly formed SPB after SPB duplication (Vallen et al., 1992). A number of mutations lead to a monopolar spindle (in which microtubules emanate only from one SPB), including mutations in *CDC31*, *KAR1*, *MPS1* and *MPS2*. One component of the SPB found in many organisms, γ-tubulin, has not yet been detected in *S. cerevisiae* (Stearns et al., 1991). In other organisms γ-tubulin appears to interact with microtubule ends to promote or initiate microtubule polymerization (reviewed in Oakley, 1992).

-Kinetochores:

Another structure that is intimately associated with microtubules is the kinetochore. Kinetochores are the specialized structures at the centromere of each chromosome that mediate attachment of microtubules during mitosis. Although kinetochores have been actively studied in yeast for many years, the proteins that comprise the kinetochore have proven elusive until recently. Three proteins that bind to yeast centromeres have been isolated

biochemically (Lechner and Carbon, 1991) and the encoding genes identified. These genes also have been isolated in other ways, including screens for mutants with altered chromosome transmission fidelity (*ctf13* and *14*) (Doheny et al., 1993) and for mutants with defective nuclear division cycles (*ndc10*) (Goh and Kilmartin, 1993). Mutants in *CBF2/CTF14/NDC10* cause cells to arrest with short spindles at the G2/M boundary (Doheny et al., 1993).

-Chromosome segregation:

A class of genes encoding proteins that might be expected to interact with microtubules are those genes that function to insure proper chromosome segregation during mitosis or meiosis. A number of independent screens have been conducted, and many mutations have been identified (for example, *cin* mutants (Hoyt et al., 1990; Stearns et al., 1990), and *chl* mutants (Kouprina et al., 1993)). Chromosome segregation mutations that also affect microtubules include the previously mentioned *ctf13* and *ctf14* (Doheny et al., 1993). Mutations in *CSE1* and *CSE2*, two genes that appear to be required for mitotic chromosome segregation, show an intermediate sensitivity to nocodazole, a microtubule-depolymerizing drug (Xiao et al., 1993). The *CIN1*, *CIN2* and *CIN4* genes were isolated independently as recessive mutations that increase chromosome instability (Hoyt et al., 1990) and also as mutations that increased sensitivity to benomyl (Stearns et al., 1990). Mutations in *CIN* genes lead to loss of microtubule structures at nonpermissive temperatures. Nuclear migration and karyogamy are also affected.

-Karyogamy:

Microtubules function during mating in yeast to bring the two nuclei together. Screens designed to isolate mutants deficient in nuclear fusion have identified genes that are affected in this migration. The *KAR* genes were originally identified as mutants that reduced karyogamy without affecting cell fusion (Conde and Fink, 1976). *KAR1* appears to be important for SPB duplication and has microtubule defects (as discussed in the section on spindle pole bodies). *KAR3* encodes a protein related to kinesin, a microtubule motor protein (Meluh and Rose, 1990) and is essential for karyogamy. *KAR3* hybrid fusion proteins localize to microtubules in the shmoo tip (Meluh and Rose, 1990). *kar3* mutant strains accumulate large-budded cells with a short mitotic spindle in a single nucleus. *BIK1*, another gene isolated in screens for defects in karyogamy, also interacts with microtubules. Either deletion or overproduction of *BIK1* causes microtubules to shorten or disappear. The Bik1p localizes to spindle pole bodies and the mitotic spindle (Berlin et al., 1990).

-Spindles and microtubule motor proteins:

Microtubules form the spindle during mitosis to segregate chromosomes to the mother and daughter cells. A number of kinesin-related proteins in addition to the *KAR3* protein discussed above have been identified that affect the functioning of the spindle; for example, *CIN8* and *KIP1* have roles in maintaining spindle integrity (Saunders and Hoyt, 1992). Cells with mutations in both *CIN8* and *KIP1* undergo spindle collapse if shifted to nonpermissive temperature early in mitosis. This collapse is alleviated if *KAR3* is also deleted, as if *KAR3* promotes the collapse in some manner (Saunders and Hoyt, 1992). These results suggest that *CIN8/KIP1*

and *KAR3* generate opposing forces in the spindle. Other yeast proteins have been isolated that have some effect on spindles. For example, mutants in the *DHC1* gene (encoding a dynein-related protein) fail to position the spindle in the daughter bud correctly (Li et al., 1993). Another gene, *SPO15*, is unable to form a bipolar spindle. The *SPO15* gene has significant homology to the mammalian microtubule-associated protein dynamin. *SPO15* also associates with microtubules *in vitro* (Yeh et al., 1991).

-Microtubule-depolymerizing drug studies:

Many mutations in tubulin genes lead to an alteration in sensitivity to microtubule depolymerizing drugs such as benomyl. A number of researchers have taken advantage of this to identify genes that have an altered response to benomyl. Isolation of mutations supersensitive to benomyl identified three mutants, all of which were allelic with the *CIN1*, *2* and *4* genes described above (Stearns et al., 1990). A more recent screen for mutants that die when exposed to benomyl at high concentration for a relatively short period, identified the *BUB1* and *BUB2* genes (Hoyt et al., 1991). These mutants fail to arrest in response to the microtubule depolymerization caused by benomyl (*BUB* stands for Budding Uninhibited by Benzimidazole). *BUB3* was isolated as a quantitative suppressor of *bub1-1* during cloning of the *BUB1* gene. The *BUB* genes are postulated to be involved in a feedback control mechanism that monitors the state of the spindle. A group of mutants possessing similar phenotypes and function was isolated in a second screen using benomyl sensitivity (Li and Murray, 1991). Mutants were selected that grew at a normal rate in the presence of concentrations of benomyl that usually slow down the cell cycle. The *MAD* (Mitosis Arrest Deficient) genes appear to assess the rate of spindle

assembly, while the *BUB* genes may monitor actual formation of the spindle (reviewed in (Murray, 1992)).

In conclusion, screens for mutations that affect structures or processes involving microtubules have identified a large number of genes, some of which have phenotypes that indicate that they may interact directly with microtubules. A number of genes isolated in screens for mutations in one structure or process are deficient in other microtubule-mediated processes also.

Genetic Analysis of Tubulin Mutants to Identify Microtubule-Interacting Elements

-Pseudoreversion analysis:

One method for identifying genes and gene products that interact with one another is to identify extragenic suppressors of a mutation. By this pseudoreversion method, described in (Jarvik and Botstein, 1975), a strain containing a conditional mutation is mutagenized and screened for cells that no longer exhibit the conditional phenotype. The suppressed strains isolated in this way are mated with another strain wildtype at the original mutant locus. Haploid progeny are obtained by sporulating and dissecting the diploid heterozygote. They are examined to determine if they exhibit the original conditional phenotype that was suppressed, if they are wildtype, or if they have acquired a novel conditional phenotype. If the suppression of the original conditional phenotype occurred by mutation of a gene that is unlinked to the original locus, then one-half of the progeny should be wildtype at the original conditional locus but carry the suppressing mutation.

These progeny can be analyzed for novel conditional phenotypes. Analysis of extragenic suppressors obtained in this manner has been of enormous value in deciphering interactions between genes in many different cellular processes.

This approach has been utilized with *tub1* mutations that arrest with a normal spindle at the nonpermissive temperature (Schatz et al., 1988). These alleles, *tub1-737* and *tub1-746*, were chosen because of the spindle morphology - the arrest might indicate a defect in a specific step in spindle elongation. Cells were incubated at the nonpermissive temperature of 11° C. for six weeks to select for spontaneous cold-resistant mutants. Cold-resistant strains were screened to eliminate intragenic revertants. When the extragenic suppressors were characterized, many of them had an altered sensitivity to benomyl and a number had other conditional phenotypes. All of the suppressors occurred in the *TUB2* gene, encoding β-tubulin.

-Unlinked noncomplementation:

Another method for isolating functionally interacting gene products is through the use of noncomplementation. Normally, when two haploids (each of which contains a different mutation) are mated to form a diploid, the mutations are complemented by the wildtype alleles contributed by the mating partner. However, if the mutations are in genes that encode proteins that interact, for example as part of a complex, the mutations may not be complemented in the diploid (see (Raff and Fuller, 1984) and (Stearns and Botstein, 1988)).

This approach has been utilized in *S. cerevisiae* to identify genes containing mutations that fail to complement *tub2* mutants (Stearns and Botstein, 1988). Mutagenized haploid cells were mated with isogenic *TUB2*

and *tub2cs* haploids. The resulting diploids were incubated at the nonpermissive temperature. Prospective noncomplementers were identified by their ability to form colonies when crossed to the *TUB2* strain but not the *tub2cs* strain. Tetrad dissection revealed mutations that were not linked to the *TUB2* locus. One unlinked mutation was isolated; it proved to be in *TUB1*. When this *tub1-1* mutant was used in a second noncomplementation screen, two mutations were identified as unlinked noncomplementers of *tub1-1*. One was in *TUB2*, while the other was in *TUB3*.

-Quantitative suppression:

A third approach to identifying interacting elements relies on observations made while cloning genes by complementation of mutant phenotypes in a number of organisms. In yeast, circular plasmids that are autonomously maintained allow the isolation of the wildtype allele of a gene that has a conditional lethal mutation at the chromosomal locus. Introduction of plasmids containing genomic DNA, followed by incubation at the nonpermissive temperature, will identify those strains containing a plasmid with DNA capable of complementing the mutation (Nasmyth and Reed, 1980). In most cases, the complementing DNA contains the wildtype allele of the gene that is mutated. However, in some cases, the suppressing element is unlinked to the mutated locus. For example, during cloning of the histidine tRNA synthetase of *S. cerevisiae*, a quantitative suppressor was isolated (Natsoulis et al., 1986). The suppressor was identified as the structural gene for $tRNA^{His}$. In this case suppression was probably due to the increase in substrate for the defective histidine tRNA synthetase, allowing the defect to be bypassed. More recently, this phenomenon has been exploited to isolate suppressors of cell cycle mutants in *S. cerevisiae* (Kitada

et al., 1993) and *Schizosaccharomyces pombe* (Hayles et al., 1986), among others.

Applying Quantitative Suppression to *tub1* Mutations

To date, isolation of genes that directly interact with microtubules through the use of genetic screens that utilize tubulin mutations has only identified new mutants in the known tubulin genes. However, quantitative suppression techniques might allow isolation of novel genes that act to regulate microtubule functions.

A bank of cold-sensitive conditional mutations (described in Schatz et al., 1988) contains *tub1* mutations that fall into three categories: Class 1, Class 2 and Class 3. Class 1 mutant strains arrest at the nonpermissive temperature as large-budded cells with no microtubules. Class 2 mutations also cause a large-budded cell arrest, but the cells exhibit excess microtubules when visualized by indirect immunofluorescence after incubation at the nonpermissive temperature. Class 3 mutants exhibit no conspicuous quantitative defects in microtubule structures, however, many alleles exhibit microtubules that are disorganized in appearance. These mutants generally do not exhibit a specific arrest phenotype at the nonpermissive temperature. Tubulin protein levels in the three classes of mutants have been examined by Laurie Connell, a post-doc in the Solomon lab: the majority of the alleles have approximately wildtype levels of protein at the nonpermissive temperature.

The Class 1 and Class 2 mutants are appropriate substrates for use in a quantitative suppression screen. Their characteristics (arrest with a defined

microtubule morphology yet with wildtype protein levels) indicate that the mutants might be defective in specific aspects of microtubule regulation. In this report I will describe the isolation of quantitative suppressors of the Class 2 extra microtubule *tub1* mutant strains. The nature of the suppressing genes has implications for understanding of the Class 2 mutations and reveals possible interactions between microtubule regulation and the cell cycle in *Saccharomyces cerevisiae*.

EXPERIMENTAL PROCEDURES

Techniques, Plasmids and Strains

See Table 2a for a list of plasmids generated in this project. The table includes a brief description of plasmid and the manipulations performed in generating it. Standard protocols were used for work with restriction enzymes, kinases, ligases, etc. (Sambrook et al., 1989). Enzymes usually were obtained from New England Biolabs, Inc. and directions supplied with the particular enzyme were followed. *Escherichia coli* strain HB101 was used for bacterial work unless noted otherwise. Yeast media (YPD, SC (complete) and SD (minimal) and supplements) were prepared as described in Sherman et al., 1986 and Katz and Solomon, 1988. Standard genetic techniques were used, as described in Guthrie and Fink, 1991. Unless indicated otherwise, all strains are derived from DBY strains, which are of S288c origin. See table 2b for a list of strains used and generated in this study.

Transformation protocols

Yeast transformations were performed using the LiAc method (Ito et al., 1983) with modifications as stated in Solomon et al., 1992. To summarize, the strain was initially grown overnight in SC dropout liquid media or supplemented SD media. Cell density was determined by hemocytometer count, and an appropriate dilution was made into 100 ml YPD media. Cells were grown at 30° until density was approximately 2 x 10^7 cells/ml. Cells were spun down, washed and incubated in Tris/EDTA/LiAc for an hour. Cells were then divided into a number of

Table 2a:

Plasmids Generated in this study

Plasmid	Description
pDK7	*CEN4 ARS1 URA3 TUB1* from genomic fragment
pDK8	*CEN4 ARS1 URA3* suppressor 1 contains *ATS1*
pDK9	*CEN4 ARS1 URA3* suppressor 2 contains *ATS2*
pDK10	*CEN4 ARS1 URA3* suppressor 3 contains *ATS3*
pDK11	deletion of Cla1 sites in pDK8 - subcloning
pDK12	deletion of HindIII sites in pDK8 - subcloning
pDK13	deletion of SphI sites in pDK8 - subcloning
pDK14	pKS+ vector with EcoRI to HindIII from pDK8 - sequencing
pDK15	pSK+ vector with EcoRI to HindIII from pDK8 - sequencing
pDK16	deletion of SphI sites in pDK11 (complete *ATS1* gene)
pDK17	pDK14 cut with SacI and closed
pDK18	pDK15 cut with ApaI and closed
pDK19	pSK^+ vector with ClaI to EcoRI fragment from pDK8
pDK20	pKS^+ vector with EcoRI to ClaI fragment from pDK8
pDK21	pBR322 with deleted (blunted out) EcoRI
pDK22	deletion of ClaI site in YEp24
pDK23	pDK21 with ClaI to SphI from pDK16
pDK24	pDK23 cut with EcoRI and PmlI and ligated with 1.2 kb *URA3* EcoRI to SmaI fragment (truncation of *ATS1*)
pDK25	pBR322 with BamHI to SphI fragment from pDK8
pDK26	pBR322 with deleted (blunted) ClaI site
pDK27	YEp24 cut with EcoRI (removes all 2-μm region)
pDK28	pDK27 cut with BamHI and SphI and ligated with 300 bp BglII to SphI fragment (3' noncoding region of *ATS1*) from pDK25
pDK29	pSK^+ vector ligated with ClaI to ClaI fragment of pDK8 (5' region of *ATS1*)
pDK30	pUC19 ligated BamHI to EcoRI fragment of pDK8

Plasmid	Description
pDK31	pDK28 cut with ClaI and SspI and ligated with ClaI to HincII fragment (5' noncoding region of *ATS1*) from pDK30 (Deletion Construction)
pDK32	YEp24 cut with BamHI and SphI and ligated with BclI to SphI fragment from pDK8 (complete *ATS1* gene)
pDK33	pLGSD5 cut with BamHI and ligated with BclI to BglII fragment (complete *ATS1* in proper orientation)
pDK34	as pDK33 but with *ATS1* in reverse orientation
pDK35	YCp50 ligated with HincII to SphI fragment from pDK32 (complete *ATS1*)
pDK36	pDK35 cut at ClaI site and 12CA5 epitope tag on ClaI fragment inserted
pDK37	YCp50 with HincII to SphI fragment from pDK8
pDK38	pDK31 cut with ClaI and SmaI, ligated with *HIS3* ClaI to SmaI fragment (replaces *URA3* from deletion vector with *HIS3*)
pDK39	pRS313 vector cut with ClaI and ApaI and ligated with BstBI and ApaI from pDK25 (complete *ATS1* on *HIS CEN* vector)
pDK40	epitope tag in EcoRI site of *ATS1* - has frameshift
pDK41	epitope tag in EcoRI site of *ATS1* - correct orientation,
pDK42	epitope tag in EcoRI site of *ATS1* - reverse orientation
pDK43	YCp405 cut with EagI and SphI and ligated with HincII to SphI fragment from pDK25
pDK44	YCp405 cut with XbaI (blunted) and EagI and ligated with BsrGI (blunted) and EagI fragment from pDK7 - complete *TUB1* gene

Table 2b:

Strain	Genotype	Description	Source
DBY2403	*MATa his3-Δ200 leu2-3,112 lys2-801 ura3-52 tub1::HIS3 tub3::TRP1* with *tub1-714-LEU2-CEN4-ARS1* (pRB614)	Class 2 extra microtubule strain	SCHATZ *et al.* 1988
DBY2412	As DBY2403 except *tub1-730* (pRB630)	"	"
DBY2414	As DBY2403 except *tub1-733* (pRB633)	"	"
DBY2418	As DBY2403 except *tub1-741* (pRB641)	"	"
DBY2426	As DBY2403 except *tub1-758* (pRB658)	"	"
DBY2433	As DBY2403 except *TUB1* (pRB658)	Wildtype control strain	"
DBY2412	As DBY2403 except *tub1-704* (pRB604)	Class 1 no-microtubule strain	"
DBY2412	As DBY2403 except *tub1-709* (pRB609)	"	"
DBY2412	As DBY2403 except *tub1-724* (pRB624)	"	"
DBY2412	As DBY2403 except *tub1-728* (pRB628)	"	"
DBY2412	As DBY2403 except *tub1-729* (pRB629)	"	"
DBY2412	As DBY2403 except *tub1-738* (pRB638)	"	"
DBY2412	As DBY2403 except *tub1-744* (pRB644)	"	"
DBY2412	As DBY2403 except *tub1-750* (pRB650)	"	"
DBY2412	As DBY2403 except *tub1-759* (pRB659)	"	"
DBY2412	As DBY2403 except *tub1-760* (pRB660)	"	"
DBY2412	As DBY2403 except *tub1-767* (pRB667)	"	"
FSY120	*MATa/α his4-619/+ leu2-3,112/leu2-3,112 lys2-801/+ ura2-52/ura3-52*		KATZ and SOLOMON 1988

Strain	Genotype	Description	Source
FSY185	*MATa/α ade2/+ his3-Δ200/his3-Δ200 leu2-3,112/leu2-3,112 lys2-801/lys2-801 ura3-52/ura3-52*		KATZ *et al.* 1990
FSY332	DBY2412 with pDK8	suppression analysis	This study
FSY336	DBY2412 with pDK7	" "	" "
FSY337	DBY2412 with PDK32	" "	" "
FSY338	DBY2412 with pWF48	" "	" "
FSY340	DBY2414 with pDK7	" "	" "
FSY341	DBY2414 with pDK16	" "	" "
FSY342	DBY2414 with pDK32	" "	" "
FSY343	DBY2412 with YCp50	" "	" "
FSY346	DBY2403 with pDK44 and pRB614	synthetic lethality analysis	" "
FSY347	DBY2426 with pDK44 and pRB658	" " "	" "
FSY348	FSY346 but *Δats1::URA3*	" " "	" "
FSY349	FSY346 but *URA3*	" " "	" "
FSY350	FSY349 with only pDK44 (wildtype for *TUB1* and *ATS1*)	" " "	" "
FSY351	FSY348 with only pDK44 (wildtype for *TUB1*, *Δats1*)	" " "	" "
FSY352	FSY349 with only pRB614 (*tub1-714*, wildtype for *ATS1*)	" " "	" "
FSY353	FSY348 with only pRB614 (*tub1-714*, *Δats1*)	" " "	" "

Strain	Genotype	Description	Source
ASY257	*tub2-412:URA3 ura3-52 ade2 his3 lys2*	suppression analysis	T. Huffaker
NMY1	*tub2-150 ura3-52*	" "	G. Barnes
	*MAT**a** prp20-1 ura3-52*	*PRP20* work	W. Forrester
M14	*MAT**a** ura3-52*	*PRP20* parental strain	" "
FSY360	FSY120 but *Δats1::URA3/ATS1*	*ATS1* deletion analysis	This study
FSY370	*MAT**a**/α his4-619/+ ura3-52/ura3-52*	*ATS1-PRP20* interaction	" "
	Δats1::URA3/+ prp20-1/+	analysis	
FSY371	*MAT**a**/α his4-619/+ ura3-52/ura3-52*	*ATS1-PRP20* interaction	" "
	Δats1::URA3/+ PRP20/PRP20	analysis-control cross with M14	

tubes, DNA was added, and incubated 30 minutes. Subsequently, a 40% PolyEthyleneGlycol$_{4000}$ (Sigma) solution was added. After another 30 minute incubation, cells were heat-shocked at 42° for 5 minutes, washed with dH_20, and plated on selective media. For suppression of a cold-sensitive *tub1* mutation, transformed cells were plated on a number of selective plates, one of which was placed at room temperature to evaluate the number of transformants, while the remainder were placed at the restrictive temperature. Occasionally the method of Elble, 1992, involving overnight incubation in LiAc, PEG_{4000} and TE followed by plating on selective media, was used when introducing a particular plasmid into a strain, and efficiency or suppression was not an issue.

Plasmid Loss Protocol

Single colonies of strains to be assayed were inoculated into liquid media nonselective for their auxotrophic markers (either SC dropout media or YPD) and allowed to grow overnight (16 to 24 hours) at 30° on a rotating drum. A hundred-fold dilution of the first overnight was inoculated into nonselective media and allowed to grow overnight again. Density of the culture was determined then by hemocytometer count. Appropriate dilutions of the second overnight culture were next spread on non-selective plates (either SC-dropout or YPD) and placed at 30° until colonies were visible. These were then transferred by replica-plating to selective media (SC dropout media) and incubated at 30 degrees. A loss event, indicating the absence of the particular plasmid, was scored if a colony was totally absent on the drop-out plate; partially missing colonies were not counted. See Figure 2-2 for a diagrammatic depiction.

Growth Rate Determinations

Growth rates were determined by inoculating single colonies of the strain to be assayed into 5 ml selective liquid media (SC-dropout or minimal with additions) in 30 ml test tubes and placed on a rotating drum at 23° (room temperature) or 30°. After growth overnight (16 hours) cell density was determined by hemocytometer counts. 10 ml of selective media in 125 ml Erlenmeyer flasks was then inoculated with enough overnight culture to achieve a density of 1 x 10^5 cells/ml and placed at the appropriate temperature. Cell number was determined via hemocytometer counts at appropriate intervals depending on incubation temperature. Dilutions of cells were plated to permissive solid media and incubated at 30° to evaluate the number of viable cells at each time point.

Sequencing

Sequencing of both strands of the region containing *ATS1* was performed utilizing the modified T7 DNA polymerase Sequenase with a modification of the di-deoxy chain termination method of Sanger (US Biochemicals). A combination of subclones in the pKS^+ and pSK^+ Bluescript vectors (Stratagene) and oligonucleotides directed to various internal sequences of *ATS1* were utilized to generate multiply overlapping sequences from both strands of the *ATS1* gene. See table 2c for a list of oligonucleotides utilized in the sequencing reactions, and figure 2-10 for a diagram of the sequencing reactions performed.

Immunofluorescence

Immunofluorescence studies of the microtubule morphology and DNA of strains were performed as described previously in Solomon et al.,

Table 2c:

Oligonucleotide Primers for Sequencing of *ATS1*:

Name	Sequence	Location
Top #2	CGCGTGTTGGCGGATGT	961 to 978
Top #3	CGGGCCAACAACGAAAA	1132 to 1148
Top #4	CTGGAGGCCCGTGGAAG	237 to 253
Top #6	ACTGATTTAAGTTACGT	-187 to -171
Bottom #1	CTTATCAGTGCTAGAGC	1013 to 997
Bottom #2	ACCGTGCTCACTCCCGG	820 to 804
Bottom #3	GCTGTTGTTTGAGCTCG	652 to 636
Bottom #4	GTCCAGCCGCACGCCAC	291 to 274

Location is given relative to the ATG in the *ATS1* open reading frame, with A=1. "Top" oligos hybridize to the non-sense strand, "Bottom" to the sense strand. Note: Top#2 is missing a T at the 7th position according to the actual *ATS1* sequence; Bottom #4 is missing a C at the 3rd position according to the sequence.

1992. Primary antibodies used included an anti-β-tubulin rabbit polyclonal antisera, 206-1 and a monoclonal antibody against α-tubulin, A1BG7. These antibodies were generated in the Solomon lab. Secondary antibody was FITC-conjugated goat anti-rabbit IgG or goat anti-mouse IgG (Cappel). DAPI (4', 6'-diamidino-2-phenylindole) was used to visualize DNA. A Zeiss Axiophot microscope was utilized for all immunofluorescence.

Bud Size Distribution

Bud sizes were determined in the following manner: An overnight culture of the strain was grown at 30° in SC dropout media. Cell density was determined by hemocytometer count and appropriate dilutions made. Cells were placed at the desired temperature and allowed to grow until mid-log phase. Cell density was then counted and bud size scored.

Southern Blotting

The protocol for isolation of DNA for Southern analysis is adapted from Holm et al., 1986 as modified in Solomon et al., 1992. DNA (usually 1 to 3 μg) was digested with restriction enzymes and subjected to gel electrophoresis on agarose gels, (0.6 to 0.8%). The gel was washed with 1.5M NaCl and 0.5M NaOH, followed by 1.5M NaCl and 1M Tris pH7.5. The DNA was next transferred to Hybond-N nylon using either a Stratagene Posiblotter for 1 hour or blotting with paper towels overnight in 6x SSC (20x SSC is 1M NaCl, 0.1M NaCitrate). The nylon was cross-linked in a Stratagene UV Crosslinker. After placing in a sealable plastic bag, the probe solution was added, the bag sealed and placed at 42° for a minimum of eight hours. Probe was removed and the nylon washed three

times at 65° for ten minutes each time, using 2x SSC + 0.1% SDS, 1x SSC + 0.1% SDS, and 0.5x SSC + 0.1% SDS. The nylon was then placed on Kodak X-OMAT film and placed at -20°.

Probe was made using the random primed hexamer protocol (Feinberg and Vogelstein, 1983). A DNA fragment was isolated on an agarose gel, separating it from the gel matrix using the GeneClean II kit (Bio101), and quantitating the DNA by 260 nm absorbance. Approximately 100 ng of DNA was boiled for 5 min, then added to a mixture of random hexamers, BSA, 50 uCi ^{32}P dATP, and 2.5 units Klenow fragment. The reaction was conducted at room temperature for a minimum of three hours. The reaction mixture was then added to 5 ml formamide, 2.5 ml 20x SSPE, 1.3 ml dH_2O, 1 ml Denhardt's solution, and 0.1 ml 10% SDS. This mixture was then added to the nylon to hybridize at 42°.

Northern Blotting

Total RNA for Northerns was isolated using the protocol in Solomon et al., 1992. RNA is run on an agarose gel containing formaldehyde, 1X MOPS and 0.5 µg/ml ethidium bromide. Usually 1, 5 and 25 µg of each sample were run per lane. The gel is then exposed to ultraviolet radiation to nick the RNA, and then transferred overnight in 10x SSC onto Hybond-N nylon using the paper-towel method. The nylon is crosslinked two times, then prehybridization solution is added. The prehybridization mix contains 1.5 ml 1M phosphate buffer, 60 µl 0.5M EDTA, 10.5 ml 20% SDS, and 3 ml 10% BSA. After 3 to 4 hours at 65°, probe is added (probe was prepared as described for Southerns) and the nylon hybridized overnight (minimum of 12 hours) at 65°. The nylon is then washed twice

in wash buffer A: 10 ml 10% BSA, 10 ml 20% SDS, 8 ml 1M Phosphate buffer, 400 µl 0.5M EDTA, and 172 ml H_2O at 65° for 15 minutes, then three times in wash buffer B: 10 ml 20% SDS, 8 ml 1M Phosphate buffer, 400 µl 0.5M EDTA, and 182 ml H_2O at 65° for 15 minutes. The nylon was placed on Kodak X-OMAT X-ray film.

Benomyl Studies

Strains to be assessed for benomyl resistance or sensitivity were grown overnight in appropriate selective media. Cell density was determined by counting cells using a hemocytometer, and concentrations were adjusted to approximate parity. Serial dilutions were made in standard 96-well plastic tissue-culture plates in liquid media or sterile water. Dilutions were then transferred to selective plates containing various concentrations of benomyl using a "frogger" - a device containing a series of 48 metal pins embedded in a plastic base, with pins arranged such that each pin fits into one well of the 96-well plate, allowing one-half of the plate to be transferred at a time. Benomyl plates were generated by adding with vigorous stirring appropriate amounts of benomyl in dimethyl sulfoxide to standard media, while still liquid prior to pouring, held at 60° (Solomon et al., 1992).

Color Assay for *CEN* segregation

JAY11 contains two adenine mutations, *ade2* and *ade3*. Normally, this double mutant forms white colonies, however JAY11 contains a *LEU2 CEN ADE3* plasmid that complements the *ade3* mutation, and so the colonies are red due to the *ade2* mutation. If cells are grown nonselectively for the *CEN* plasmid, white sectors will be generated in the

red colony. Stability of the *CEN* plasmid can be monitored by performing a plasmid loss experiment (see above), determining the percentage of totally white colonies at the beginning and the end of the experiment. The number of totally white colonies at the beginning of the experiment is subtracted from the final total, to arrive at a value for the intervening time. If the number of generations are known, then a percentage loss per generation can be calculated (see Koshland et al., 1985).

Disruption of *ATS1*

YEp24 was digested with EcoRI to remove the 2-μm sequences but retain the *URA3* gene. Next this derivative was digested with BamHI and SphI and ligated to a 300 bp BglII-SphI fragment containing noncoding sequences 3' of the *ATS1* gene. Finally, this construct was digested with ClaI and SspI, and ligated to a ClaI to HincII fragment containing 5' noncoding *ATS1* sequence. This generated a plasmid containing a *URA3* gene flanked by 5' and 3' noncoding *ATS1* sequence. Digestion with XmnI and SphI yields a linear fragment of approximately 1880 bp with ends derived from *ATS1* locus sequence.

Truncation Construction

The EcoRI site in pBR322 was removed by digesting with EcoRI, treating with Klenow for 30 minutes in the presence of 1mM dNTPs at room temperature, heating to 65° to inactivate, and then ligating with T4 DNA ligase overnight. This vector (pDK21) was then digested with ClaI and SphI, and the ClaI to SphI fragment of *ATS1* ligated to it. This construct (pDK23) was digested with EcoRI and PmlI, and ligated with a 1.2 kb EcoRI to SmaI fragment containing the *URA3* gene. The resulting

plasmid, pDK24, contains the *ATS1* gene interrupted at the EcoRI site, then two novel amino acids are introduced prior to a stop codon. A linear fragment containing the truncation and with ends directing integration at *ATS1* was generated by digestion of pDK24 with ClaI and SphI.

Overexpression constructions

pLGSD5 vector (Guarente et al., 1982) was used as the base plasmid for construction of the overexpression vector. pLGSD5 was digested with BamHI. A BclI to BglII DNA fragment of 1.1 kb containing the *ATS1* coding region was ligated into this BamHI site such that 24 bp separate the ATG in *ATS1* from the *CYC1* leader of pLGSD5. Insertion of the *ATS1* fragment was possible in either orientation - the direction of insertion was determined by diagnostic restriction digests with EcoRI and HindIII. pDK33 contains *ATS1* in the proper orientation; pDK34 in the opposite orientation.

RESULTS

Isolation of Suppressors of Class 2 Mutants

-Isolation of Class 2 suppressors:

DBY2412 (containing the *tub1-730* mutation) was transformed with a genomic library contained on *URA3 CEN* plasmids (Rose et al., 1987). Cesium chloride-prepared DNA was added to four tubes containing DBY2412. YCp50 DNA and buffer alone (no DNA added) were also added to individual tubes. The contents of each tube were divided among three selective plates. Two were placed at the nonpermissive temperature of 15° and the last at 30° (see figure 2-1).

After two weeks, 29 transformants were isolated that grew at the nonpermissive temperature from an estimated total of 3200 transformants. (this is estimated to be approximately one complete genome's worth, based on Rose et al., 1987). Three colonies were large, the remaining 26 were very small. Upon restreaking, only the 3 large strains formed colonies. Two of these large colonies were from the same plate and may not be independent.

-Plasmid loss:

In order to determine if the *URA3* plasmids of the three cold-resistant strains contained a copy of *TUB1* or *TUB3*, the strains were taken through a plasmid loss procedure (see figure 2-2). If the *URA3* plasmid contains a copy of an α-tubulin gene, then the cells would be able to tolerate the loss of the pRB630 (*LEU2 tub1-730*) plasmid when grown nonselectively. After growth in YPD liquid media and growth on YPD plates, colonies were

Figure 2-1:

Transformation protocol for isolation of suppressors of cold-sensitive *tub1* mutants. A strain bearing a plasmid containing a mutated version of *TUB1*, and deleted chromosomal copies of *TUB1* and *TUB3* is transformed with a plasmid containing a region of genomic DNA (Rose et al., 1987). These transformed cells are then placed on plates that select for the presence of the genomic DNA plasmid, and incubated at permissive and nonpermissive temperatures. Incubation at permissive temperature allows evaluation of the efficiency of transformation, while incubation at nonpermissive temperatures allows isolation of plasmids containing genes that suppress the cold-sensitivity of the *tub1* mutation.

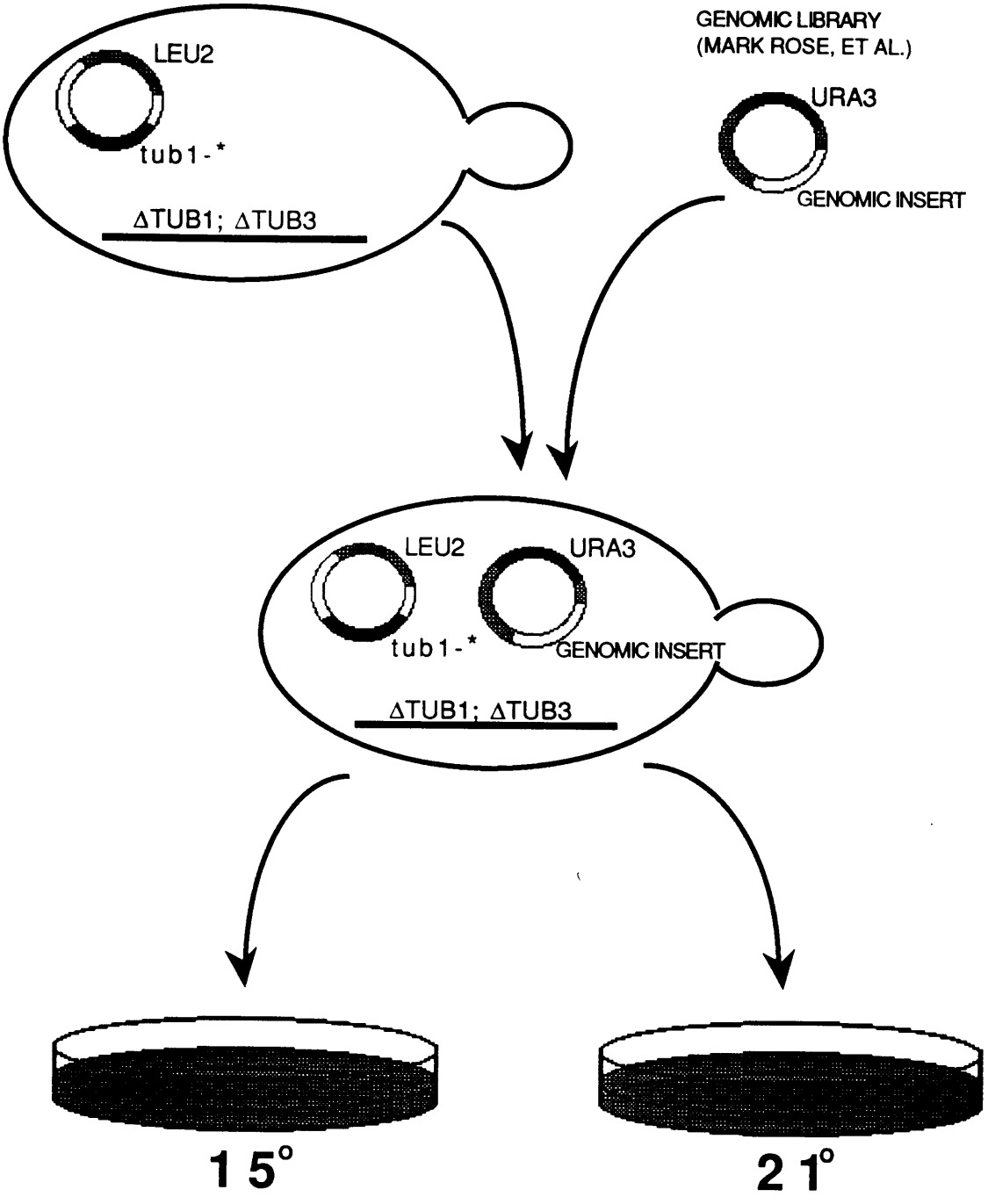
GENOMIC LIBRARY
(MARK ROSE, ET AL.)
LEU2
tub1-*
ΔTUB1; ΔTUB3
URA3
GENOMIC INSERT
LEU2
URA3
tub1-*
GENOMIC INSERT
ΔTUB1; ΔTUB3
15°
21°

Figure 2-2:

The protocol for evaluating loss events of various plasmids in different strains. The strain to be evaluated (usually containing two differing plasmids) is inoculated into liquid media nonselective for both plasmids. After an overnight growth, the culture is diluted and allowed to grow overnight. Appropriate dilutions are then plated to permissive solid media and incubated until colonies are visible. The plate is then replica-plated to various selective media, to identify colonies that have lost one of the plasmids. Only colonies that are completely absent are scored as a loss; partial colonies indicate a loss event that occurred after plating to solid media.

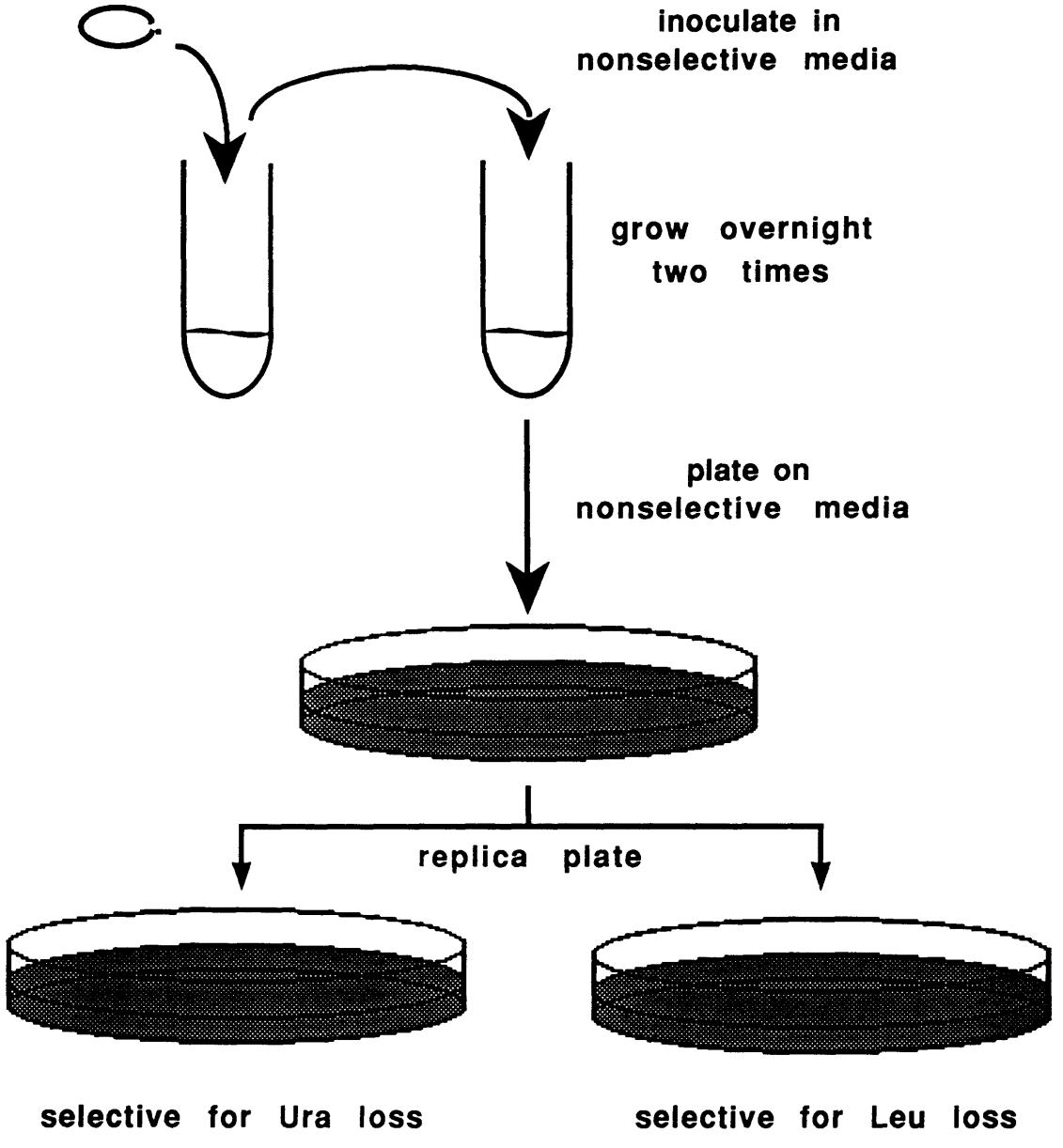
inoculate in
nonselective media
grow overnight
two times
plate on
nonselective media
replica plate
selective for Ura loss
selective for Leu loss

transferred to plates selective for the presence of each plasmid. All three strains failed to give rise to any colonies that had lost pRB630, indicating that the *URA3* plasmids did not contain *TUB1* or *TUB3*.

-Isolation of the suppressor plasmids:

The *URA3* genomic plasmids were isolated from the three suppressed strains. Each strain was grown in liquid media at 15° for 5 days. DNA was harvested from 1.5 ml of each strain and used to transform *Escherichia coli* strain HB101. Individual Amp^R transformants were grown in LB broth with ampicillin and plasmid DNA isolated. pRB630 and *URA3* genomic plasmids were distinguished by restriction digest of the isolated plasmids. For example, digestion of *TUB1* and *TUB3* with EcoRI generates fragments of known size, and so can be used to indicate if the suppressing plasmids contain a gene coding for α-tubulin. (*TUB2*, encoding β-tubulin, would not be likely to be detected in this screen, as overexpression of β-tubulin is extremely deleterious to the cell (Weinstein and Solomon, 1990).) pDK8 contains *ATS1*, the suppressing element from the first cold-resistant strain, pDK9 contains *ATS2* and pDK10 contains *ATS3*. By initial restriction digests all three plasmids appeared to be independent.

-Re-introduction of suppressing plasmids into DBY2412:

To test if the cold-resistance observed in the initial suppressed strains was due to the presence of the plasmid, the isolated plasmids pDK8, 9 and 10 were transformed into DBY2412 and plated directly at the nonpermissive temperature. All three plasmids gave rise to colonies at the nonpermissive temperature, but the size and number of colonies varied between plasmids (see figure 2-3). pDK8 (*ATS1*) suppressed *tub1-730* to the greatest extent,

Figure 2-3:

Suppression of the cold-sensitivity of DBY2412. The uppermost block of photographs shows selective plates containing DBY2412 (*tub1-730*) transformed with the vector YCp50 and incubated at either 15° or room temperature for two weeks. The second block shows DBY2412 transformed with pDK8 (*ATS1*). The third and fourth blocks show DBY2412 transformed with pDK9 (*ATS2*) and pDK10 (*ATS3*), respectively. pDK8 shows the greatest extent of suppression, and was further characterized.

YCp50

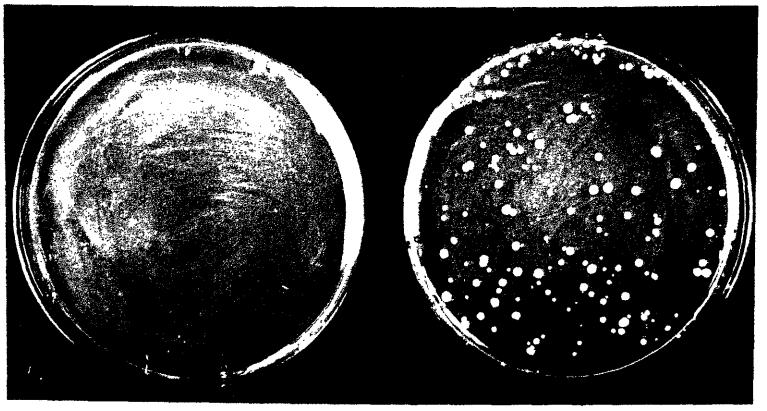

pDK8

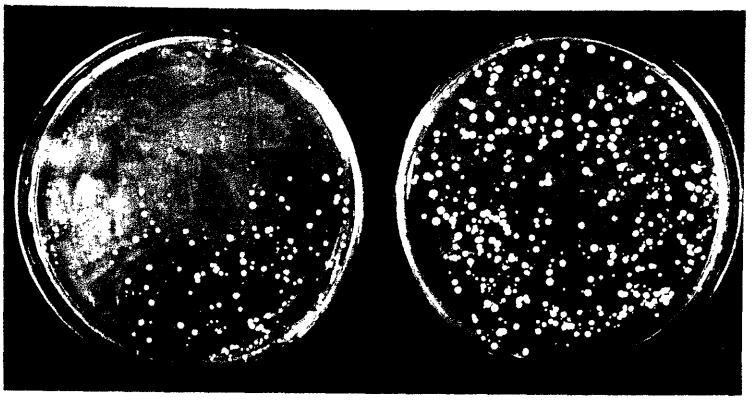

pDK9

pDK10

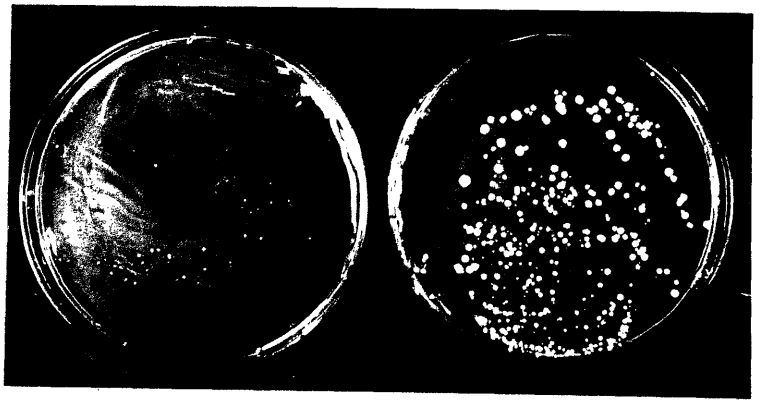

by both colony size and number at the nonpermissive temperature. Based on this result, *ATS1* suppression was further examined. The suppression with *ATS2* and *ATS3* was felt to be too weak to warrant further characterization.

-Suppression of *tub1-730* cold-sensitivity is not due to a genetic alteration:

In order to determine if the presence of the plasmid was the determining factor for suppression of the cold-sensitivity of the *tub1-730* mutation, strains that lacked the plasmid were isolated. DBY2412 transformed with YCp50, pDK7 (*TUB1*) and pDK8 (*ATS1*) were taken through the plasmid loss protocol. Colonies that resulted from cells that no longer contained a *CEN URA3* plasmid were identified.

One representative each from DBY2412 strains that had originally been transformed with YCp50, pDK7 (*TUB1*) and pDK8 (*ATS1*) was then grown at 15° to assess the cold-sensitivity of the *tub1-730* allele in each strain. If the suppression originally observed in the pDK8 transformed cells had been due to a genomic alteration, the absence of the pDK8 plasmid should make no difference in the suppression of *tub1-730*. However, after incubation at the nonpermissive temperature, strains that had formerly been suppressed but were now lacking pDK7 or pDK8 failed to grow. This indicates that the suppression observed originally was not due to a genetic alteration in the genome. Taken with the results from the re-transformations of *ATS1* into DBY2412, the suppression of the cold-sensitivity of *tub1-730* requires the presence of the *ATS1* plasmid.

Characterization of the *ATS1* Suppression

-Suppression of Class 2 extra microtubule mutants:

Does the suppressor of the cold-sensitivity of *tub1-730* only act on that allele of *TUB1*, or can *ATS1* suppress other mutations in *TUB1*? To determine if *ATS1* suppression was allele-specific, pDK8 was transformed into the remaining four Class 2 extra microtubule mutants, DBY2403 (*tub1-714*), DBY2414 (*tub1-733*), DBY2418 (*tub1-741*), and DBY2426 (*tub1-758*). Transformants of all four strains produced colonies at the nonpermissive temperature. When pDK8 was transformed into two Class 1 mutations, DBY2408 (*tub1-724*) and DBY2410 (*tub1-728*), no colonies formed at 15°. Suppression by *ATS1* is specific to the Class 2 mutations, rather than allele-specific or general for *tub1* mutations.

-Growth in liquid media:

Excess *ATS1* allows growth of *tub1-730* mutant strains under nonpermissive conditions. Growth rates were determined for the mutant *tub1-730* strain transformed with various plasmids. DBY2412 transformed with pDK7 (*CEN TUB1*) and pDK16 (*CEN ATS1*) plasmids were grown overnight in liquid media, then diluted and shifted to the nonpermissive temperature of 15°. The number of viable cells in a population of DBY2412 (*tub1-730*) did not increase during the course of the experiment, unlike strains containing the *ATS1* plasmid or a *TUB1* plasmid (see figure 2-4).

-Microtubule morphology in suppressed strains:

The state of the microtubules was examined in a Class 2 extra microtubule strain and suppressed strains bearing plasmids containing *ATS1*.

Figure 2-4:

Excess *ATS1* allows growth in liquid media at 15°. DBY2412 (*tub1-730*) or DBY2412 containing pDK7 (*CEN TUB1*) or pDK16 (*CEN ATS1*) were grown in liquid media at 15°. Cell number was determined and dilutions placed on selective plates. The graph shows the number of viable cells/ml over the course of the experiment. DBY2412 does not increase in viable cell count, while DBY2412 containing either excess *TUB1* or *ATS1* increased in viable cells.

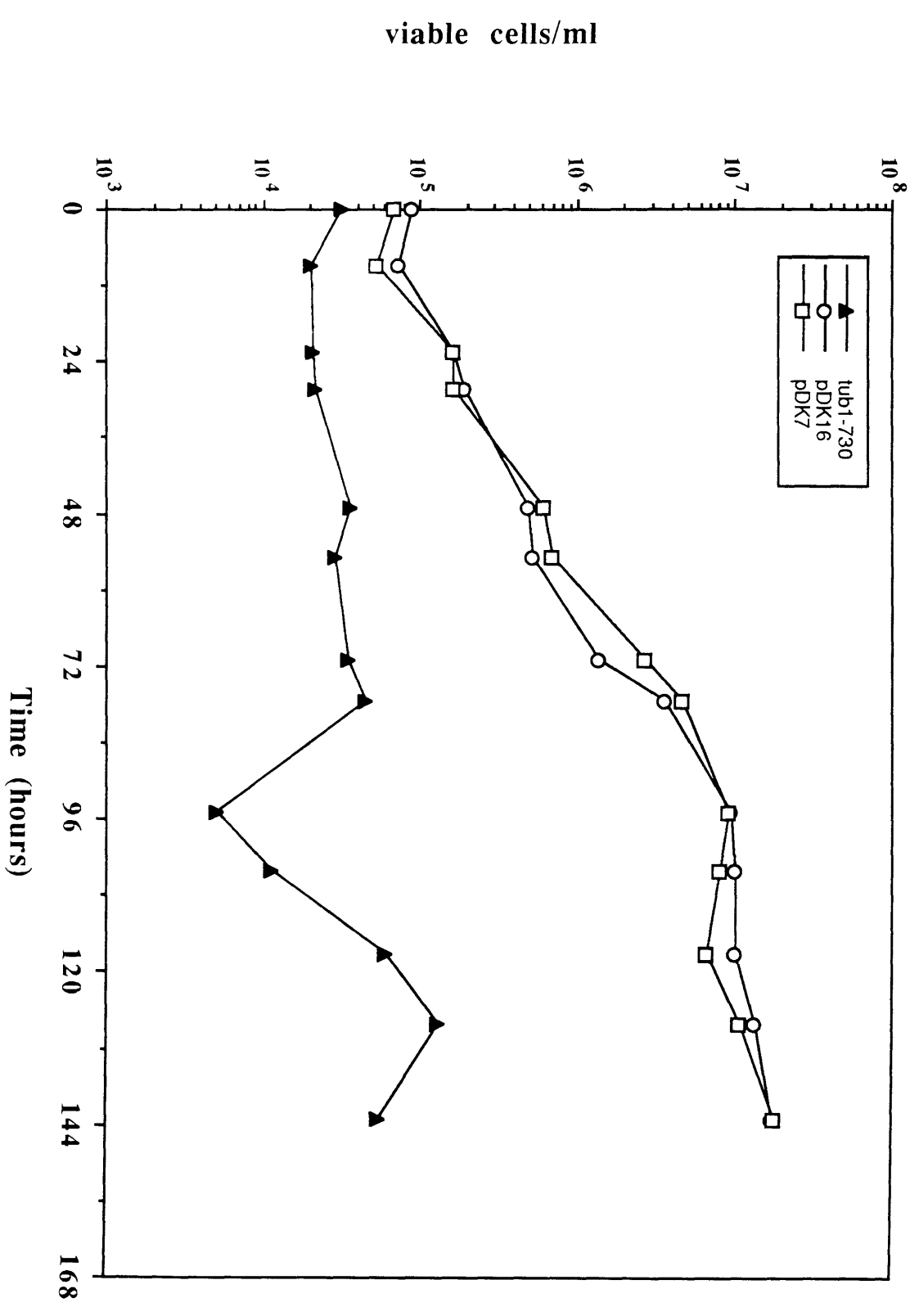
viable cells/ml
10^8
10^7
10^6
10^5
10^4
10^3
tub1-730
pDK16
pDK7
0
24
48
72
96
120
144
168
Time (hours)

Figure 2-5:

Excess *ATS1* suppresses the extra microtubule phenotype of DBY2414 (*tub1-733*). DBY2414 (*tub1-733*) transformants were examined for microtubule morphology after 20 hours at 13°. The following classes were scored: cells with no microtubules, cells with a single dot of staining, cells with a short bar (approximately one-half the cell diameter) or in budded cells with a spindle, and finally cells with large structures (greater than one-half the cell diameter) or budded cells containing a spindle and with large cytoplasmic microtubules. pDK7 is a *CEN TUB1* plasmid, pDK16 is a *CEN ATS1* plasmid, and pDK32 is a 2-μm *ATS1* plasmid.

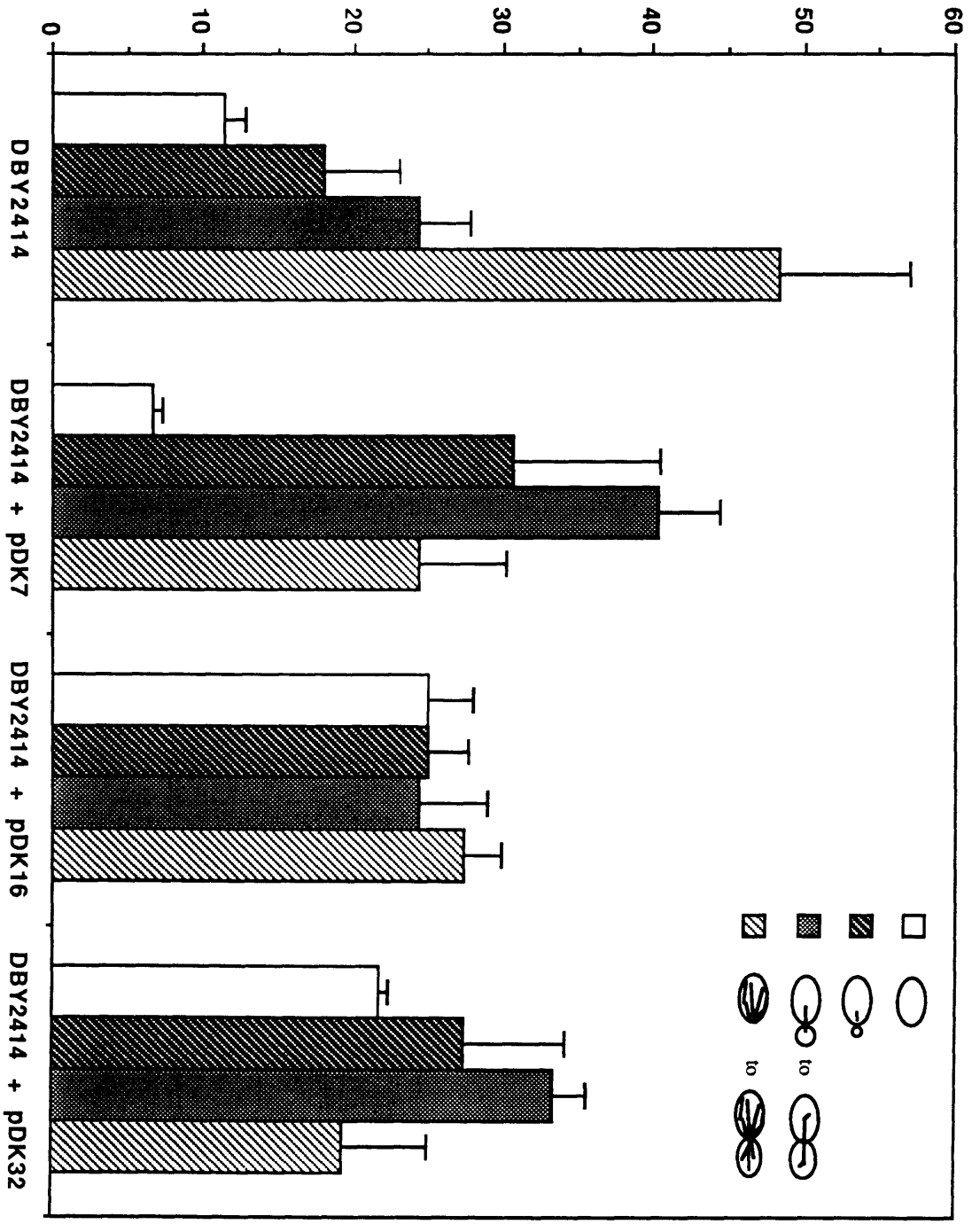
% of Cells with Indicated MT Structures
0
10
20
30
40
50
60
DBY2414
DBY2414 + pDK7
DBY2414 + pDK16
DBY2414 + pDK32

Transformants of DBY2414 (*tub1-733*) containing pDK7 (*TUB1*), pDK8 (*ATS1* on *CEN*) or pDK32 (*ATS1* on 2-μm) were grown selectively at the nonpermissive temperature of 13° for 20 hours and then fixed and prepared for immunofluorescence. Cells were examined for their microtubule morphology and the following classes scored: cells with no microtubules, cells with a single dot of staining, cells with a short bar (approximately one-half the cell diameter) or in budded cells with a spindle, and finally cells with a large structure (greater than one-half the cell diameter) or budded cells containing a spindle and with large cytoplasmic microtubules (see figure 2-5, and also figure 1-1 for a graphic depiction of these various morphologies). Approximately 50% of the *tub1-733* cells contained excess microtubules. *TUB1* transformed cells had a reduced number of cells with large microtubule structures. Cells bearing *ATS1* on a *CEN* plasmid had an intermediate distribution of structures, while cells with *ATS1* on a 2-μm plasmid had a distribution resembling that of the *TUB1* containing cells. Both *ATS1* containing strains had a higher percentage of cells with no microtubule staining than either the *tub1-733* or the *TUB1* transformed strains.

-Bud size distributions in suppressed strains:

The distribution of bud sizes is aberrant in the extra microtubule mutants of *TUB1*. Cells arrest at the nonpermissive temperature with a predominantly large-budded phenotype. To assess the degree to which this phenotype is alleviated in mutant strains containing *ATS1* suppressor plasmids, DBY2414 (*tub1-733*) was transformed with YCp50, pDK7 (*TUB1*), pDK8 (*CEN ATS1*), and pDK32 (2-μm *ATS1*). Transformants were grown for 23 hours at 15°. Cells were scored as having no buds, small buds

Figure 2-6:

Excess *ATS1* suppresses the bud distribution phenotype of DBY2414 (*tub1-733*). DBY2414 was transformed with YCp50, pDK7 (*TUB1*), pDK8 (*CEN ATS1*) or pDK32 (2-μm *ATS1*). Cells were incubated at approximately 15° for 23 hours and then the distribution of bud sizes evaluated. Buds were scored as either no bud, small (less than 75% of the mother), large (greater than 75% of the mother) or three or more cells together. 75% of the cells in a YCp50 transformed DBY2414 culture contain cells with a large-budded phenotype. Transforming pDK7 (*TUB1*) into DBY2414 restores the bud size distribution to a more normal distribution. Introduction of *ATS1* on either high or low copy plasmids alters the distribution, reducing the large-budded class. The distribution is not identical to *TUB1*-transformed cells, however; especially noticeable is the increase in the no-budded class of cells. The bud size distribution is not greatly different between strains containing *CEN* or 2-μm *ATS1* plasmids.

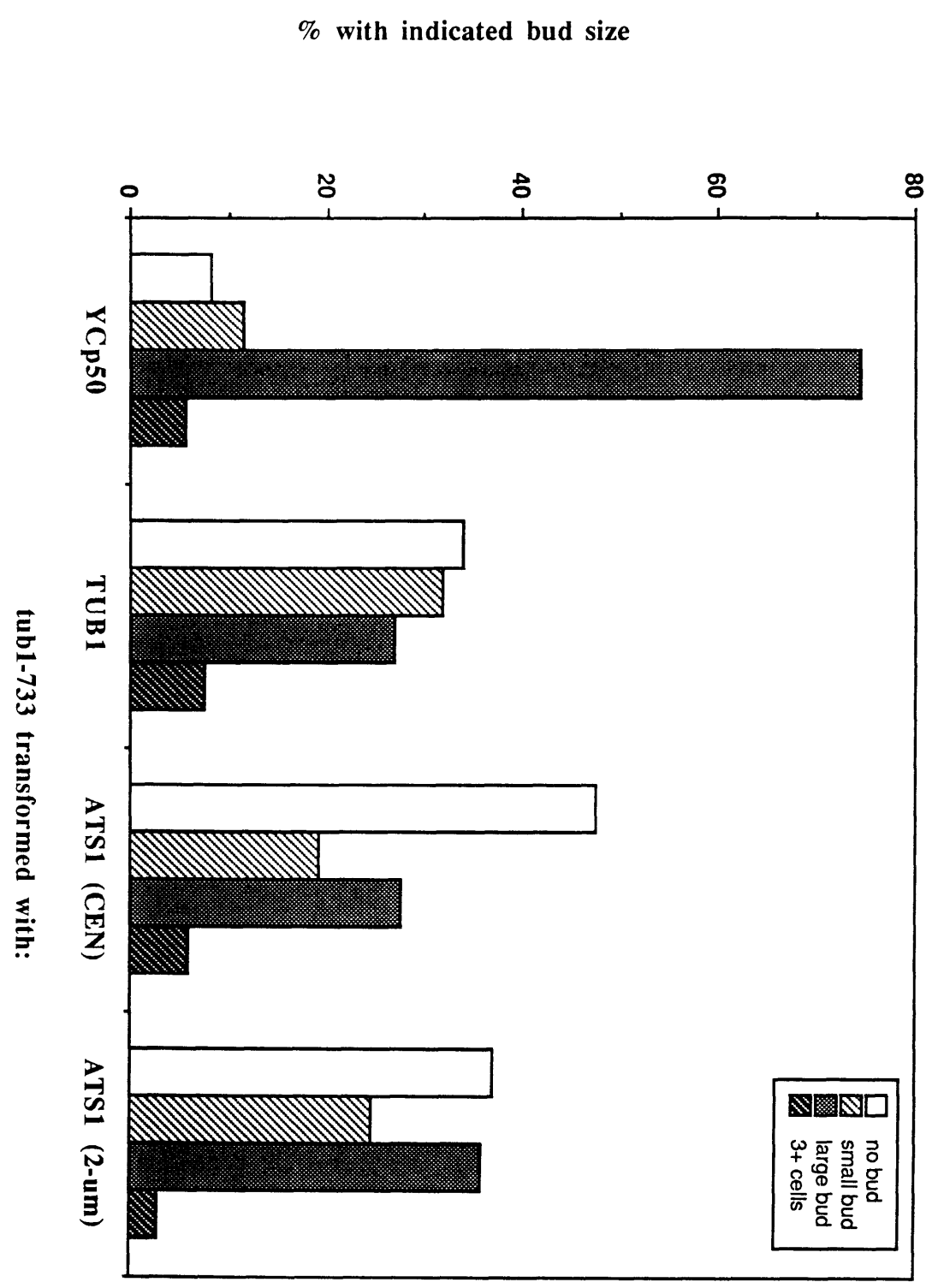
% with indicated bud size
0
20
40
60
80
no bud
small bud
large bud
3+ cells
YCp50
TUB1
ATS1 (CEN)
ATS1 (2-um)
tub1-733 transformed with:

(less than 75% of the mother), large buds (greater than 75% of the mother), or clumped with three or more cells together (see figure 2-6). A DBY2414 strain containing YCp50 had a large budded phenotype in approximately 75% of the cells. Transforming pDK7 into DBY2414 restores a more normal bud size distribution. Introduction of excess *ATS1* into DBY2414 also alters the bud size distribution, reducing the percentage of cells in the large-budded class. The distribution is not identical to that seen with *TUB1* transformed cells; most noticeable is the increase in the no bud class of cells. This increase correlates with the observed increase in the no-microtubule group in the microtubule morphology experiment discussed above. The bud size distribution is not greatly different between strains containing *CEN* or 2-μm *ATS1* plasmids, although pDK32 transformed cells have a distribution more closely resembling pDK7 transformed cells.

-Benomyl sensitivity of *tub1-730* is not altered in suppressed strains:

DBY2412 (*tub1-730*) is sensitive to the microtubule depolymerizing drug benomyl (Schatz et al., 1988). In order to determine if this sensitivity was altered in strains containing extra copies of *ATS1*, serial dilutions of various strains were plated to solid media containing various concentrations of benomyl.

Two independent isolates of DBY2412 transformed with pDK7 or pDK16 and one isolate transformed with YCp50, along with an untransformed strain of DBY2412, were grown overnight in liquid media, and then serial 10-fold dilutions were made in 96-well plates. These dilutions were transferred to SC-Ura media containing 0, 15, 30 or 45 μg/ml of benomyl (see figure 2-7). As expected, the Ura$^-$ DBY2412 control strain failed to grow on any of the plates. Patches were seen for all other strains on

Figure 2-7:

15 μg/ml benomyl **0 μg/ml benomyl**

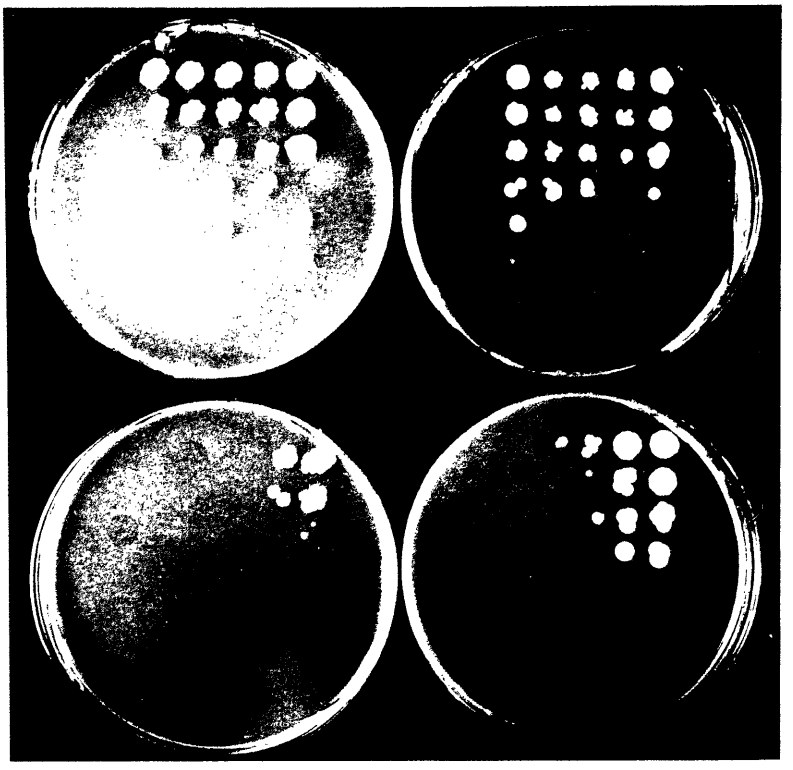

45 μg/ml benomyl **30 μg/ml benomyl**

Excess *ATS1* does not alter the DBY2412 (*tub1-730*) benomyl sensitivity phenotype. From left to right on each SC-Ura+benomyl plate: DBY2412 (no patches grew on any plate), DBY2412 with YCp50, DBY2412 with pDK16 (*CEN ATS1*): 2 columns, and DBY2412 with pDK7 (*CEN TUB1*): 2 columns. From the top of each plate, in each column, are 10-fold dilutions of a liquid culture. Concentrations of benomyl are as marked for each plate.

0 μg/ml and 15 μg/ml plates. DBY2412 transformed with pDK7 (*TUB1*) was able to grow on 45 μg/ml benomyl, unlike the other strains, although at an approximate 100-fold reduction relative to dilutions placed on no-benomyl plates. Individual colonies were present in the highest concentration patches at 30 μg/ml benomyl for strains transformed with pDK16 (*ATS1*), but not YCp50. This is only a marginal difference, however, and may reflect only a difference in concentration of cells patched, and not a true difference in sensitivity. We conclude that excess *ATS1* does not significantly alter the sensitivity to benomyl exhibited by DBY2412.

Sequence of *ATS1*

-Identification of the region of pDK8 responsible for suppression:

A restriction map of pDK8 was generated by digestion with various restriction enzymes both singly and in combination. One enzyme digestion is of note: digestion with NotI indicated that the genomic region contained one site for that rare 8-base cutter. Studies (Link and Olson, 1991) indicate that there are only approximately 38 NotI sites in the *Saccharomyces cerevisiae* genome.

The plasmid library was constructed through insertion of genomic yeast DNA into the BamHI site of YCp50 (Rose et al., 1987). The genomic DNA was cut with Sau3AI and size selected. The isolated genomic fragments were then ligated into the BamHI site. In pDK8, this insertion regenerated a BamHI site on the EcoRI side of the insert. BamHI, HindIII, ClaI, and EcoRI sites flank the insert on one side, while SalI, SphI and ApaI flank the insert on the other. Double digests with combinations of these

Figure 2-8:

The various domains on the suppressing plasmid pDK8. The genomic region containing *ATS1* is approximately 6 kilobases in extent; the entire plasmid is approximately 14 kb. A number of restriction sites were mapped in the genomic DNA, and are indicated here. Sites were determined by restriction digests with various combinations of enzymes that only occur in the backbone and enzymes that occur in the genomic DNA.

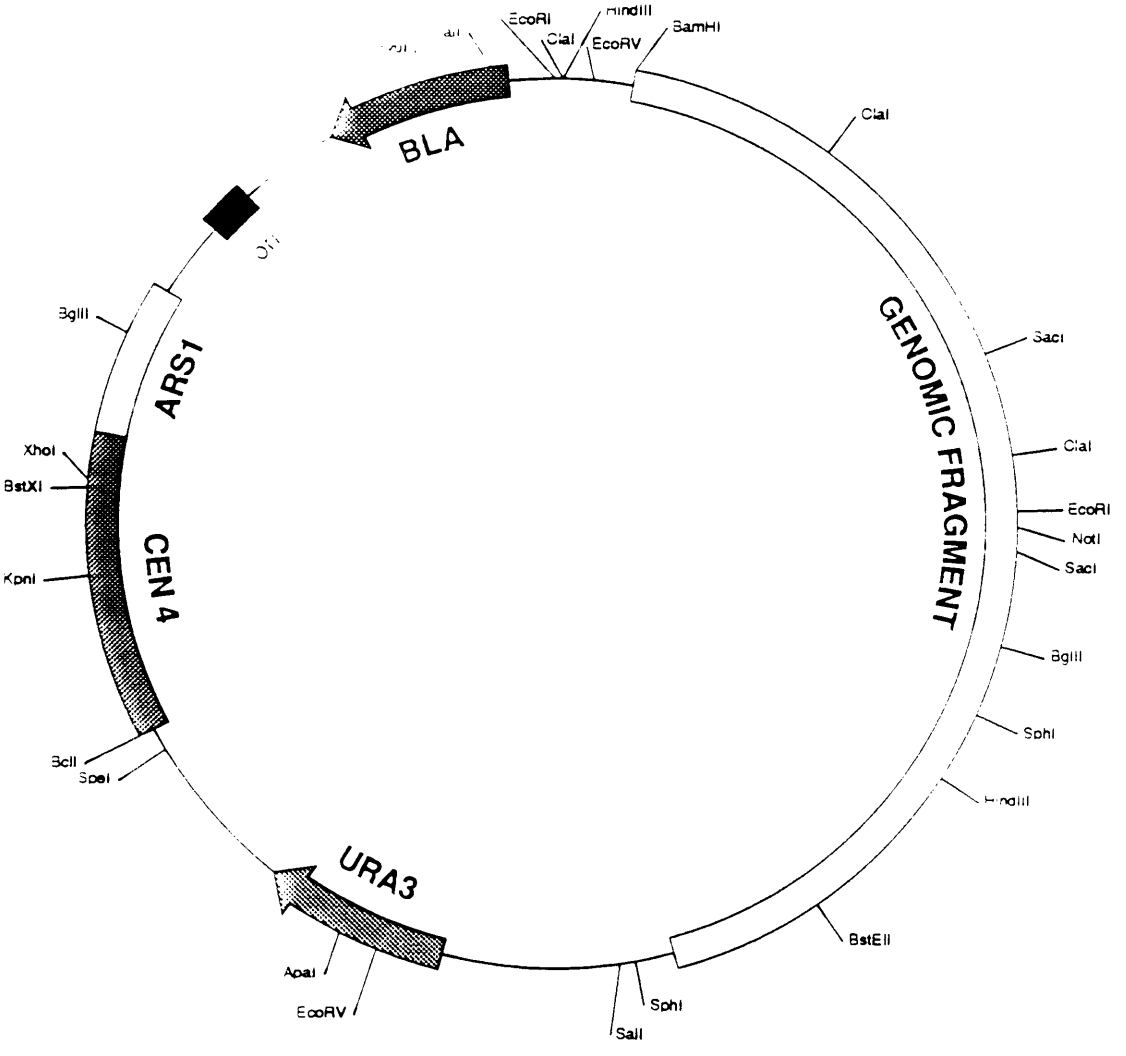
EcoRI
ClaI
HindIII
EcoRV
BamHI
ClaI
BLA
GENOMIC FRAGMENT
SacI
ClaI
EcoRI
NotI
SacI
BglII
SphI
HindIII
BstEII
SphI
SalI
ApaI
EcoRV
URA3
BclI
SpeI
CEN 4
KpnI
XhoI
BstXI
ARS1
BglII

Figure 2-9:

Constructions used to determine the region of pDK8 responsible for suppression of the cold-sensitivity of DBY2412. pDK11 is a deletion of the regions between ClaI sites in pDK8. pDK12 is a deletion of DNA between HindIII sites in pDK8. pDK13 is a deletion of DNA between SphI sites in pDK8. pDK16 was generated by deleting the SphI region in pDK11. Suppression was evaluated by introducing the plasmids into DBY2412 (*tub1-730*) and incubating at the nonpermissive temperature. pDK16 complemented the cold-sensitivity, and this region was sequenced.

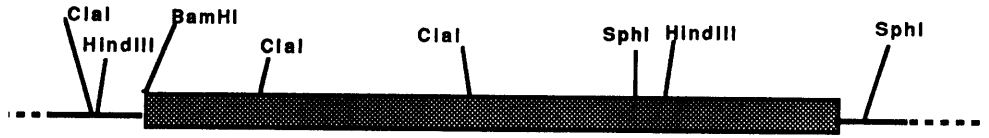

pDK8 GENOMIC FRAGMENT: 6 KILOBASES

SUPPRESSION

+

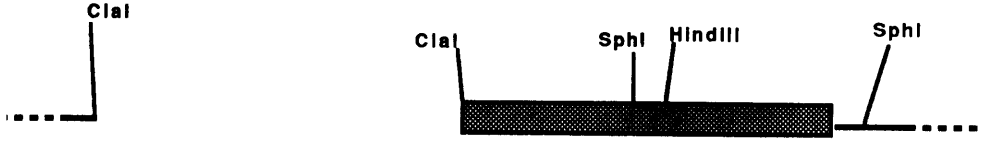

pDK11 ClaI DELETION: Δ2.8 KILOBASES

+

pDK12 HindIII DELETION: Δ4.5 KILOBASES

−

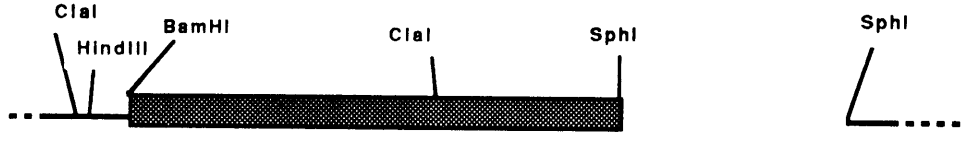

pDK13 SphI DELETION: Δ1.5 KILOBASES

+

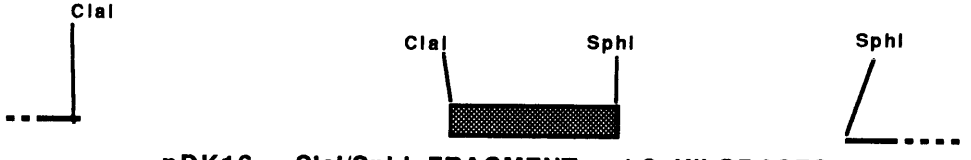

pDK16 ClaI/SphI FRAGMENT: 1.3 KILOBASES

+

enzymes and enzymes whose sites were to be mapped localized sites within the genomic insert of pDK8. Digestion of pDK8 with HindIII, followed by recircularization with T4 DNA ligase, yielded plasmid pDK12. In a similar manner, pDK11 was generated from a ClaI digest, and pDK13 from an SphI digest. (See figure 2-8 for diagram of restriction sites in pDK8.)

DBY2412 was transformed with pDK11, pDK12, pDK13, pDK7 and YCp50. Plates containing transformants were placed at room temperature and at 15° to evaluate the ability of each plasmid to rescue the cold-sensitivity of *tub1-730*. These transformations indicated that the region between the second ClaI site and the SphI site in the genomic region of pDK8 was necessary for suppression of the cold-sensitivity (see figure 2-9). A plasmid (pDK16) was constructed that contained just the region between the ClaI and SphI sites. When introduced into DBY2412, pDK16 transformed cells formed colonies at the nonpermissive temperature, indicating that the ClaI to SphI region was sufficient for suppression.

-Sequencing of suppressing region:

Based on the results of the subcloning, it was decided to sequence the ClaI to SphI region of the genomic insert of pDK8. Subclones containing DNA that covered the entire ClaI to SphI region were generated. Single-stranded DNA sequencing using the dideoxy nucleotide method resulted in the generation of a continuous sequence from the SphI to the ClaI sites.

I obtained a series of primers that corresponded to sequences between the ClaI and SphI sites. These primers (see table 2a) allowed the sequencing of both strands of DNA from the SphI site to the ClaI site and beyond. Regions were sequenced multiple times in both directions to insure that the

Figure 2-10:

Schematic representation of the sequencing reactions performed in the *ATS1* region. Each line indicates a separate sequencing reaction, with direction of sequencing indicated by the arrow. The major open reading frame is indicated as a hatched box, along with a few of the restriction sites utilized for constructions.

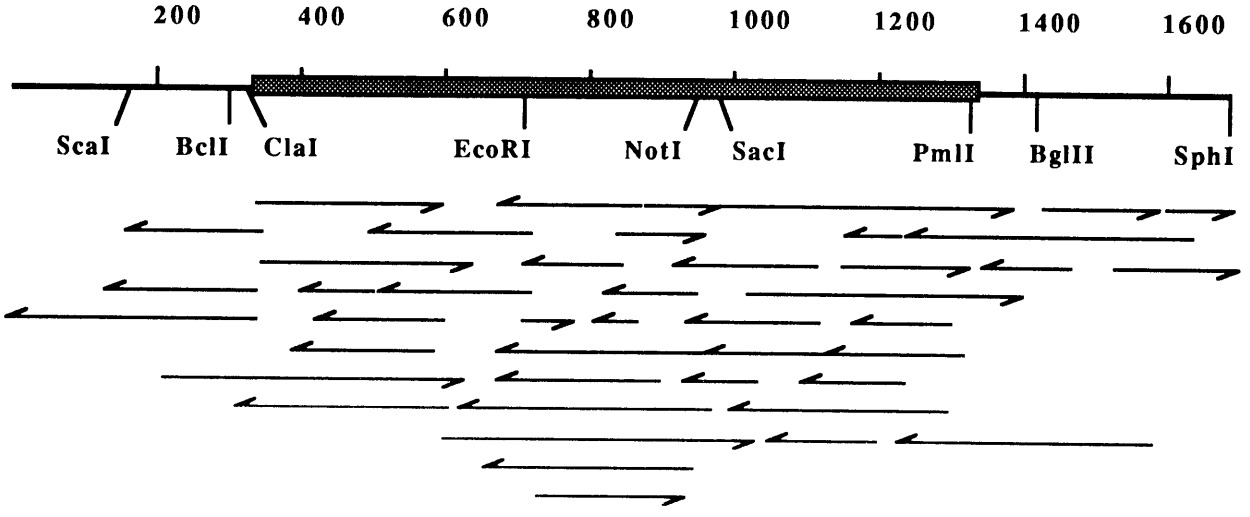
200
400
600
800
1000
1200
1400
1600
ScaI
BclI
ClaI
EcoRI
NotI
SacI
PmlI
BglII
SphI

Figure 2-11:

The nucleotide and amino acid sequence generated during sequencing of the *ATS1* region. Numbering is from the 'A' in the ATG that begins the *ATS1* open reading frame. Bases 5' of this are indicated by negative numbers. Numbering for the nucleotide sequence is indicated to the left, while numbering for the amino acid sequence is to the right.

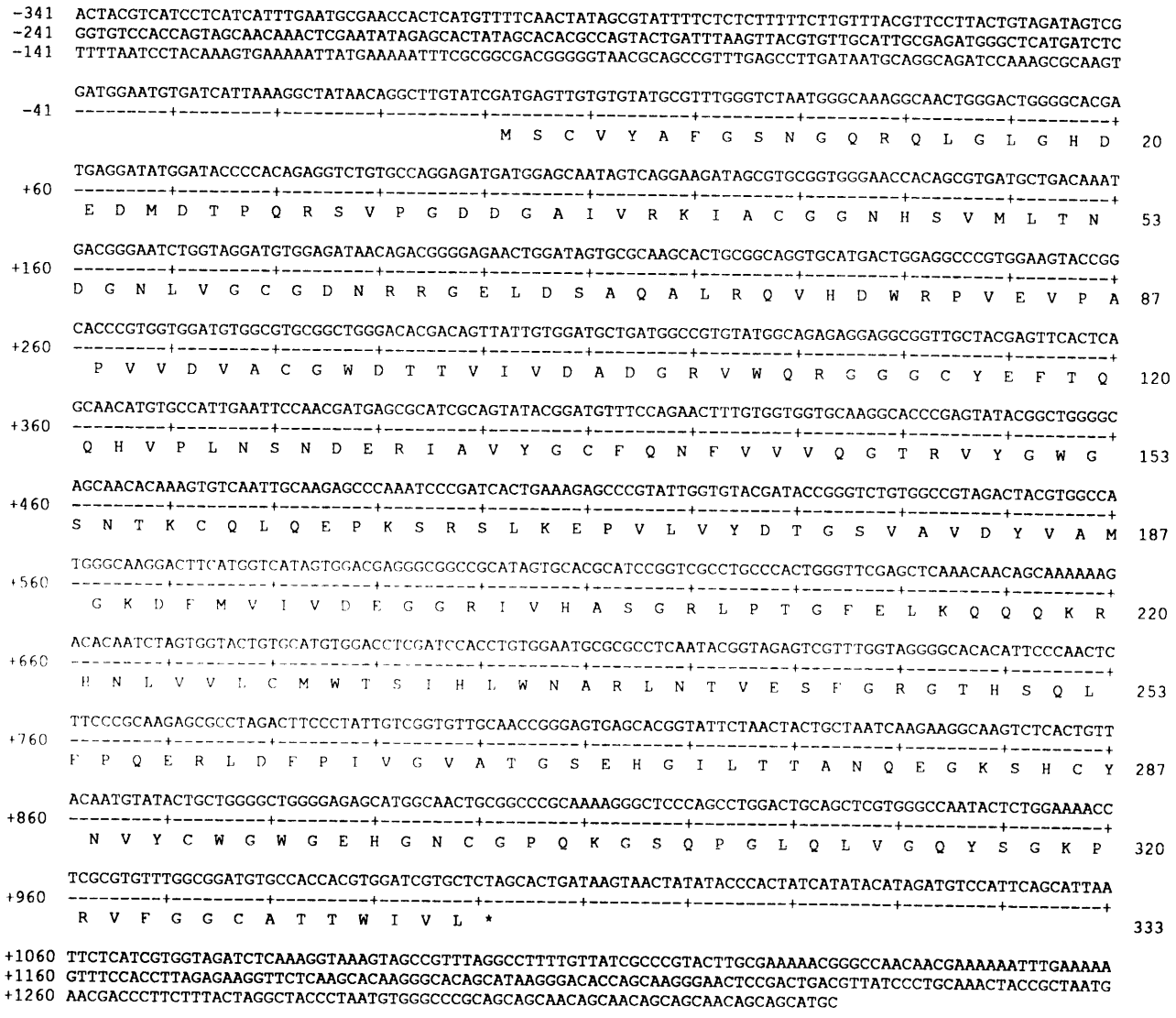
-341 ACTACGTCATCCTCATCATTTGAATGCGAACCACTCATGTTTTCAACTATAGCGTATTTTCTCTCTTTTTCTTGTTTACGTTCCTTACTGTAGATAGTCG
-241 GGTGTCCACCAGTAGCAACAAACTCGAATATAGAGCACTATAGCACACGCCAGTACTGATTTAAGTTACGTGTTGCATTGCGAGATGGGCTCATGATCTC
-141 TTTTAATCCTACAAAGTGAAAAATTATGAAAAATTTCGCGGCGACGGGGGTAACGCAGCCGTTTGAGCCTTGATAATGCAGGCAGATCCAAAGCGCAAGT
GATGGAATGTGATCATTAAAGGCTATAACAGGCTTGTATCGATGAGTTGTGTGTATGCGTTTGGGTCTAATGGGCAAAGGCAACTGGGACTGGGGCACGA
-41
M S C V Y A F G S N G Q R Q L G L G H D 20
TGAGGATATGGATACCCCACAGAGGTCTGTGCCAGGAGATGATGGAGCAATAGTCAGGAAGATAGCGTGCGGTGGGAACCACAGCGTGATGCTGACAAAT
+60
E D M D T P Q R S V P G D D G A I V R K I A C G G N H S V M L T N 53
GACGGGAATCTGGTAGGATGTGGAGATAACAGACGGGGAGAACTGGATAGTGCGCAAGCACTGCGGCAGGTGCATGACTGGAGGCCCGTGGAAGTACCGG
+160
D G N L V G C G D N R R G E L D S A Q A L R Q V H D W R P V E V P A 87
CACCCGTGGTGGATGTGGCGTGCGGCTGGGACACGACAGTTATTGTGGATGCTGATGGCCGTGTATGGCAGAGAGGAGGCGGTTGCTACGAGTTCACTCA
+260
P V V D V A C G W D T T V I V D A D G R V W Q R G G G C Y E F T Q 120
GCAACATGTGCCATTGAATTCCAACGATGAGCGCATCGCAGTATACGGATGTTTCCAGAACTTTGTGGTGGTGCAAGGCACCCGAGTATACGGCTGGGGC
+360
Q H V P L N S N D E R I A V Y G C F Q N F V V V Q G T R V Y G W G 153
AGCAACACAAAGTGTCAATTGCAAGAGCCCAAATCCCGATCACTGAAAGAGCCCGTATTGGTGTACGATACCGGGTCTGTGGCCGTAGACTACGTGGCCA
+460
S N T K C Q L Q E P K S R S L K E P V L V Y D T G S V A V D Y V A M 187
TGGGCAAGGACTTCATGGTCATAGTGGACGAGGGCGGCCGCATAGTGCACGCATCCGGTCGCCTGCCCACTGGGTTCGAGCTCAAACAACAGCAAAAAAG
+560
G K D F M V I V D E G G R I V H A S G R L P T G F E L K Q Q Q K R 220
ACACAATCTAGTGGTACTGTGCATGTGGACCTCGATCCACCTGTGGAATGCGCGCCTCAATACGGTAGAGTCGTTTGGTAGGGGCACACATTCCCAACTC
+660
H N L V V L C M W T S I H L W N A R L N T V E S F G R G T H S Q L 253
TTCCCGCAAGAGCGCCTAGACTTCCCTATTGTCGGTGTTGCAACCGGGAGTGAGCACGGTATTCTAACTACTGCTAATCAAGAAGGCAAGTCTCACTGTT
+760
F P Q E R L D F P I V G V A T G S E H G I L T T A N Q E G K S H C Y 287
ACAATGTATACTGCTGGGGCTGGGGAGAGCATGGCAACTGCGGCCCGCAAAAGGGCTCCCAGCCTGGACTGCAGCTCGTGGGCCAATACTCTGGAAAACC
+860
N V Y C W G W G E H G N C G P Q K G S Q P G L Q L V G Q Y S G K P 320
TCGCGTGTTTGGCGGATGTGCCACCACGTGGATCGTGCTCTAGCACTGATAAGTAACTATATACCCACTATCATATACATAGATGTCCATTCAGCATTAA
+960
R V F G G C A T T W I V L * 333
+1060 TTCTCATCGTGGTAGATCTCAAAGGTAAAGTAGCCGTTTAGGCCTTTTGTTATCGCCCGTACTTGCGAAAAACGGGCCAACAACGAAAAAATTTGAAAAA
+1160 GTTTCCACCTTAGAGAAGGTTCTCAAGCACAAGGGCACAGCATAAGGGACACCAGCAAGGGAACTCCGACTGACGTTATCCCTGCAAACTACCGCTAATG
+1260 AACGACCCTTCTTTACTAGGCTACCCTAATGTGGGCCCGCAGCAGCAACAGCAACAGCAGCAACAGCAGCATGC

sequence generated was correct. (See figure 2-10 for a diagram of the region sequenced and individual sequencing reactions.)

One major open reading frame was detected, originating just 3' of the ClaI site and continuing for approximately one kilobase toward the SphI site (see figure 2-11 for the complete nucleotide and amino acid sequences). This open reading frame is capable of coding for a protein of 333 amino acids. The protein has an isoelectric point of 6.7. It is unusually rich in glycine and valine, containing 43 and 37 residues, respectively. It also has a slightly higher percentage of leucine and glutamine residues than expected. The predicted molecular weight of the Ats1 protein is 36.5 kDa. Computer analysis using the Genetics Computer Group program "PeptideStructure" predicts that *ATS1* contains no extensive regions of β-pleated sheets or α-helices. Similarly, there appear to be no regions capable of forming a transmembrane domain. There is one possible glycosylation site.

-Proteins with similarity to the predicted *ATS1* protein:

Computer analysis indicated that the Ats1p consists of a series of seven internal tandem repeats, each approximately 50 amino acids in length (see figure 2-12). A number of residues are conserved in each repeat. These are boxed in figure 2-12, with a rough consensus sequence indicated underneath the repeats. Dashes indicate spaces that have been introduced to maximize the similarities between repeats.

Recently a large (greater than 17 kilobase) region of chromosome I has been sequenced (Clark et al., 1992; Ouellette et al., 1993). By sequence comparison the *ATS1* locus occurs in this region. This localization also agrees with my initial restriction mapping, as chromosome I contains one NotI site at the approximate location that sequence comparison predicts

Figure 2-12:

The amino acids of *ATS1* arranged as a series of seven tandem repeats. Dashes indicate spaces inserted to maximize the similarities between repeats. Each repeat is approximately 50 amino acids long. Boxed amino acids are those conserved between repeats, and are also indicated below the repeats diagram. Compare the conserved amino acids depicted here with those conserved in RCC1, in figure 2-13.

ATS1 Repeat Structure

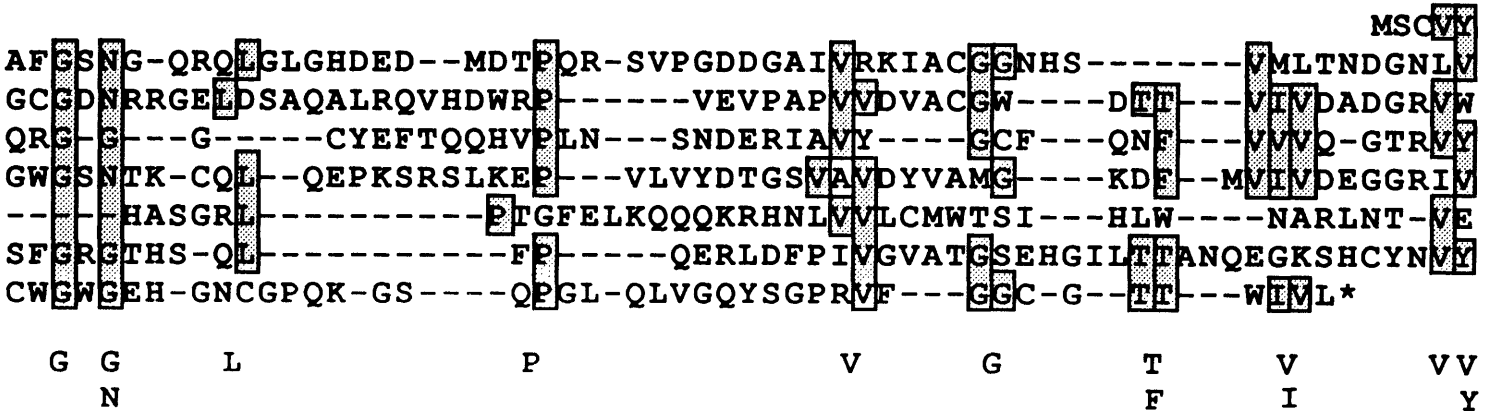

ATS1 should occur. In those sequence reports, *ATS1* is referred to as *FUN28* (FUN stands for Function Unknown Now).

When protein databases are probed with the open reading frame for *ATS1*, it exhibits significant similarity to a series of related proteins. The first protein in this group to be described, RCC1, is a mammalian gene of 421 amino acids. It consists of a series of seven tandem repeats, as does *ATS1*. Figure 2-13 shows the RCC1 protein arranged as a series of repeats. The second *ATS1* repeat is lined up with the repeats in RCC1. Stars (*) under the residues in the *ATS1* repeat indicate the number of times that specific *ATS1* residue occurs in the RCC1 repeats. The residues that are most conserved generally correspond to the residues that are conserved in the *ATS1* repeats (compare the consensus sequence in figure 2-12 with the stars in figure 2-13).

RCC1 was initially isolated as a gene that could rescue a temperature sensitive mutation in a golden hamster cell line (Ohtsubo et al., 1987). This cell line, *ts*BN2, when shifted to the nonpermissive temperature, prematurely initiated chromosome condensation, as if entering mitosis (Nishimoto et al., 1978). Subsequent biochemical and genetic analysis indicated that the RCC1 protein associated with a small ras-related protein, Ran/TC4 (Bischoff and Ponstingl, 1991a; Bischoff and Ponstingl, 1991b). The complex is capable of binding chromatin (Ohtsubo et al., 1989), although some reports indicate that it might be specifically localized to kinetochores (Bischoff et al., 1990). A number of models concerning the functioning of RCC1 have been advanced; the most prevalent is that it is functioning as a checkpoint protein, maintaining coordination between the state of DNA synthesis and mitosis in the cell. (For a more complete discussion of RCC1 and related proteins, refer to the Discussion.) Homologs of RCC1 have been identified

Figure 2-13:

Comparison of an *ATS1* protein repeat with the repeats in RCC1. The RCC1 protein is depicted at the top, arranged to demonstrate its seven tandem repeats. The second *ATS1* repeat is lined up under the RCC1 repeats. Below each amino acid of the *ATS1* repeat a star (*) has been placed to indicate the presence of that amino acid at that position in an RCC1 repeat. The number of stars indicates the number of times that the same amino acid occurs in RCC1 repeats. Comparison of residues that are highly conserved in RCC1 to *ATS1* residues that are conserved (figure 2-12) demonstrates that these amino acids are conserved in both proteins.

Comparison of ATS1 Region with RCC1 Protein Sequence:

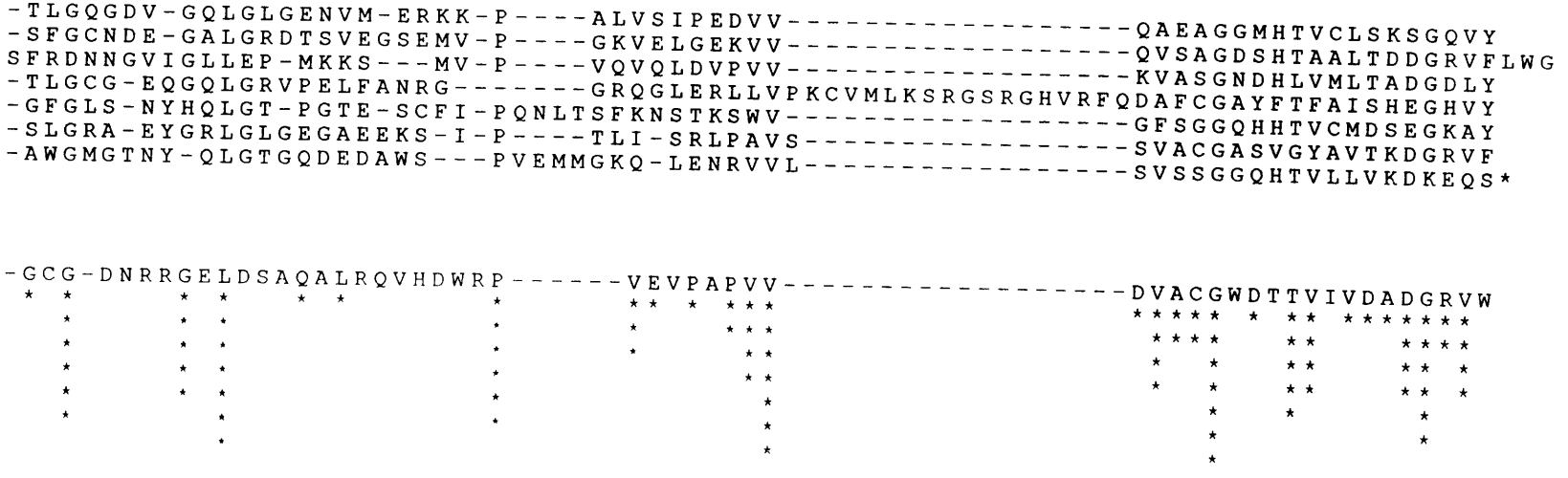

in *Drosophila* (BJ1 (Frasch, 1991)), *Xenopus* (Nishitani et al., 1990), *Schizosaccharomyces pombe* (*pim1* (Matsumoto and Beach, 1991)) and *Saccharomyces cerevisiae* (*ATS1* and *SRM1/PRP20*).

The other *S. cerevisiae* protein with similarity to *ATS1* and RCC1 is *SRM1/PRP20*. This gene has been isolated a number of times, utilizing a number of different screens (Aebi et al., 1990; Clark and Sprague, 1989; Fleischmann et al., 1991). *SRM1/PRP20* is arranged as seven tandem repeats, as is *ATS1* and RCC1. The manner in which *SRM1/PRP20* functions has not been determined. Two Ran/TC4-related genes, *GSP1* and *GSP2* (Belhumeur et al., 1993) were isolated as high-copy suppressors of the *prp20-1* temperature sensitive mutant. Deletion of *SRM1/PRP20* is lethal in haploid strains (Aebi et al., 1990; Clark and Sprague, 1989). To date *S. cerevisiae* is the only organism in which two different RCC1-like and Ran/TC4-like proteins have been identified.

Effects of *ATS1* Deletions

-Deletion of *ATS1* is not lethal, but does have some consequence:

To delete the chromosomal copy of *ATS1*, two different constructs were made. The first (pDK24) contains the first 126 amino acids of the *ATS1* coding region, with the remainder replaced with *URA3* DNA. The construction generates a relatively clean truncation of *ATS1*; i.e. there are only two altered amino acids after the site of insertion of *URA3*, and then a stop codon is encountered. An integrating fragment containing this allele can be generated by digesting pDK24 with ClaI and SphI. The second construct (pDK31) contains 5' and 3' noncoding sequence of *ATS1*,

Figure 2-14:

This figure diagrams the truncation and deletion alleles of *ATS1*. The truncation allele consists of the first third of *ATS1*, interrupted after EcoRI by *URA3* DNA. This insertion results in the replacement, after the EcoRI site, of two amino acids and then a stop codon is encountered.

The deletion allele consists of a complete deletion of the *ATS1* open reading frame and its replacement with *URA3* sequence. 5' and 3' sequences are intact, allowing them to be used for directing integration to the *ATS1* chromosomal locus.

Construction of Truncation Allele of ATS1

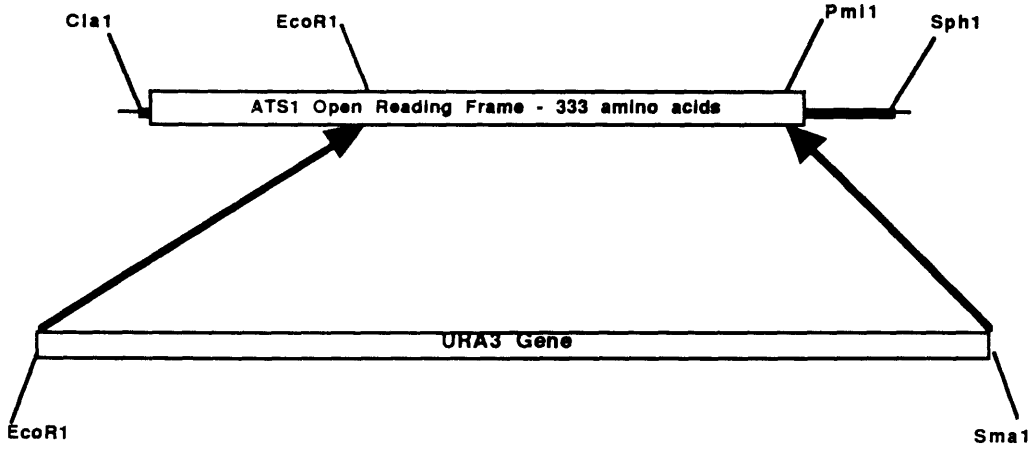

Construction of Deletion Allele of ATS1

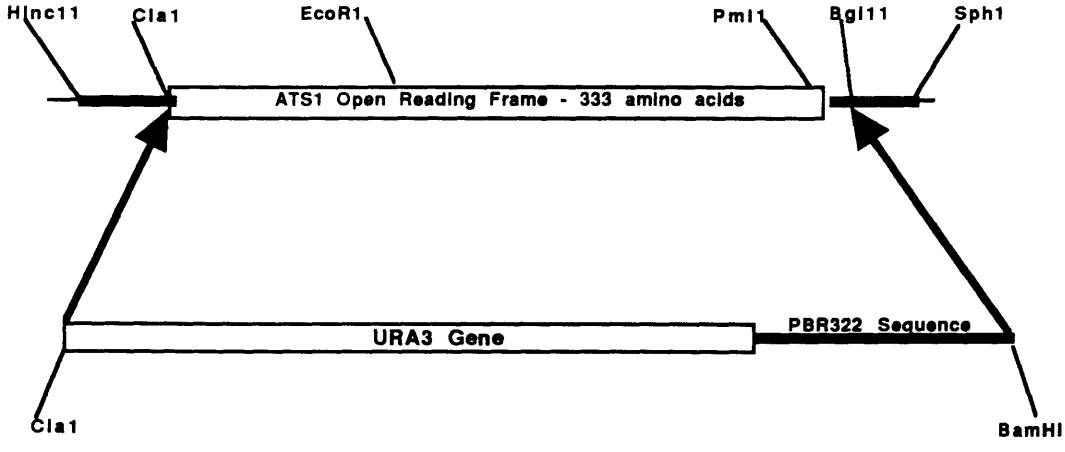

interrupted by *URA3* DNA. An 1880 bp integrating fragment containing this complete deletion allele can be generated by digesting pDK31 with XmnI and SphI. (See figure 2-14 for diagrams of each construct.)

To assess the effect of deleting a chromosomal copy of *ATS1*, the diploid strain FSY120 was transformed with linear DNA from XmnI SphI digest of pDK31. Ura^+ transformants were isolated and sporulated. Dissection of the resulting asci and examination of the colonies resulting from germination of the spores at 30° revealed that Ura^+ and Ura^- colonies were equally viable. Thus, deletion of *ATS1* in FSY120 at 30° confers no severe phenotype. This result agrees with the recent report on *FUN28* (Ouellette et al., 1993).

Although deletion of *ATS1* reveals that it is not an essential gene, are there conditions under which *ATS1* is required? To determine this, sporulated diploid spores were dissected and allowed to germinate and incubate at a range of temperatures: 11, 13, 15, 30, 37 and 42°. No colonies formed from any spore at 42°. Examination of spores at other temperatures revealed a slow-growth phenotype at extreme temperatures. Ura^+ cells formed smaller colonies at 11 and 37° than Ura^- colonies, in the same length of time at the same temperature (see figure 2-15). At 11°, out of 43 spores 14 formed small colonies. All 14 were Ura^+, including one aberrant 1 Ura^-:3 Ura^+ tetrad. This phenotype could be seen at higher temperatures, such as 13° C, but was less dramatic. At 37° 17 small colonies were formed from 31 spores deposited. Of these 17, 14 were Ura^+. The penetrance of the slow growth phenotype was somewhat variable. Occasional colonies that were Ura^+ could be found that were the same size as their Ura^- siblings, for example.

Figure 2-15:

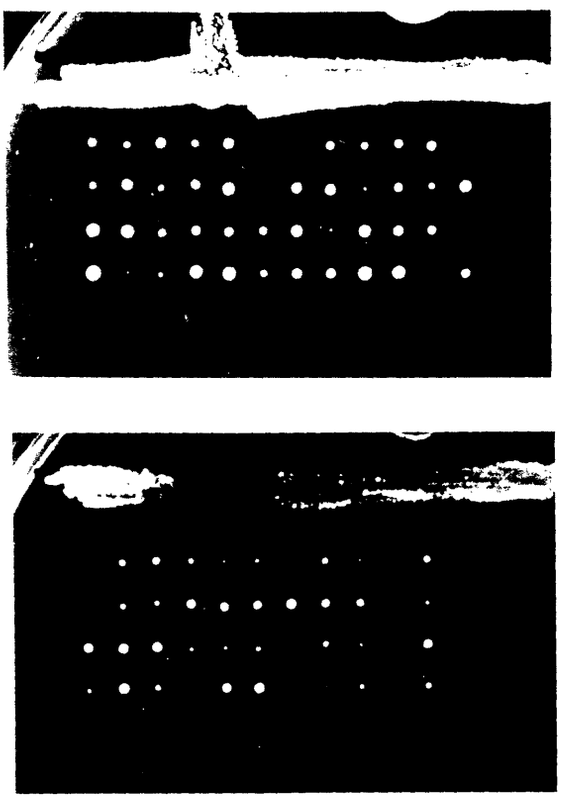

Colonies resulting from tetrads dissected and incubated at extreme temperatures. A diploid strain heterozygous for *Δats::URA3* was sporulated and asci dissected and incubated at 11 degrees C. (top) or 37 degrees C. (bottom). At 11 degrees, 43 spores formed colonies. Of these, 14 are noticeably smaller than their siblings. All 14 are Ura+. For example, tetrad #1 (from the left) contains two Ura+ (1a, b) and two Ura- (1c,d) colonies. Tetrad #3 (from the left) is an aberrant tetrad: 3a is Ura-, 3b-d are Ura+. At 37 degrees C. of 31 spores, 17 were smaller, and of these, 14 were Ura+. As an example, tetrad #8 (rightmost) contains two Ura+ (8b, d) and two Ura- (8a, c) colonies.

Crosses were performed to determine if the incomplete penetrance of the slow growth phenotype was in fact due to the assorting of an already occurring heterozygous mutation in FSY120. Based on colony morphologies within a tetrad, two small Ura$^-$ strains and two large Ura$^-$ colonies were crossed, as were two small Ura$^+$ and two large Ura$^+$ colonies. Finally, pairwise combinations between the various small and large Ura$^+$ and Ura$^-$ colonies were constructed, for a total of eight crosses. The three diploid strains resulting from Ura$^-$ x Ura$^-$ colonies were transformed with the linear integrating fragments from pDK24 (the truncation allele) and pDK31 (the deletion allele) or the 2-μm *ATS1* plasmid pDK32. A total of 17 diploids were sporulated, and approximately twenty tetrads from each diploid strain were dissected, with ten placed at 11° and ten at 30°. Based on these dissections, no indication that a second gene was assorting independently of the *Δats1::URA3* alleles that might alter the growth of the strains containing a deletion of *ATS1*. Strains heterozygous for the deletion allele continued to exhibit the slow growth phenotype, although once again with variable penetrance. If there is another gene that is affecting the growth of the strains containing a deletion of *ATS1*, the effect it is having is too subtle to be consistently detectable.

-Effects of benomyl on wildtype strains in which *ATS1* has been deleted or overexpressed:

One common phenotype of mutations that affect microtubule structures is alteration in the sensitivity to microtubule destabilizing drugs such as benomyl. If *ATS1* is acting as a microtubule destabilizer, then it is possible that elimination of *ATS1* might render cells more resistant to the effects of benomyl. In a similar fashion, overexpression of *ATS1* might

Figure 2-16:

Deletion of *ATS1* does not affect benomyl resistance of haploids derived from wildtype FSY120. FSY120 derived strains were grown in SC-Ura or SC media, 100-fold serial dilutions made, and then transferred to SC-UraAde or SC-Ade plates containing varying concentrations of benomyl. Strains used were from tetrad dissections of sporulated FSY120 transformed with either pDK32 (2-μm *ATS1 URA3*), the deletion construction *Δats1::URA3* or the truncation construction *tΔats1::URA3*. Each plate is divided into four quarters. The upper right contains three columns of FSY120 pDK32 segregants, the upper left contains four FSY120 *ATS1* deletion segregants, while the bottom sections contain two sets of *ATS1* truncation segregants. The photograph at the top of the page shows SC-Ade plates, with from top to bottom, left to right, 0, 5, 10, 15, 10, 25, and 30 μg/ml of benomyl. The bottom photograph shows SC-UraAde plates with the same amounts of benomyl as the plates in the top photograph. Segregants that lack *URA3* fail to form patches on SC-UraAde plates in the bottom photograph. As can be seen by inspecting Ura^+ and Ura^- segregants within each tetrad, no alteration in benomyl resistance was detected in strains containing a deletion or truncation of *ATS1*.

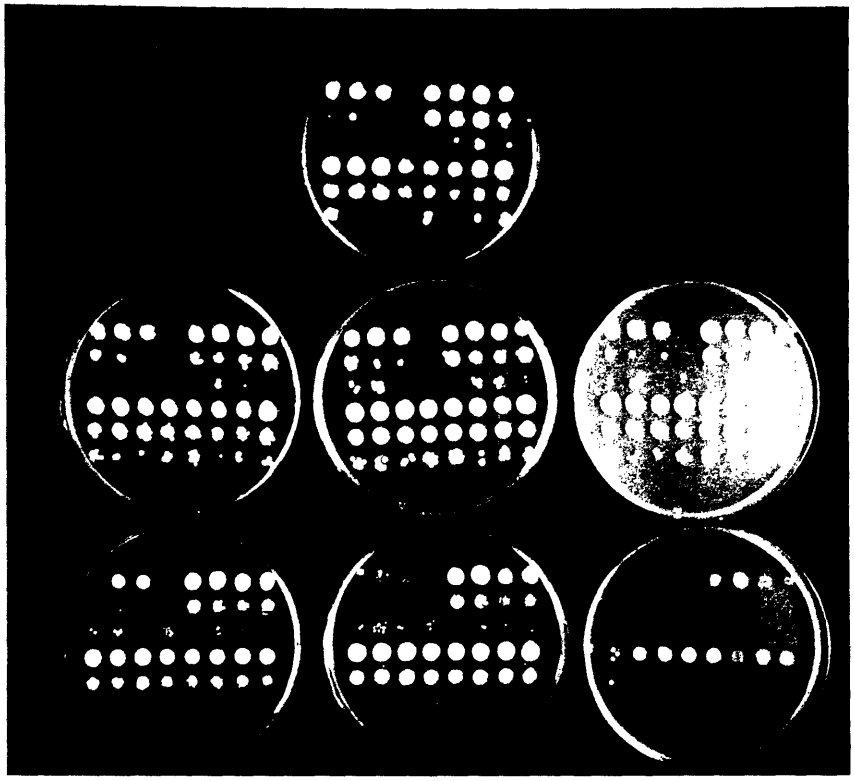

SC-Ade

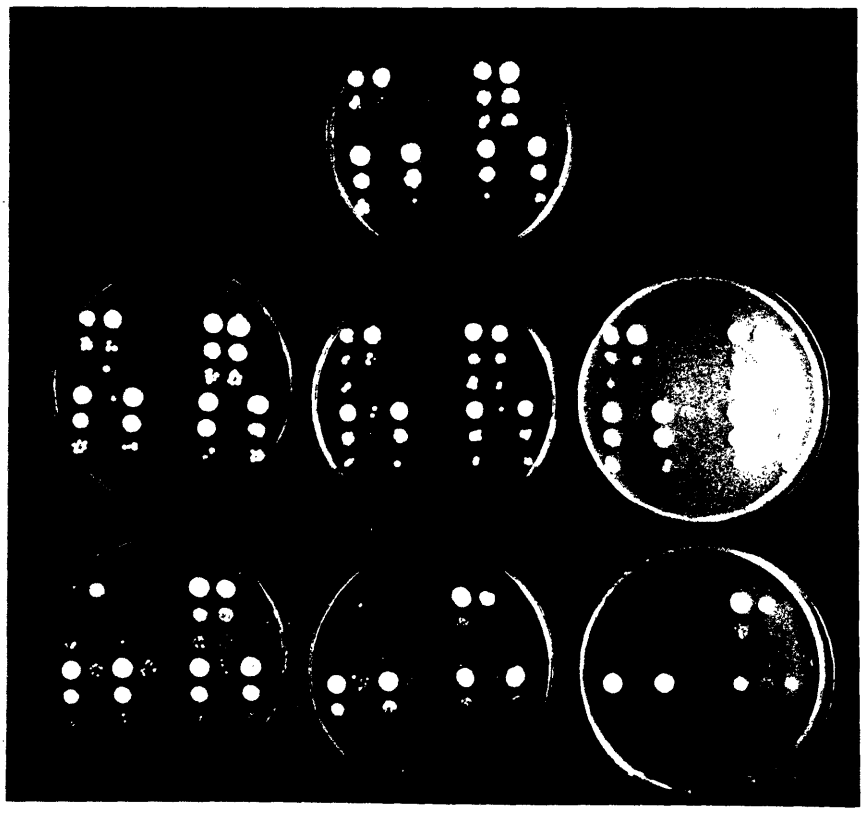

SC-UraAde

enhance the effects of benomyl in a wild-type strain. To test these possibilities, strains containing deletions, truncations or excess copies of *ATS1* were plated on plates containing various concentrations of benomyl.

Overexpression or elimination of *ATS1* in wild-type strains has no significant impact on susceptibility to the microtubule depolymerizing drug benomyl. The following strains were used in this experiment: three colonies from a tetrad dissection of FSY120 transformed with pDK32 (*ATS1* on a 2-μm plasmid), one complete tetrad resulting from an FSY120-derived strain heterozygous for *Δats1::URA3*, and two tetrads derived from diploids heterozygous for a *URA3*-marked truncation of *ATS1*. 100-fold serial dilutions of each strain were made in 96-well plates after growth overnight in liquid media. These dilutions were then transferred to SC-Ade or SC-UraAde containing 0, 5, 10, 15, 20, 25 or 30 μg/ml of benomyl. After growth at 30 degrees, the ability of each strain to form patches was assessed (see figure 2-16). Strains containing pDK32 failed to form patches at 25 μg/ml benomyl, the same concentration that affected sister strains that lacked pDK32. Comparison of strains from tetrads containing deletions or truncations of *ATS1* with their wild-type (at the *ATS1* locus) counterparts similarly failed to reveal any significant alteration in the extent of benomyl resistance or sensitivity.

Overexpression of *ATS1* in Various Backgrounds

-Overexpression of *ATS1* in wildtype cells:

Overexpression of *ATS1* in the extra microtubule mutant strains is capable of restoring growth at the nonpermissive temperature.

Figure 2-17:

Excess *ATS1* does not affect doubling times of wildtype strains at either 15° or room temperature. A strain isogenic with the extra microtubule mutant strains but wildtype at *TUB1* (DBY2433) was transformed with pDK32 (2-μm *ATS1*) or YCp50. Two independent isolates of each were grown in liquid media at either 15° or room temperature. Strains containing excess *ATS1* did not significantly differ in growth rate from vector-containing strains at either temperature.

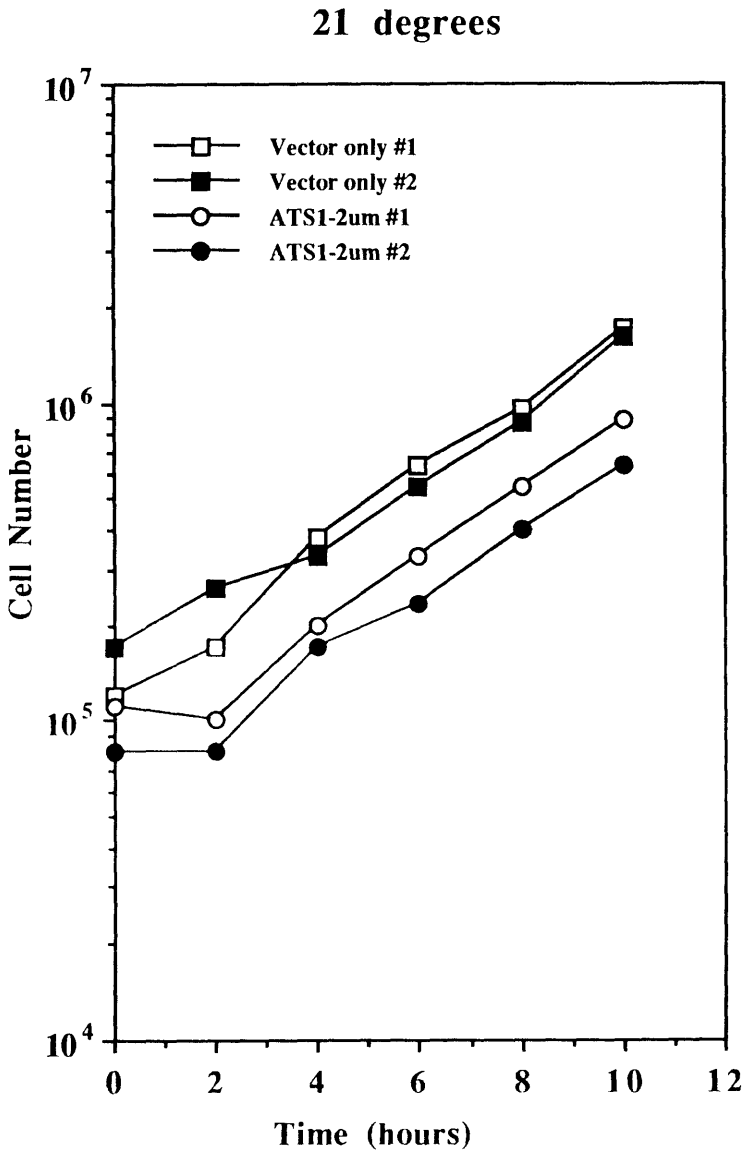
21 degrees
Vector only #1
Vector only #2
ATS1-2um #1
ATS1-2um #2
Cell Number
10^7
10^6
10^5
10^4
0
2
4
6
8
10
12
Time (hours)

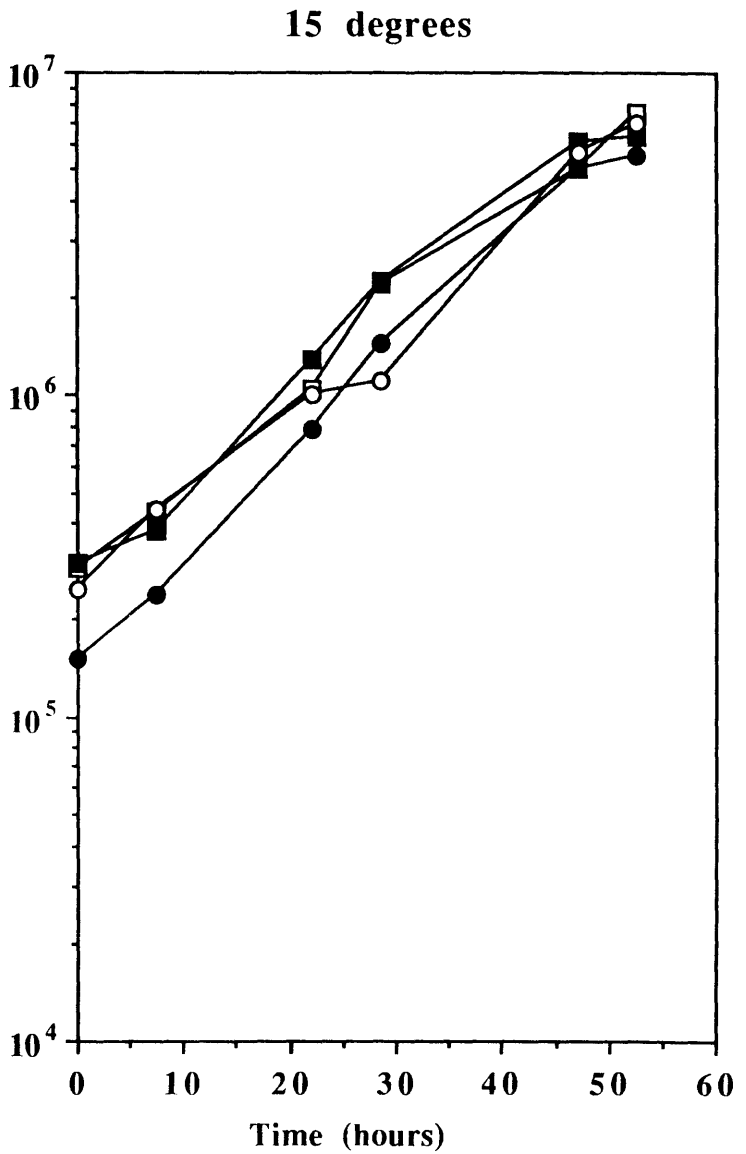
15 degrees
10^7
10^6
10^5
10^4
0
10
20
30
40
50
60
Time (hours)

Overexpression of *ATS1* in wildtype cells might have an effect on the growth rate also, either at normal temperatures or reduced temperatures. DBY2433 (isogenic with the *tub1* mutants but containing pRB539 *TUB1*) was transformed with YCp50 or pDK32. Two transformants of each were grown in selective liquid media at 15° or room temperature. Cell numbers were counted over the course of the experiment: 52 hours for the 15° grown cells and 10 hours for the room temperature experiment. As shown in figure 2-17, the growth rates of the vector transformed and *ATS1* transformed cells are nearly identical. Overexpression of *ATS1* in DBY2433 does not seem to affect the growth rate of the wildtype strain at room temperature or 15°.

-Does excess *ATS1* affect bud size distributions in wildtype cells?

Overexpression of *ATS1* in the extra microtubule mutant background is capable of suppressing the large-budded arrest phenotype connected with the *tub1* mutation. Does overexpression of *ATS1* in a *TUB1* background alter the distribution of bud size? Such an alteration would be indicative of an increase in the duration of a particular phase of the cell cycle, potentially a more subtle phenotype than just an alteration in the doubling time of the strain overexpressing *ATS1*. DBY2433 (*TUB1*) containing YCp50, pDK7, or pDK32 were grown in selective liquid media at 15° or room temperature. Bud size distributions were determined after 4 hours for room temperature cultures, and 21 hours for 15° cultures (see figure 2-18). At room temperature, a high proportion of the cells had no buds (averaging 50% of the cells), approximately 35% of the population had a small bud, and the remainder were large-budded or clumped. There was no difference between any of the strains containing the various plasmids. At 15°, there was some variation between the YCp50 transformed DBY2433 cells and the cells

Figure 2-18:

Excess *ATS1* does not alter bud size distributions in wildtype cells. FSY182 was transformed with YCp50, pDK7 (*TUB1*) or pDK32 (2-mm *ATS1*). Cells were grown, then diluted and incubated at room temperature for 4 hours or 15° for 21 hours. Buds were scored as either no bud, small (less than 75% of the mother), large (greater than 75% of the mother) or three or more cells together. Bud size distribution at room temperature is shown to the left, 15° incubated cells to the right.

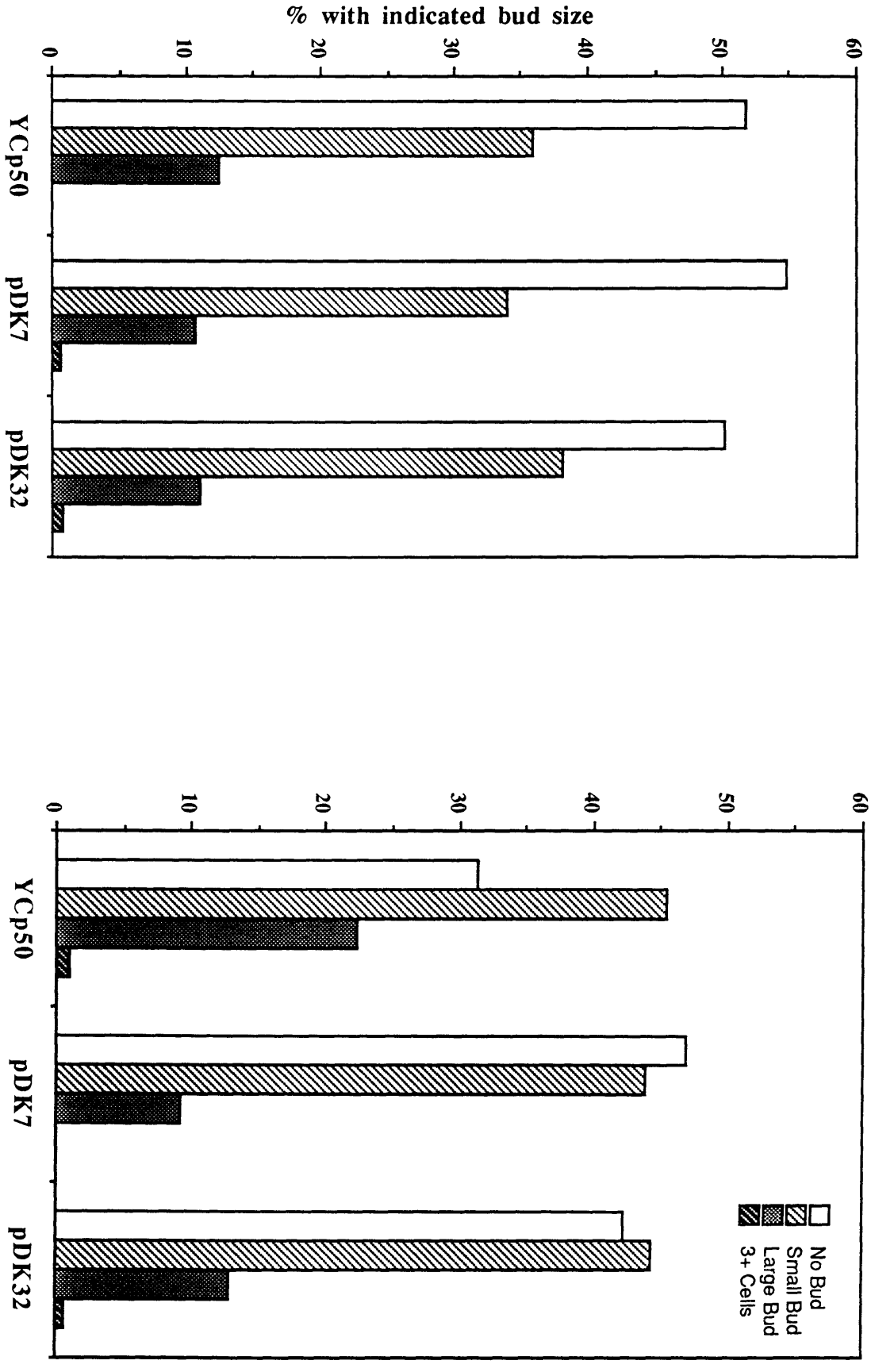
% with indicated bud size
0
10
20
30
40
50
60
YCp50
pDK7
pDK32
No Bud
Small Bud
Large Bud
3+ Cells

containing *TUB1* or *ATS1* plasmids. The percentage of no-budded cells in the population was lower in the YCp50 bearing cells, down to 30% as compared to approximately 45% for the other two strains. The large-budded class was higher in percentage (22%) in YCp50 cells, while *TUB1* and *ATS1* cells had a large bud in 10% and 12% of the population. These differences may indicate that strains containing excess α-tubulin or *ATS1* spend proportionately less time in or near mitosis, or possibly longer in G1, as compared to cells without any excess of either protein.

-High level overexpression of *ATS1*:

Although overexpression of *ATS1* in moderate amounts (on *CEN* and 2-μm plasmids) had no effect, it remains possible that greatly overexpressing *ATS1* in wildtype cells might have a phenotype. Such high level overexpression is possible using the *GAL1,10 -CYC1* promoter region. *ATS1* was placed under the control of this promoter, generating pDK33 with *ATS1* in the correct orientation relative to the promoter and pDK34 with *ATS1* in the reverse orientation (see figure 2-19 for a diagram of the constructions).

pDK33, pDK34 and pLGSD5 were transformed into FSY183 and FSY185. Both strains were chosen because they have been demonstrated to have a high level of induction from the *GAL1,10 -CYC1* promoter when grown in galactose. When streaked for single colonies on SCGal-Ura plates, pDK33 transformants gave rise to colonies in the same amount of time as pDK34 and pLGSD5 containing strains.

Growth in SCGal-Ura liquid media also gave no detectable difference between strains overexpressing *ATS1* and control strains. Cells were grown in SCRaffinose-Ura media, to which galactose was added at the beginning of the experiment. At intervals cells were plated and incubated at 30°. Based

Figure 2-19:

Schematic diagram of galactose-regulated overexpression constructions of *ATS1*. pDK33 contains a BclI to BglII fragment of *ATS1* that has been inserted into the BamHI site of pLGSD5. This places the ATG of *ATS1* 24 base pairs from the *CYC1* leader sequence. pDK34 contains *ATS1* in the reverse orientation.

Galactose-regulated Overexpression of ATS1

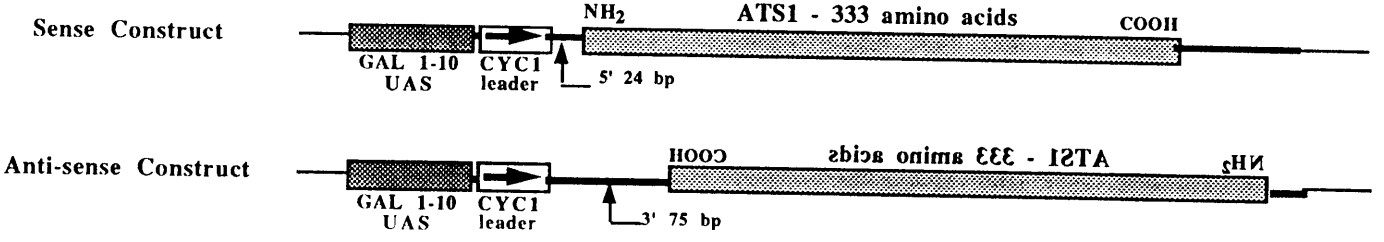

Figure 2-20:

Galactose-induced overexpression of *ATS1*. Growth in SCGal-Ura liquid media gives no detectable difference between strains overexpressing *ATS1* and control strains. The upper panel shows a graph of growth rates for cells were grown in SCRaffinose-Ura media, to which galactose was added at the beginning of the experiment. At intervals cells were plated and incubated at 30°. Based on these plates, cells doubled every 1.5 hours for pDK33 (Gal-*ATS1*), pDK34 (Gal *ATS1* in reverse orientation) and pLGSD5 (control vector). The lower panels show the results of Northerns on RNA from cells grown in galactose and glucose. The panel on the left shows RNA (from pLGSD5 and pDK33 containing cells grown in galactose) and probed with an *ATS1* probe. On the right is an *ATS1* probed Northern of RNA from pDK33 containing cells grown in either galacose or glucose. Specific *ATS1* message is only detected from cells containing pDK33 grown in galactose medium.

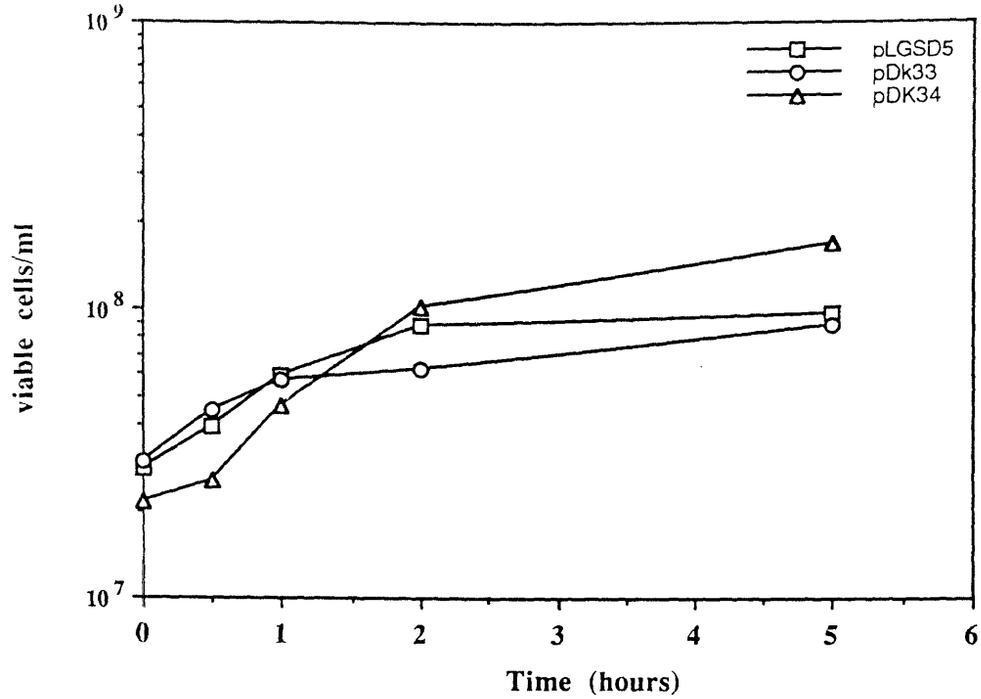

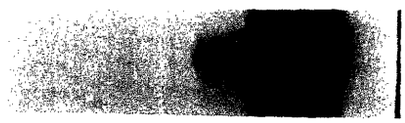

1 25 5 1 5 25

µg/ml RNA

pLGSD5 pDK33

1 5 1 5 25 50

µg/ml RNA

pDK33

galactose glucose

on these plates, cells doubled every 1.5 hours for pDK33, pDK34 and pLGSD5 (see figure 2-20).

To determine if *ATS1* was being overexpressed, cells containing pDK33 or pLGSD5 were grown in SC-Ura and SCGal-Ura media. Total RNA was isolated and run on a formaldehyde agarose gel. After transfer to Hybond-N nylon the blot was probed with *ATS1* (see figure 2-20). One specific band was seen in lanes containing RNA from galactose-grown cells harboring pDK33. No message was detected from pDK33 containing cells grown in glucose, even with 50 μg of RNA.

-Effects of high level overexpression of *ATS1* on benomyl resistance/sensitivity:

Previous experiments involving alteration in the level of *ATS1* in strains (both *tub1* mutants and wild-type) had indicated that both deletion and overexpression of *ATS1* did not affect benomyl sensitivity or resistance. It is possible, however, that drastic overproduction of *ATS1* might have an impact on microtubule structures, rendering them more susceptible to benomyl-induced depolymerization.

FSY120 transformed with pLGSD5, pDK33 (*ATS1* in correct orientation in pLGSD5) or pDK34 (*ATS1* in reverse orientation in pLGSD5) was inoculated into glucose- or galactose-containing media and grown at 30° overnight. 10-fold serial dilutions were made in a 96-well plate and were then patched to SC-UraAde or SCGal-UraAde plates containing 0, 10, 15, 20, 25, or 30 μg/ml benomyl. These were then incubated at 30° (see figure 2-21).

Strains containing pDK33 or pDK34 did not differ significantly from a strain containing the pLGSD5 control vector on SC-UraAde media.

Figure 2-21:

High level overexpression of *ATS1* does not affect benomyl resistance in FSY120. The wildtype strain FSY120 was transformed with pLGSD5, pDK33 (Gal *ATS1*) or pDK34 (Gal *ATS1* in the reverse orientation). Transformants were grown overnight in SC-Ura or SCGal-Ura media. 10-fold serial dilutions were transferred to SC-UraAde or SCGal-UraAde plates containing benomyl and incubated at 30°. The upper photograph shows six SC-UraAde plates, containing (from left to right, top and bottom) 0, 10, 15, 20, 25 and 30 μg/ml benomyl. The lower set of plates are SCGal-UraAde plates containing 0, 10, 15, 20 and 25 μg/ml benomyl. On each plate, from left to right, are serial dilutions of FSY120 containing pLGD5 (galactose-grown), pDK34 (galactose), 2 columns of pDK33 (galactose), 1 column of pLGSD5 (glucose-grown), pDK34 (glucose) and 2 columns of pDK33 (glucose).

SC-UraAde

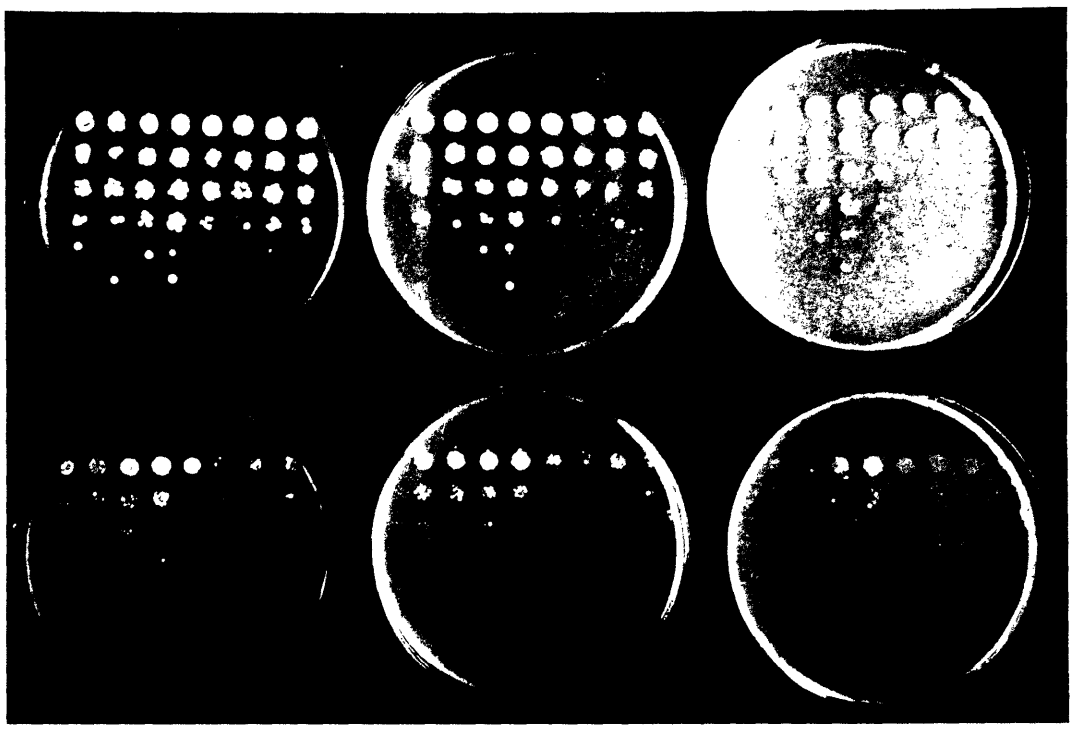

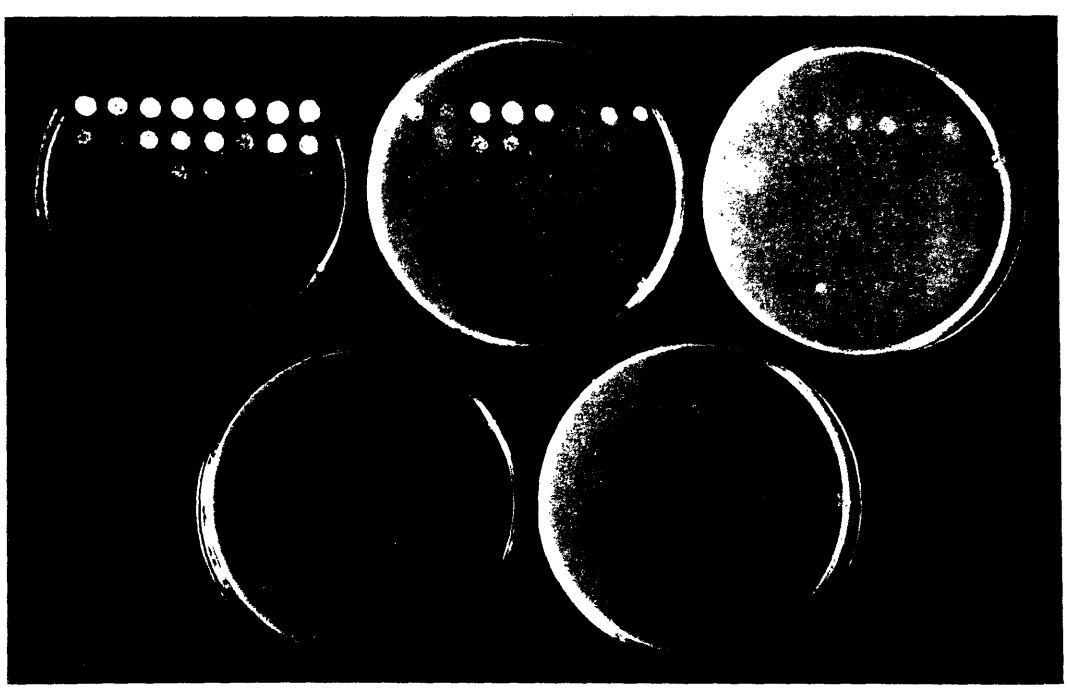

SCGal-UraAde

Growth on SCGal-UraAde was uniformly weaker when compared to growth on SC-UraAde, probably due to the poorer carbon source. Patches failed to form at benomyl concentrations above 10 μg/ml, whereas patches still formed at 30 μg/ml benomyl on glucose plates. The strains that grew the best, both on glucose and galactose media, contained pDK33. The differences detected were very minor and are probably attributable to slight differences in concentrations of cells deposited in each patch.

-High level overexpression of *ATS1* in no-microtubule *tub1* mutants:

Initial experiments indicated that *ATS1* was not capable of suppressing two Class 1 no microtubule mutants, *tub1-724* and *tub1-728*. Eleven Class 1 mutants are available. pLGSD5 and pDK33 were transformed into each strain to determine if high level overexpression of *ATS1* has any effect in those strains.

Transformants were grown overnight in SC-UraLeuAde media, and diluted in 96 well plates. DBY2412 (*tub1-730*) containing pDK7 (*TUB1*) was used as a positive control. Dilutions were transferred to SC-UraLeuAde or SCGal-Ura plates, and incubated at 15, 18, 30 or 37°. There was essentially no difference between pLGSD5 and pDK33 transformed strains on either SC or SCGal plates at any temperature (see figure 2-22) We conclude that overexpression of *ATS1* in the no-microtubule mutants does not suppress the cold-sensitivity associated with the *tub1* mutations. Similarly, overexpression of *ATS1* does not negatively affect the no-microtubule mutant strains. Overexpression might have been deleterious if the *ATS1* product acted as a microtubule destabilizer, for example (see Discussion).

Figure 2-22:

High level overexpression of *ATS1* does not affect phenotypes associated with Class 1 no-microtubule mutant strains. Four panels of plates are shown. On each plate there are two columns of each mutant strain, one transformed with pDK33 (Gal-*ATS1*) and the other with pLGSD5, with 4 strains per plate. The top row of plates in each panel is SC-UraLeuAde plates, while the lower plates are SCGal-Ura. The strains are, in order from left to right across each panel: DBY2399 (*tub1-704*), DBY2401 (*tub1-709*), DBY2408 (*tub1-724*), DBY2410 (*tub1-728*), DBY2411 (*tub1-729*), DBY2417 (*tub1-738*), DBY2421 (*tub1-744*), DBY2425 (*tub1-750*), DBY2427 (*tub1-759*), DBY2428 (*tub1-760*), DBY239), DBY2432 (*tub1-767*) and DBY2412(*tub1-730*). DBY2412 does not contain either pDK33 or pLGSD5, instead, both columns are cells containing pDK7 (*TUB1*), to serve as a positive control. The upper left panel shows plates incubated at 37°, the upper right at 30°, the lower left at 18° and the lower right at 15°.

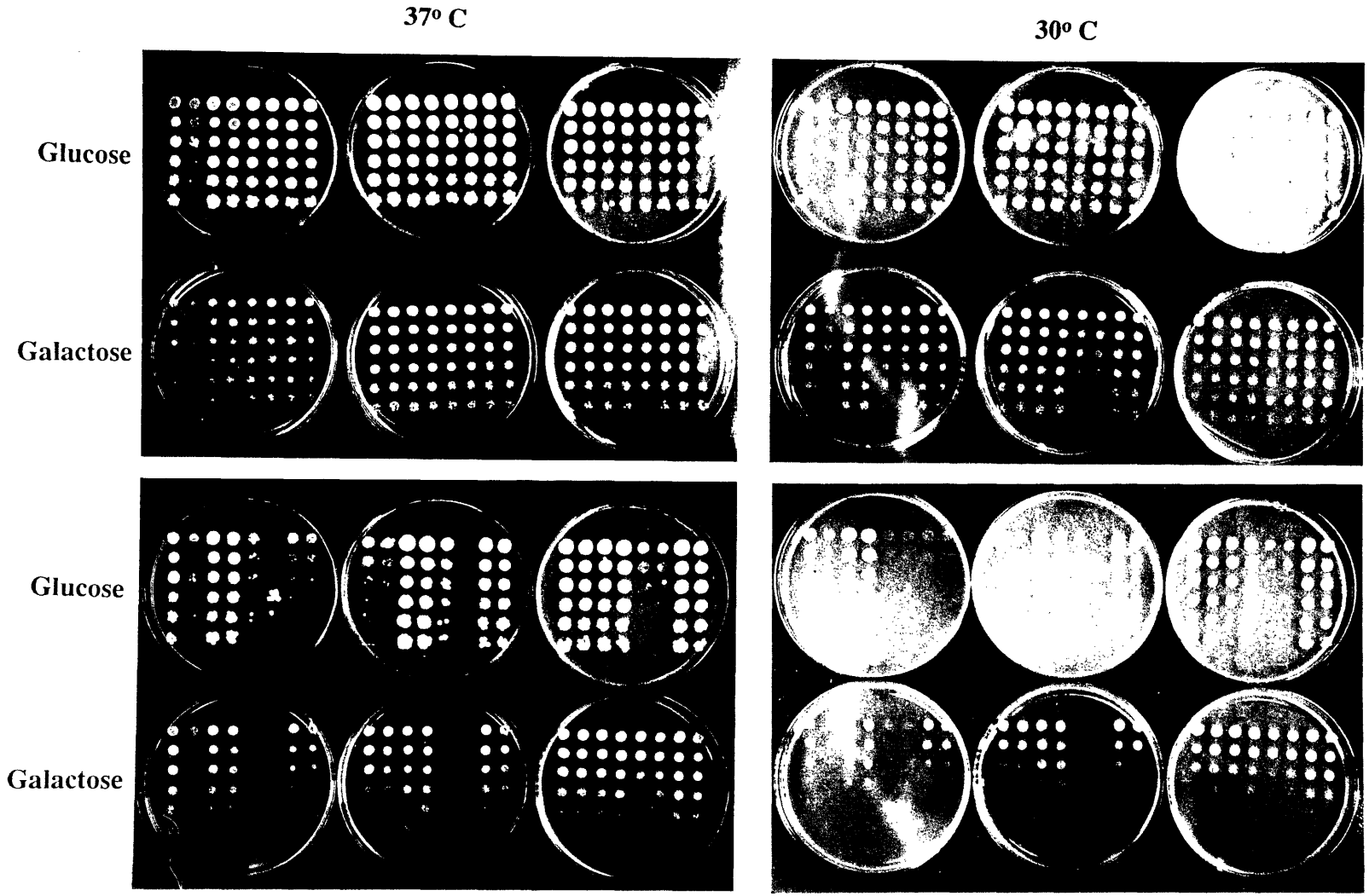
37° C
30° C
Glucose
Galactose
Glucose
Galactose
18° C
15° C

-Overexpression of *ATS1* in two *tub2* mutants:

Is extra *ATS1* capable of suppressing any mutant that exhibits excess microtubules, or does the suppression only occur in Class 2 mutant strains? We obtained two strains with mutations in the β-tubulin gene *TUB2*. These mutations, *tub2-150* and *tub2-412*, generate excessive microtubules at their respective nonpermissive temperatures. Extra copies of *ATS1* were then introduced into the strains to determine if the excess was capable of suppression.

tub2-150 is a benomyl-requiring mutation in β-tubulin (G. Barnes, personal communication). A *tub2-150 ura3-52* strain was transformed with YCp50, pDK35, pDK36 and pDK32. Transformants were isolated on SC-UraAde (30 μg/ml benomyl) plates. Isolates were picked and grown in selective liquid media containing benomyl for 16 hours. Cell density was determined, appropriate dilutions were made in a 96 well tissue culture tray, and transferred to SC-UraAde plates containing decreasing concentrations of benomyl. No alteration in the benomyl requirement was detected in strains containing excess *ATS1* (either *CEN* plasmid or 2-μm plasmid borne) as compared to vector controls (see Figure 2-23).

tub2-412 is a β-tubulin mutation that confers a cold-sensitive phenotype at 14° and arrests with excess microtubules (T. Huffaker, personal communication). Strains ASY257 and 259 (*tub2-412:URA3, ade2, lys2, his3, ura3-52*) were transformed with pRS313 (*HIS CEN* plasmid) and pDK39 (*ATS1* fragment on pRS313). Transformants were plated on SC-HisLeuUra media and incubated at either 30° or 13°. Whereas 1000+ colonies grew at the permissive temperature, no colonies appeared on plates incubated at the nonpermissive temperature. Thus, in two strains, each bearing β-tubulin mutations that generate excess microtubules, overexpression of *ATS1* did not suppress phenotypes associated with the mutations.

Figure 2-23:

The benomyl requirement of *tub2-150* is not alleviated by excess *ATS1*. The photograph shows six SC-Ura plates containing the indicated amount of benomyl. Ten-fold dilutions of the following strains were transferred to each plate and incubated at 30° - from left to right on each plate: 2 columns of *tub2-150* with pDK32 (2-μm *ATS1*), 2 columns of pDK36 (*CEN ATS1*), 2 columns of pDK35 (*CEN ATS1*) and 2 columns of YCp50 vector. No alteration in benomyl requirement of *tub2-150* was detected with excess *ATS1*.

15 µg/ml
20 µg/ml
25 µg ml
0 µg/ml
5 µg/ml
10 µg/ml

ATS1 and *SRM1/PRP20*

-*SRM1/PRP20* suppresses extra microtubule mutants:

ATS1 has significant similarity to another yeast gene, *SRM1/PRP20*. In order to determine the relationship between *ATS1* and *SRM1/RP20*, a number of strains and plasmids were obtained from Wayne Forrester at the University of Wisconsin at Madison. pWF48 is a 2-μm *URA3* plasmid containing *PRP20*. This plasmid was introduced by transformation into DBY2412 (*tub1-730*) to assess *PRP20*'s ability to suppress the cold-sensitivity of the *tub1* mutation. At the same time, *ATS1* on 2-μm (pDK32) and *TUB1* (pDK7) were also transformed into DBY2412, plated, and placed at 15°. *PRP20* was capable of generating colonies at the nonpermissive temperature (see figure 2-24).

-Suppression of DBY2412's bud size distribution phenotype by excess *PRP20:*

DBY2412 (*tub1-730)* containing YCp50, pDK7 (*TUB1*), pDK32 (2-μm *ATS1*) or pWF48 (2-μm *PRP20*) were grown in SC-HisLeuUra liquid media at 15° for 20 hours. Bud size distribution was determined for each strain by microscopy (see figure 2-25). YCp50 transformed strains arrested with approximately 60% of the cells having a large bud. When DBY2412 contained pDK7, this group was reduced to approximately 15% of the population and a high proportion of cells do not have a bud. Strains containing excess *ATS1* or *PRP20* also have a reduced number of cells with a large bud: 22% and 18%, respectively. Thus, excess *ATS1* and *PRP20* suppress the large-budded arrest phenotype of DBY2412 with approximately equal efficiency.

Figure 2-24:

PRP20 is capable of suppressing the cold-sensitivity associated with DBY2412 (*tub1-730*). This figure shows photographs of plates containing transformants of DBY2412 grown at the nonpermissive temperature of 15° for two weeks. The upper left shows DBY2412 transformed with YCp50, the upper right DBY2412 transformed with pDK7 (*CEN TUB1*), the lower left DBY2412 transformed with pDK32 (2-μm *ATS1*) and the lower right pWF48 (2-μm *PRP20*). Both *ATS1* and *PRP20* plasmids allow colonies to form at the nonpermissive temperature. However, colonies are not as large as those formed by *TUB1* transformed cells.

YCp50

pDK7 (*TUB1*)

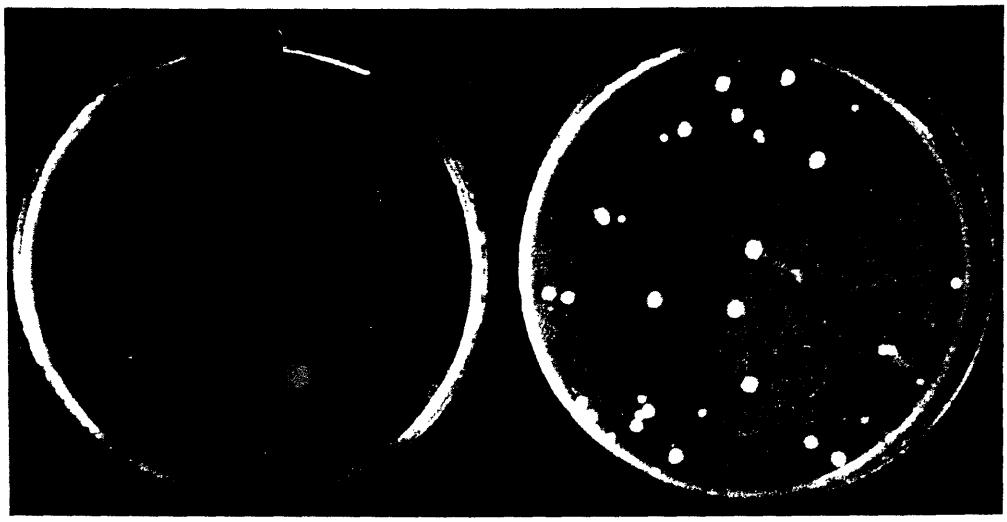

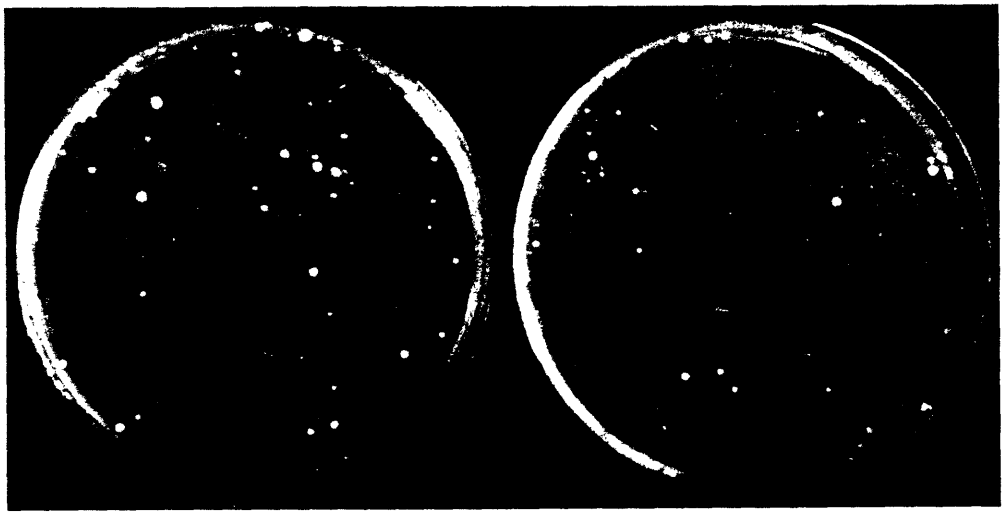

pDK32 (2-μm *ATS1*)

pWF48 (2-μm *PRP20*)

Figure 2-25:

Excess *PRP20* suppresses the bud distribution phenotype of DBY2412 (*tub1-730*). DBY2412 was transformed with YCp50, pDK7 (*TUB1*), pDK32 (2-μm*ATS1*) or pWF48 (2-μm *PRP20*). Cells were incubated at approximately 15° for 20 hours and then the distribution of bud sizes evaluated. Buds were scored as either no bud, small (less than 75% of the mother), large (greater than 75% of the mother) or three or more cells together. YCp50 transformed DBY2412 generates cells with a large-budded phenotype approximately 60% of the time. Transforming pDK7 (*TUB1*) into DBY2412 restores the bud size distribution to a more normal distribution. Introduction of *ATS1* on high copy plasmids alters the distribution, reducing the large-budded class. Introduction of *PRP20* also restores the distribution of bud sizes to a distribution approximating that of *TUB1* transformed strains.

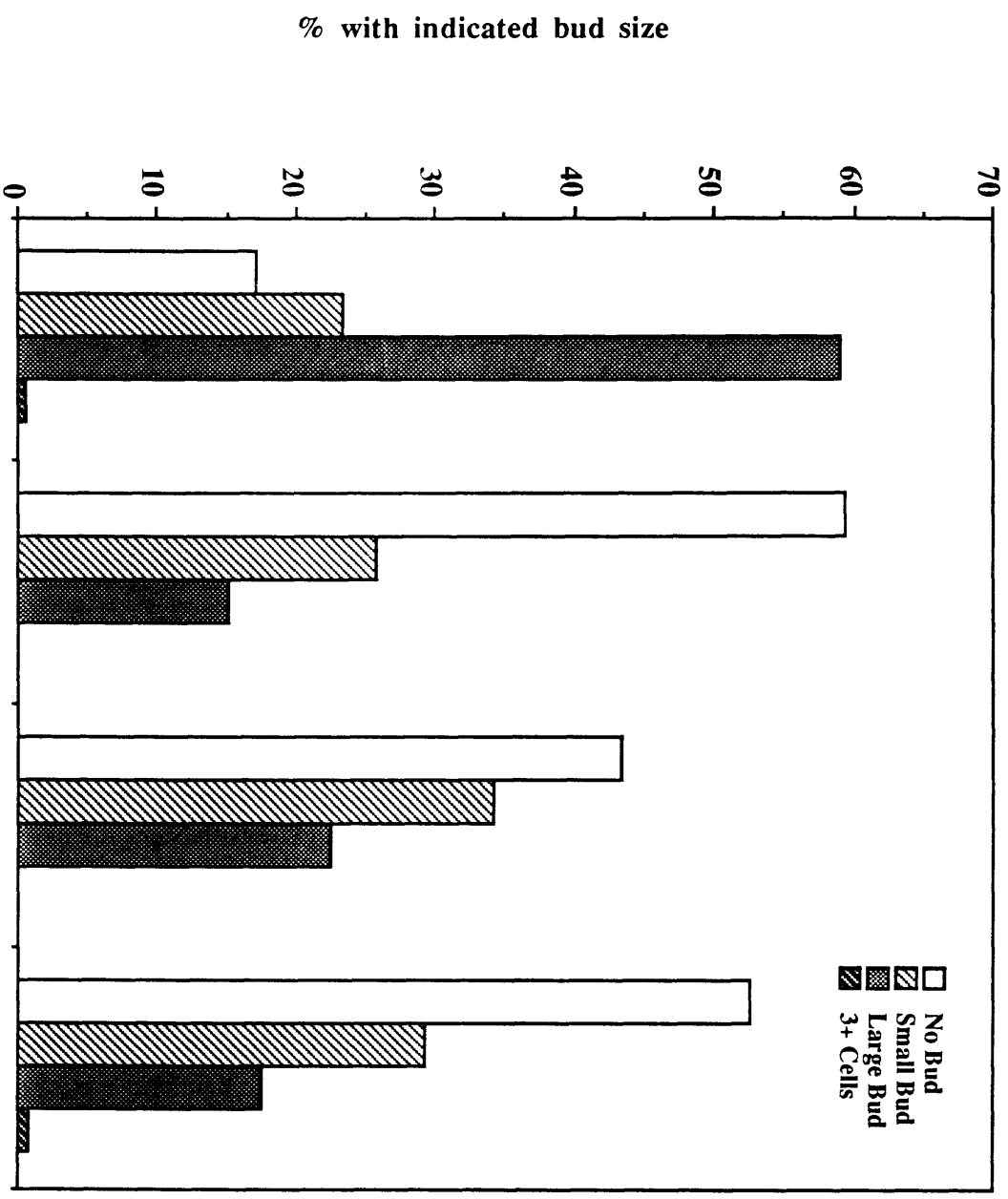
% with indicated bud size
0
10
20
30
40
50
60
70
Vector
TUB1
ATS1
PRP20
No Bud
Small Bud
Large Bud
3+ Cells
tub1-730 transformed with:

-Overexpression of *ATS1* in *prp20-1:*

By a number of criteria, *PRP20* seems able to function in a manner similar to *ATS1*. Are the two proteins functionally interchangeable in the cell in general? To answer this question, a temperature-sensitive mutation in *PRP20* was obtained from Wayne Forrester. This strain, F9-1d, is *prp20-1 ura3-52*. F9-1d was transformed with YCp50, pDK32 (2-μm *ATS1*), pWF48 (2-μm *PRP20*), pLGSD5 (Gal-*LacZ*) and pDK33 (Gal-*ATS1*). Transformants containing each plasmid were isolated at room temperature. They were plated on SC-Ura or SCGal-Ura media and incubated at 33° and 37°. The only strain that grew at either temperature was the pWF48 transformed strain. Thus, overexpression of *ATS1* in a strain containing the *prp20-1* mutation is incapable of rescuing the temperature-sensitivity associated with that allele. We conclude that *ATS1* is not functionally interchangeable with *PRP20*.

***-prp20-1* microtubule phenotype:**

Personal communication with Wayne Forrester indicated that *prp20-1* mutant strains might exhibit an aberrant microtubule structure upon arrest at the nonpermissive temperature of 37°. To confirm this, a *prp20-1* mutant strain and its parental strain M14 were grown in liquid media at room temperature, then switched to 37°. After 30, 60 and 90 minutes, aliquots were removed and fixed for immunofluorescence. The microtubules were stained with antibody against α-tubulin, and visualized with secondary antibody coupled to fluorescein. Cells bearing the *prp20-1* mutation arrest with a microtubule structure reminiscent of wild-type cells at the early bud stage in which they have a short or absent spindle with a cytoplasmic microtubule directed toward the newly emerged bud. However, in the

Figure 2-26:

prp20-1 mutants exhibit an aberrant microtubule structure upon arrest. The upper immunofluorescence micrograph shows a group of *prp20-1* cells grown under permissive conditions (room temperature) for one hour. The lower panel shows the same strain one hour after a shift to 37°. Cells at the nonpermissive temperature arrest with a number of cytoplasmic microtubules not directed toward new buds, unlike the cells grown at permissive temperatures.

prp20-2 after 1 hour at room temperature

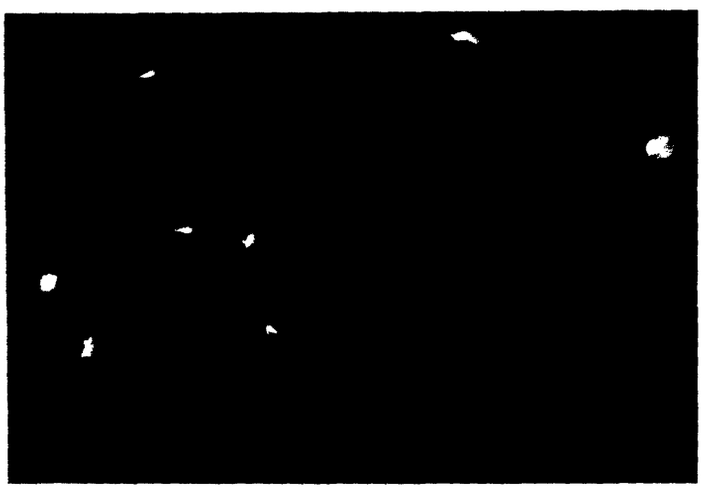

prp20-2 after 1 hour at 37 degrees C.

prp20-1 mutants, there are extra cytoplasmic microtubules, usually two or three, which are not directed at the site of the bud. A high percentage of cells exhibit this phenotype as compared to control parental cells (see figure 2-26).

-Does *ATS1* affect the stability of *CEN* plasmids?

One report on RCC1, the mammalian protein that is similar to *ATS1* and *SRM1/PRP20*, indicated that it might localize to kinetochores (Bischoff et al., 1990). Briefly, an anti-kinetochore antiserum recognized a protein CENP-D, as a band on a Western blot. Fragments of this protein were microsequenced and all corresponded almost exactly with RCC1 protein sequence. As kinetochores are the site at which microtubules attach to chromosomes in many organisms, including *S. cerevisiae*, we wished to assess the role, if any, of *ATS1* at the kinetochore. To accomplish this, we used a strain, JAY11, which allows loss events of centromere-based plasmids to be monitored. We calculated the loss rate for JAY11 strains containing YCp50, pDK16 (*CEN ATS1*), pDK32 (2-μm *ATS1*), and deletions of *ATS1* (see Table 2d).

The experiment was conducted over a 24 hour period, using 4 independent cultures of JAY11 containing YCp50, 2 with pDK16, 2 with pDK32, and 4 with a deletion of *ATS1*. The average percentage loss rate per generation for the marker plasmid in strains containing YCp50 was 6.8%, with a wide variability (from 3% to 16%). The loss rates for the marker plasmid in strains with plasmid-borne versions of *ATS1* were almost identical, 3.1% for pDK16 and 3.2% for pDK32. Excess *ATS1* appears to reduce the loss rate of the *ADE3 CEN* plasmid, but deletion of *ATS1* had the same effect - loss rates were between 3.2% and 4.1% per generation.

Table 2d:

Does *ATS1* affect the stability of *CEN* plasmids? JAY11 transformants containing YCp50, pDK16, pDK32, or *Δats1::URA3* were taken through a modified plasmid loss protocol. The percentage of white colonies (indicative of a loss of the *LEU2 ADE3 CEN* plasmid) at the beginning of the experiment is subtracted from the percentage of white colonies at the end, and divided by the number of generations to arrive at a % loss per generation. Cultures were grown in either YPD or SC-Ura for 24 hours, and plated on YPD or SC-Ura plates.

Table 2d:

Cultures...		JAY11 with:					
Grown In:	Plated On:	YCp50 #1	YCp50 #2	pDK16	pDK32	*Δats1::URA3* #1	*Δats1::URA3* #2
YPD	SC-Ura	8.1	3.6	5.2	4.2	3.9	5.6
	YPD	7.8	6.0	2.3	3.8	3.1	0.7
SC-Ura	SC-Ura	16.0	4.6	4.0	2.6	2.4	5.6
	YPD	3.0	5.6	1.0	2.2	3.3	4.6
Average:		8.7	5.0	3.1	3.2	3.2	4.1

Synthetic Interactions

-Rationale:

Deletion of *ATS1* in wildtype backgrounds has only a minor effect, that of slowed growth at high or low temperatures. This may be due to a redundancy of the *ATS1* function. One gene in yeast that is known to be similar in structure and has at least some overlapping function is *PRP20*. Perhaps deletion of *ATS1* in *prp20-1* mutants might exacerbate the temperature sensitivity of *prp20-1*, leading to a lethal phenotype at all temperatures. Alternately, *ATS1* function could only be necessary under certain conditions, conditions that normally do not occur in wildtype cells. One set of mutations, the Class 2 extra microtubule *tub1* mutations, seems to require *ATS1* in excess to suppress the cold-sensitivity associated with the *tub1* mutations. In those mutants, the chromosomal *ATS1* locus is presumably functional. Deletion of this basal level might lead to a synthetic lethal phenotype. We examined both of these possibilities.

-Is a *Δats1::URA3 prp20-1* double mutant viable?

In order to assess the viability of a double mutant of *PRP20* and *ATS1*, two **a** strains, one containing *prp20-1* and *ura3-52* (F63-7d) and the other a parental strain containing only *ura3-52* (M14) were obtained from Wayne Forrester. These were crossed with two α strains from tetrad dissections, one strain containing a deletion of *ATS1* and the other containing a truncation of *ATS1*. Diploids resulting from the matings were placed on sporulation plates. Strains were dissected and placed at 15° C, room temperature, or 30°.

Figure 2-27:

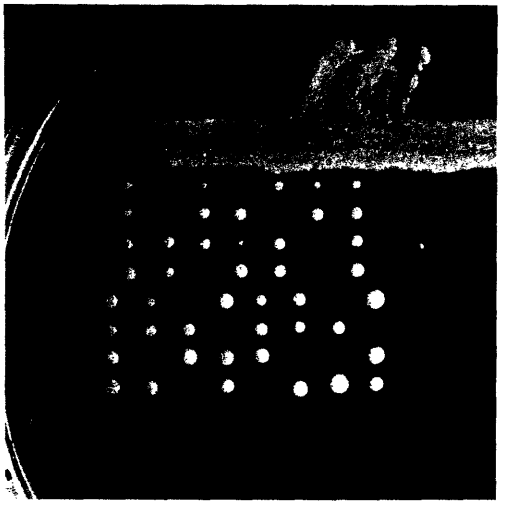

Δats1::URA3 prp20-2 double mutants are viable. A *prp20-2* strain (F63-7d) was crossed with a *Δats1::URA3* strain and sporulated. Asci were dissected and incubated at 30 degrees. Although 17 out of 60 spores deposited (approximately 25% of the colonies) form only a small colony or fail to grow, one-half of these small or absent colonies are *ATS1*, while all of them are *prp20-2*. This indicates that there is another gene, unlinked to the *ATS1* locus, that when combined with the *prp20-2* mutation is deleterious.

If the combination of *Δats1::URA3* and *prp20-1* was lethal, then one-quarter of the spores should fail to germinate. Tetrads were scored for Ura$^+$ and temperature sensitivity at 37° to identify cells containing the individual mutations in *ATS1* and *PRP20*. 25% of the spores failed to grow or gave rise to small colonies (see figure 2-27), but this phenotype only correlated with the presence of the *prp20-1* mutation and not the presence of the *Δats1* allele. 50% of the slower growing strains were Ura$^-$, indicating that another gene, unlinked to *ATS1*, was responsible for the temperature sensitivity when in combination with *prp20-1*. This gene has not been further characterized.

-Synthetic interactions between *ATS1* mutants and Class 2 mutants:

Initial attempts to obtain integrations of the XmnI to SphI fragment of pDK31 (which contains the *Δats1::URA3* construct) in *tub1* Class 2 mutant backgrounds were unsuccessful in identifying strains in which *ATS1* had been deleted. pDK44, containing *TUB1* on a *LYS2 CEN* plasmid, was constructed and transformed into DBY2403 (*tub1-714*) and DBY2426 (*tub1-758*). DBY2412 (*tub1-730*) was not used; the *lys2-801* amber allele has apparently reverted to Lys$^+$ in this strain. Successful transformants containing pDK44 were identified in both DBY2403 and DBY2426.

DBY2403 and DBY2426 containing pDK44 were transformed with linear XmnI - SphI DNA fragments to delete the chromosomal *ATS1* locus. 23 Ura$^+$ colonies were isolated from the *tub1-714* background, 20 from the *tub1-758* strain. Southern blots on the various putative integrants indicated that 10 of the *tub1-714* strains contained a deletion of *ATS1*, 7 remained Ats1$^+$, and 6 were indeterminate. For the potential disruptants in the *tub1-758* background, 12 contained deletions of *ATS1*, 6 were wildtype, and 2 gave abnormal bands on Southern blots.

Plasmid loss experiments were conducted on *tub1-714* and *tub1-758* strains that contained pDK44 and either *Δats1::URA3* or *ATS1*. If the deletion of *ATS1* is deleterious in combination with the extra-microtubule *tub1* mutations, then strains containing the deletion would be unable to lose pDK44, containing *TUB1*. However, strains wildtype at the *ATS1* locus should be able to lose both pDK44 and pRB614/658 (containing *tub1-714/758*) at equal frequencies. A number of different plasmid loss experiments, conducted in both the *tub1-714* and *tub1-758* backgrounds, demonstrated that strains containing a deletion of *ATS1* lost the *TUB1* plasmid much less frequently than the *tub1* plasmid, while strains wildtype for *ATS1* lost the two plasmids with equal frequency. Over the course of a number of experiments, 28 loss events involving the *TUB1* plasmid pDK44 were detected compared to 376 losses of the *tub1* plasmid, when examining 11083 colonies in the *Δats1::URA3* background. This compares to 106 loss events for the *TUB1* plasmid and 116 loss events for the *tub1* plasmid, with 6585 colonies scored in the *ATS1* background (see figure 2-28).

-Determination of growth rates at various temperatures:

The large difference in the number of loss events detected for pDK44 as compared to pRB614/658 in *ATS1* deletions suggests that double mutants (*Δats1 tub1*) are under strong negative selection. To determine if such selection actually existed, growth rates were determined for strains containing various combinations of the mutations. FSY350 is wild-type (*ATS1* and containing pDK44, the *TUB1 LYS2 CEN* plasmid). FSY351 contains a deletion of *ATS1* and pDK44. FSY352 is *ATS1* but contains pRB614, the *tub1-714 LEU2 CEN* plasmid. Finally, FSY353 is a double mutant: *Δats1::URA3* and bearing pRB614. Cells were grown in synthetic

Figure 2-28:

Chart of the percentage loss of plasmids in strains containing *Δats1::URA3* versus strains that are *ATS1*. Each strain contained two plasmids, a *LEU2 CEN tub1* plasmid (either pRB614 or pRB658) and a *LYS2 TUB1 CEN* plasmid (pDK44). Cells were grown in media permitting the loss of both plasmids at permissive temperature (22°) and plated to YPD plates. Loss of each plasmid was scored by replica-plating to SC-Lysine or SC-Leucine plates. The data reported in this figure are a compilation of a number of independent experiments, involving both *tub1-714* and *tub1-758* strains. Individual results did not deviate from the combined results reported here. In the *ATS1* strains, 106 loss events were seen with pDK44 and 116 loss events for pRB614/58, out of 6585 colonies examined. In the *Δats1::URA3* strains, 28 loss events were seen with pDK44 and 376 with pRB614/58, out of 11083 colonies examined.

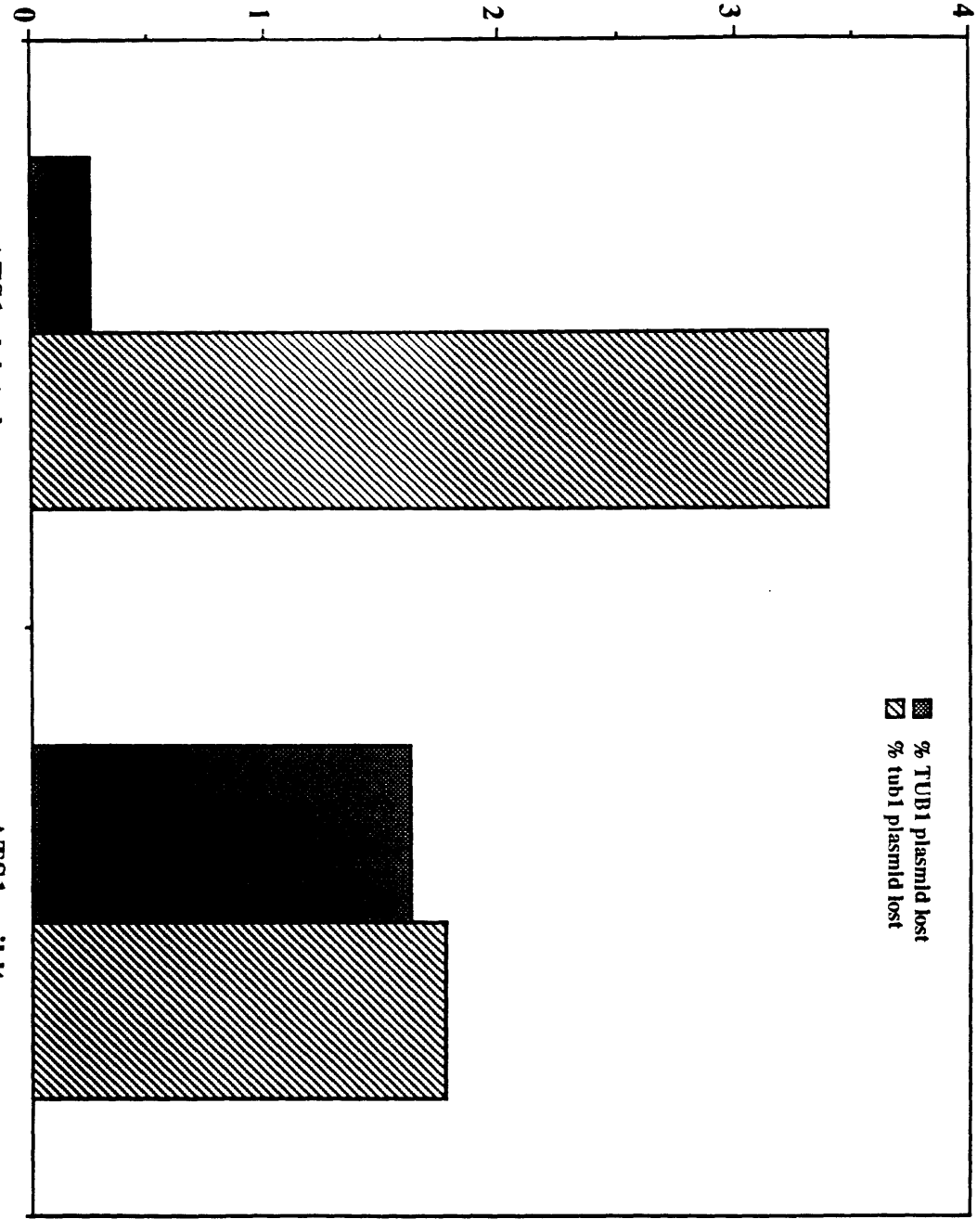
% of total colonies scored
0
1
2
3
4
% TUB1 plasmid lost
% tub1 plasmid lost
ATS1 deleted
ATS1 wildtype
tub1 Extra Microtubule Mutant Background

Table 2e

Doubling times for strains derived from the plasmid loss assay (figure 2-28). FSY250 is *ATS1* and contains pDK44 (*TUB1*). FSY351 is *Δats1::URA3* and contains pDK44. FSY352 is *ATS1* and contains pRB614 (*tub1-714*), while FSY353 is *Δats1::URA3* and contains pRB614. Doubling times at 37° are the average of two experiments, while doubling times at 18° are the average of three experiments. The alteration in growth rate for various strains is depicted as a percentage of the doubling time of FSY350, the strain containing wildtype alleles of *TUB1* and *ATS1*.

Table 2e:

Strain	Genotype	37 °C. doubling time (hours)	37 °C. relative %	30 °C. doubling time (hours)	30 °C. relative %	18 °C. doubling time (hours)	18 °C. relative %
FSY350	wild-type	2.16	100.0 %	1.47	100.0 %	4.4	100.0 %
FSY351	*Δats1*	2.08	103.8 %	1.61	91.3 %	4.6	95.7 %
FSY352	*tub1-714*	1.98	109.1 %	1.63	90.2 %	8.9	49.4 %
FSY353	*Δats1 tub1-714*	2.62	82.4 %	1.81	81.2 %	11.3	38.9 %

medium at various temperatures, counting the number of cells and plating to synthetic medium to determine the percentage of viable cells in the culture.

The expectation from the plasmid loss data was that the double mutant would grow poorly at 22°, the temperature at which the plasmid loss experiments were conducted. Further, as temperatures were reduced, it was expected that the double mutant would fail to grow. As shown in Table 2e, the double mutant did not exhibit drastic growth defects at any temperature checked. However, it was the slowest growing strain at all temperatures. Also, the colonies generated by plating for viable cells during the growth rate experiments were smaller for the double mutant than for the other strains (see figure 2-29).

-Can the growth rate results be explained by a genetic alteration in the double mutant?

One explanation for the discrepancy between the plasmid loss results and the growth rate determinations is that the double mutant strain is actually a triple mutant. By this model, a suppressing mutation in the *Δats1* strain during or prior to the plasmid loss experiment allowed the loss of the *TUB1* plasmid. Therefore, all 28 isolates that had lost pDK44 would contain a suppressor allowing for the loss, and so are able to grow, as observed in the growth rate experiments. In order to check this possibility, the pDK44 plasmid was transformed into FSY353.

If FSY353 contains a suppressing mutation that initially allowed the loss of pDK44, then if FSY353 containing pDK44 is taken through another round of plasmid loss, cells should be able to lose both plasmids, unlike the parental *Δats1::URA3* strain. However, when tested, FSY353 transformants containing pDK44 and pRB614 were deficient in their ability to lose the

Figure 2-29:

A *Δats1 tub1-714* double mutant generates small colonies at 30° C. The upper left photograph shows a plate containing FSY350 (*ATS1 TUB1*) grown at 30° for two days. The lower left panel shows FSY351 (*Δats1 TUB1*) colonies, while the upper right shows FSY352 (*ATS1 tub1-714*). The double mutant FSY353 (*Δats1 tub1-714*) is shown on the lower right. Colonies of the double mutant consistently were smaller than those formed by the wildtype or single mutant strains.

ATS1 TUB1

ATS1 tub1-714

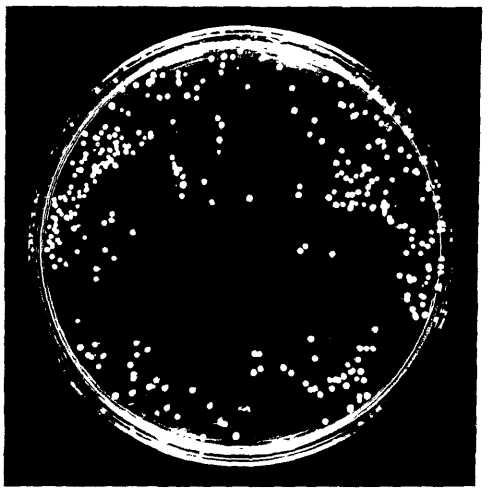

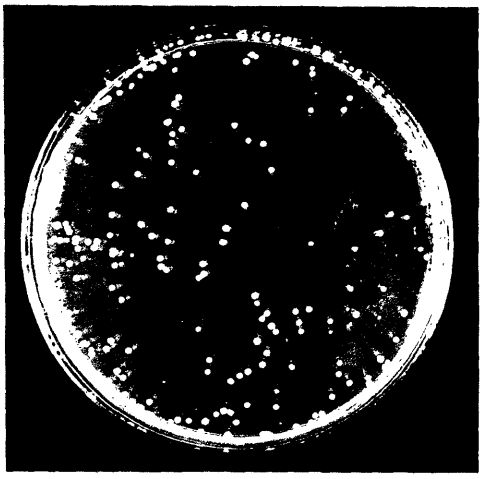

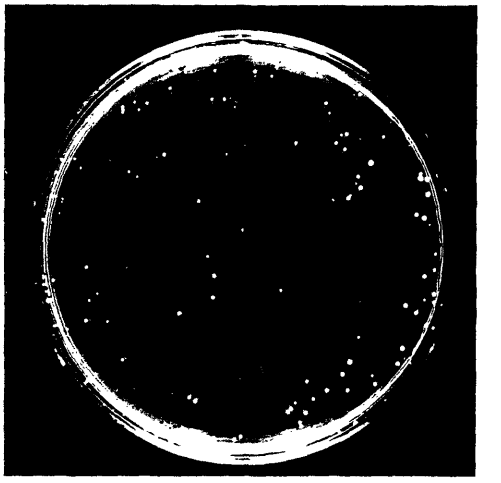

Δats1::URA3 TUB1

Δats1::URA3 tub1-714

TUB1 plasmid (see figure 2-30). This result indicates that FSY353 had not suffered a suppressing mutation.

-Copy number of the plasmids:

Another explanation for the difference in loss events detected for the *TUB1* plasmid versus the tub1 plasmids in the *ATS1* deletion strains is that the copy number of the *TUB1* plasmid has been elevated. This would have the effect of decreasing the apparent loss rate for the plasmid. Southern blots were performed on FSY348, 349, 350, 351, 352 and 353 to determine the level of each plasmid. DNA was isolated from each strain, quantitated, digested with restriction enzymes, equivalent amounts run on an agarose gel and transferred to nitrocellulose. This was probed with a fragment of *TUB1* that would hybridize to the *tub1* sequences of both pDK44 and pRB614. Restriction enzymes were chosen that would give a different size band after digestion of each plasmid. Comparison of the pRB614 and pDK44 bands showed no difference in intensities between the bands in both *Δats1::URA3* and *ATS1* strains (see figure 2-31). Thus, an alteration in the copy number of the *TUB1* plasmid in the *Δats1::URA3* strain does not explain the differences in plasmid loss.

-Can the observed difference in growth rates explain the difference in plasmid loss?

Calculations were performed to determine if the observed growth rate could account for the observed difference in colonies without the pDK44 or pRB614/58 plasmids after the plasmid loss protocol. Over the time course of the plasmid loss protocol, to what extent does the doubling time of the *Δats1::URA3 tub1-714* mutant have to be increased, in order to generate the

Figure 2-30:

Can the growth rate results be explained by a genetic alteration in the double mutant? To determine this, four strains were used, two strains from the original plasmid loss experiment (figure 2-28) and two strains resulting from a transformation of pDK44 back into strains that are *Δats1::URA3* but had lost the pDK44 plasmid. Cells were grown in media permitting the loss of both plasmids at permissive temperature (22°) and plated to YPD plates. Loss of each plasmid was scored by replica-plating to SC-Lysine or SC-Leucine plates. In the original *ATS1* strain, 6 loss events were seen with pDK44 and 9 loss events for pRB614, out of 516 colonies examined. In the original *Δats1::URA3* strains, 4 loss events were seen with pDK44 and 77 with pRB614, out of 2606 colonies examined. For the first re-transformant, 1113 colonies were examined: 0 loss events with pDK44 and 28 with pRB614 were seen. 1519 colonies were scored for the second re-transformant, with 2 loss events of pDK44 and 84 with pRB614 observed.

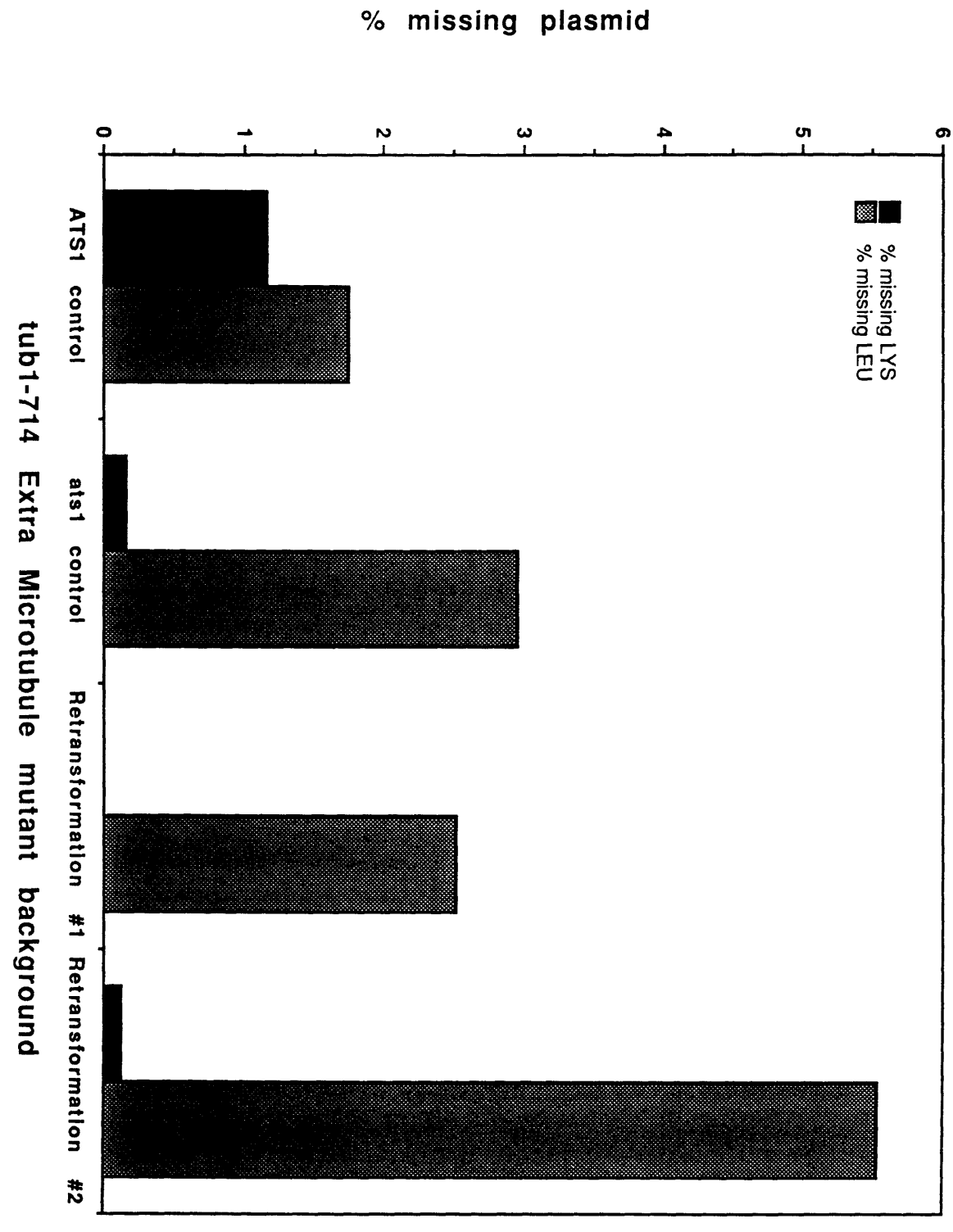
% missing plasmid
0
1
2
3
4
5
6
% missing LYS
% missing LEU
ATS1 control
ats1 control
Retransformation #1
Retransformation #2
tub1-714 Extra Microtubule mutant background

Figure 2-31:

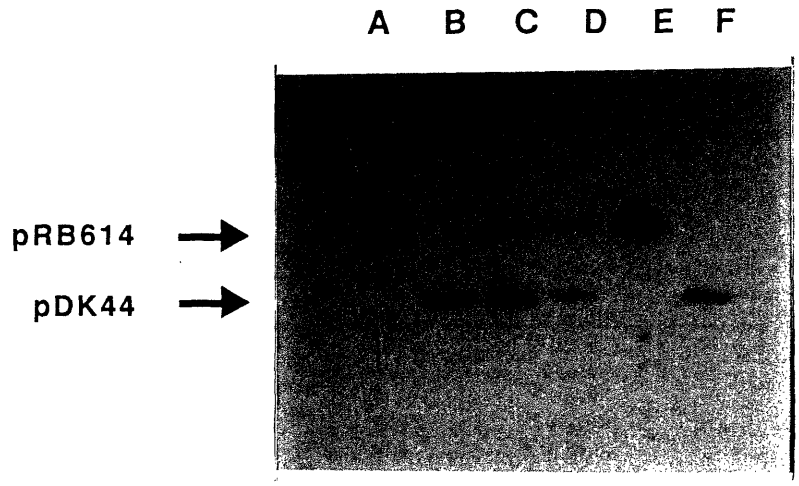

Copy number of plasmids does not explain the observed differences in plasmid loss. If the pDK44 (*LYS2 TUB1*) plasmid had a higher copy number in strains heterozygous for *Δats1::URA3*, then losses would be seen at a lower frequency. Lane A: FSY353 (*Δats1* pRB614 (*tub1-714*)) DNA; Lane B: FSY351 (*Δats1*, pDK44); Lane C:FSY348 (*Δats1* pRB614 pDK44); Lane D: FSY346 (*ATS1* pRB614 pDK44); Lane E: FSY352 (*ATS1* pRB614); Lane F: FSY350 (*ATS1*, pDK44). DNA isolated from each strain was digested, run on a gel, and probed with an internal fragment of *TUB1*. The intensity of the pDK44 and pRB614 bands in Lane C are comparable to one another, as they are in Lane D. If the copy number of pDK44 had been elevated in FSY348, then the band intensities within Lane C would not have been in the same proportion as the band intensities in Lane D.

6-fold difference in Lys$^-$ colonies that we observe? Based on the initial concentrations of cells, and using the experimentally derived doubling time for FSY350 (*ATS1 TUB1*) of 1.47 hours, an increase of 0.3 hours per doubling over the rate of FSY350 would generate a 6-fold difference in Lys$^{-/+}$ colonies at the end of the plasmid loss protocol. This rate (1.77 hours per doubling) is consistent with the observed doubling time of 1.81 hours.

A second calculation was done. Over the course of the plasmid loss protocol, can the experimentally-derived growth rates give rise to the observed difference in Lys$^-$ to Leu$^-$ colonies obtained? Starting with the growth rates for each strain, and assuming at the start of the experiment that they were equally represented in the population, by the end of the plasmid loss protocol the ratio of the two strains approximates the observed differences in the colony types obtained experimentally. It is quite possible, then, that the dramatic phenotype observed in the plasmid loss experiments, apparent decreased loss of the *TUB1* plasmid in the *Δats1 tub1* background, may be due entirely to the alteration in growth rate (see Discussion section).

DISCUSSION

I initially began the series of experiments described here in order to isolate genes encoding proteins controlling the functions of microtubules in the yeast *Saccharomyces cerevisiae*. In yeast, numerous experiments argue that neither the primary structure of the tubulin proteins nor quantitative regulation of tubulin protein levels are major regulatory factors (Katz et al., 1990; Schatz et al., 1986 - as reviewed in the Introduction). Another possibility is that associated proteins and structures might control microtubule organization and interactions. Previous work involving genetic screens for identifying such factors, screens for either pseudo-reversion of conditional mutations in the tubulin genes (Schatz et al., 1988) or unlinked noncomplementation of such mutations (Stearns and Botstein, 1988), yielded only novel mutations in the tubulin genes themselves. The screens were unsuccessful in uncovering any genes specifying interacting proteins. Quantitative suppression of conditional mutant alleles of the tubulin genes might reveal other interacting factors, however.

Quantitative suppression analyses are based on the hypothesis that the excess product will act within its normal domain of function, but that the excess will facilitate that function, thereby compensating for the defect in the mutant being suppressed. For example, an excess of a protein that acted to reduce the number or length of microtubules in the cell might rescue the extra microtubule Class 2 mutants. Such a protein could act by decreasing microtubule stability, severing microtubule polymers, or altering the association constants between dimers and the ends of microtubules. Conversely, a protein that acted to stabilize microtubules might be predicted

to rescue the no-microtubule Class 1 mutants. However, expecting to isolate suppressors of this general type makes assumptions about the nature of the cold-sensitivity in the *tub1* mutations, assumptions that may not be valid.

Isolation of *ATS1*

Introduction of genomic library plasmids into the cold-sensitive DBY2412 (*tub1-730*) strain identified three independent plasmids that were capable of generating colonies at the nonpermissive temperature of 15°. The suppression of the cold-sensitivity was plasmid-dependent. Re-introduction of the plasmids into cold-sensitive *tub1-730* mutant suppressed the cold-sensitivity, while removal of the plasmids from suppressed strains restored the cold-sensitivity to those strains. The level of suppression varied between plasmids (see figure 2-3). The plasmid having the greatest suppressing effect (pDK8) was further characterized. The suppressing element carried on pDK8 was named *ATS1*, for Alpha Tubulin Suppressor.

The *ATS1* suppressing element was isolated by subcloning of the genomic insert on the pDK8 plasmid. The *ATS1* region then was sequenced. The *ATS1* gene encodes a protein of 333 amino acids with a predicted molecular weight of 36.5 kDa. The Ats1p residues can be arranged as a series of seven tandem repeats, each repeat approximately 50 amino acids in length (figure 2-12). The protein is unusually rich in glycine and valine. No secondary structures can be predicted from the primary sequence.

Characterization of *ATS1* Suppression

The extent of the suppression seen with *ATS1* was evaluated by assessing the suppression of phenotypes associated with the Class 2 mutations. Class 2 strains, in addition to being cold-sensitive, arrest with a large-budded morphology and excess cytoplasmic microtubules. The extent of suppression of each of these phenotypes was evaluated. Other aspects of *ATS1* functioning were also investigated, including the effects of overexpression of *ATS1* in other backgrounds and the effects on the cell of a deletion of *ATS1*.

-Microtubule phenotypes:

The excess microtubule morphology *tub1-733* cells exhibit at nonpermissive temperatures is suppressed when cells carry excess copies of *ATS1* (figure 2-5). *ATS1* on either *CEN* or 2-μm plasmids is capable of restoring microtubule morphology distributions to a state comparable to, but not identical to, *tub1-733* cells transformed with *TUB1*. There also is an increase in the no-microtubule class of cells in strains containing excess *ATS1*. Perhaps above a certain level of *ATS1*, another factor becomes limiting for suppression in the Class 2 mutants, and so microtubule morphologies are not restored to the same level as with *TUB1* strains.

-Bud size distribution:

Excess *ATS1* suppresses the large-budded phenotype exhibited by strains containing the *tub1-730* and *tub1-733* mutations at the nonpermissive temperature (see figures 2-6 and 2-25). The extra microtubule mutations cause cells to arrest with a large-budded phenotype when cells are incubated

at restrictive temperatures. Overexpression of *ATS1* in DBY2412 (*tub1-730*) restores the bud size distribution to normal (comparable to *TUB1* transformed cells). In DBY2414 (*tub1-733*), the extent of suppression is not as great - the distribution is not identical to that of a strain with *TUB1*. This difference in level of suppression may be due to differences in the *tub1* alleles: a *tub1-730* strain arrests with slightly less than 60% of the population in the large-budded class, while *tub1-733* strains arrest with 75% of the population in the large-budded class.

-Class specificity of suppression:

ATS1, when transformed into all five Class 2 extra microtubule mutant strains, suppresses the cold-sensitivity associated with the mutations. The Class 2 strains all contain independent mutations. Peter Schatz, when isolating the original *tub1* mutations, mapped the region in which the mutations occurred using "healer" fragments (Schatz et al., 1988). Linear fragments of DNA containing various lengths of *TUB1* sequence were transformed into *tub1* strains, and the minimum length of *TUB1* required to rescue the cold-sensitivity of the mutation was determined. Although *tub1-730*, *tub1-741*, and *tub1-758* all fall in the same interval, they arose from three independent mutagenesis reactions. *tub1-730* and *tub1-741* arose from misincorporation mutagenesis reactions in which guanine and thymine respectively were limiting, while *tub1-758* was generated in an NH_2OH mutagenesis. Thus, each extra-microtubule mutant is an independent allele, and the mutations giving rise to the extra-microtubule phenotype are not localized to one specific region in the *TUB1* gene. As no high resolution tertiary structure is available for tubulin, it is possible that the extra microtubule mutations localize in a higher-order domain. Because the Class

2 mutant alleles are all independent, suppression by *ATS1* is not allele-specific.

Experiments indicate that excess *ATS1* is incapable of suppressing Class 1 mutant strains. These mutants arrest with a large bud, similar to the Class 2 mutants, but with no microtubules after incubation at the nonpermissive temperature. Each of the eleven Class 1 mutant strains was transformed with pDK33, containing the *ATS1* gene driven by the *GAL1,10-CYC1* promoter region. Strains containing this plasmid, and grown on galactose, failed to yield colonies at nonpermissive temperatures. *ATS1* is therefore not a general suppressor of *tub1* mutations.

I obtained two strains containing mutations in the *TUB2* β-tubulin gene that are reported to generate excess microtubules. However, excess *ATS1* did not suppress defects (cold-sensitivity and benomyl requirements) associated with the mutations (see figure 2-23 and the summary table 3a). Thus, *ATS1* is not a general suppressor of mutants that exhibit enhanced microtubule arrays.

-Effects of deletion of *ATS1*:

When one copy of the *ATS1* gene is deleted in a diploid and the resulting heterozygote sporulated and tetrads dissected, all four spores germinate and give rise to colonies at all temperatures checked. However, spores containing the *Δats1::URA3* allele that are placed at low temperatures (11°) or high temperatures (37°) give rise to colonies that are smaller than their *ATS1* counterparts (figure 2-15). This result indicates that, although *ATS1* is not an essential gene, its abrogation does yield some mild phenotypes.

Table 3a:

Strain	Suppression with excess: YCp50	*TUB1*	*ATS1*	*PRP20*
Class1 *tub1* alleles: (No-microtubule)				
tub1-704	-	+++	-	**ND**
tub1-709	-	+++	-	**ND**
tub1-724	-	+++	-	**ND**
tub1-728	-	+++	-	**ND**
tub1-729	-	+++	-	**ND**
tub1-738	-	+++	-	**ND**
tub1-744	-	+++	-	**ND**
tub1-750	-	+++	-	**ND**
tub1-759	-	+++	-	**ND**
tub1-760	-	+++	-	**ND**
tub1-767	-	+++	-	**ND**
Class 2 *tub1* alleles: (Extra microtubule)				
tub1-714	-	+++	++	++
tub1-730	-	+++	++	++
tub1-733	-	+++	++	++
tub1-741	-	+++	++	++
tub1-758	-	+++	++	++
***tub2* alleles:**				
tub2-150	-	**ND**	-	**ND**
tub2-412	-	**ND**	-	**ND**

Summary of suppression of phenotypes exhibited by various alleles of *TUB1* and *TUB2*, upon introduction of excess plasmid-borne *ATS1*, *PRP20*, *TUB1*, or vector. For more detail, refer to Results section.

One gene with which *ATS1* has been shown to associate is *TUB1* (this study). It seemed possible that disruption of *ATS1* in the Class 2 *tub1* mutant background might be deleterious. Examination of the phenotypes of the double mutant might provide some clue as to the functioning of the *ATS1* protein. A linear fragment of DNA bearing the *Δats1::URA3* construct was transformed into two Class 2 *tub1* mutants strains, DBY2403 (*tub1-714*) and DBY2426 (*tub1-758*), each of which had previously been transformed with pDK44, a *LYS2 CEN TUB1* plasmid. Strains containing an copy of the *Δats1::URA3* fragment integrated at the *ATS1* locus were identified by Southern blotting.

When attempting to generate the double mutant by loss of pDK44 (*LYS2 CEN TUB1*), it was observed that colonies that had lost pDK44 were detected almost an order of magnitude less frequently in strains containing a deletion of *ATS1* as compared to strains wildtype at the *ATS1* locus. However, when a strain that contained both the *tub1* and *Δats1* alleles was examined, its growth rate was only mildly affected (approximately 10% to 20% increase in doubling time) when compared to strains containing either mutation alone, or a wildtype strain. This disparity in results was not due to a suppressing mutation in the double mutant, nor was it due to increased copy number of the pDK44 plasmid relative to the pRB614 plasmid bearing the *tub1-714* mutation.

Calculations that take into account the differences in doubling time for strains that have lost pDK44 during the plasmid loss protocol indicate that, over the course of the plasmid loss experiments, the difference in growth rate could conceivably account for the disparity in observed loss events for the pDK44 plasmid in *Δats1* strains compared to *ATS1* strains. Another calculation, designed to see how much of a difference in growth rate would

have to exist to generate the relative differences in plasmid loss seen experimentally, also agreed with the observed growth rate for the double mutant.

A number of assumptions have been made to perform these calculations: 1) plasmid loss rate is equal for pDK44 in both *ATS1* and *Δats1* strains, 2) plasmids are lost at an early point in the plasmid loss protocol, and 3) plasmids are lost at approximately the same time in both strains. If any of these assumptions are false, the results of the calculations deviate from the experimentally-determined values. If, for example, plasmids are not lost until well into the plasmid loss experiment, but are still lost at equal frequency, then the observed difference in plasmid loss between the two strains would be minimized.

I believe the calculations and their underlying assumptions to be valid. However, if they are not correct and the difference in growth rate does not explain the results obtained in the plasmid loss experiments, then we return to the initial conundrum: why is there a large, biased, difference in recovery of Lys^- colonies and yet no major defect detectable in the double mutant?

-Effects of overexpression of *ATS1*:

Overexpression of *ATS1*, either on low (*CEN*) or high (2-μm) plasmids, or with the *GAL1,10-CYC1* promoter, yielded no phenotypes in wildtype cells. Growth rates and bud size distributions were unaltered in cells with excess *ATS1* (figures 2-17 and 2-18) and microtubule structures appeared normal by indirect immunofluorescence. Galactose-induced overexpression also failed to reveal any effects of excess *ATS1* (figure 2-20). Class 1 no-microtubule mutants containing excess *ATS1* were not suppressed, but the cold-sensitivity associated with the mutations was not

exacerbated, either. It is possible that *ATS1* overexpression does not affect cells because, above a certain level of *ATS1*, a necessary substrate or factor becomes limiting. Alternately, the factor or substrate is not expressed in the cells or under the conditions that have been examined so far. If either of these explanations is true, then the excess *ATS1* would, in both cases, have a minimal effect on the cells in which it was overexpressed.

Homologs of *ATS1*

A mammalian homolog, RCC1 (Ohtsubo et al., 1987), a *Drosophila melanogaster* homolog (BJ1) (Frasch, 1991), a *Xenopus laevis* homolog (Nishitani et al., 1990), a *Schizosaccharomyces pombe* homolog (*pim1*) (Matsumoto and Beach, 1991) and another *Saccharomyces cerevisiae* homolog in addition to *ATS1* (*SRM1/PRP20*) (Aebi et al., 1990; Clark and Sprague, 1989) have been identified. All of the genes encode proteins containing regions that can be arranged as a series of seven repeats of 50 to 60 amino acids each. All are nuclear proteins and many have been shown to bind to chromatin or DNA. A number of them (BJ1, *pim1*, RCC1 and *Xenopus* RCC1) have been postulated to be involved in maintenance of chromatin structure or cell-cycle control (for a review see Dasso, 1993).

-An *ATS1* homolog in mammalian cells:

The mammalian RCC1 protein was the earliest protein identified in the group of proteins which are similar to *ATS1*. A temperature sensitive cell line, *ts*BN2, prematurely condenses its chromosomes upon shift to nonpermissive temperatures (Nishimoto et al., 1978) when in S phase.

RCC1 mutants in G1 will arrest in G1, rather than continue through S phase. After long incubation at the nonpermissive temperature, most cells eventually arrest in G1. The RCC1 gene was cloned by complementation of this temperature-sensitivity (Ohtsubo et al., 1987) using a human cDNA library. The genomic RCC1 locus in *ts*BN2 cells was later shown to contain a serine to phenylalanine missense mutation. This mutated sequence could not suppress the temperature-sensitivity of the *ts*BN2 line (Uchida et al., 1990). Analysis of the cloned gene revealed that it encoded a protein of 421 amino acids. The residues in the RCC1 protein can be arranged as a series of seven internal repeats of approximately 60 amino acids each (Ohtsubo et al., 1987). The premature chromosome condensation phenotype of mutant RCC1 resembles the normal steps cells undergo at the onset of mitosis. In keeping with this observation, premature condensation requires the activity of the cdc25C protein (Seki et al., 1992). RCC1 has been shown to interact with a ras-like protein called Ran/TC4 by a number of criteria (Bischoff and Ponstingl, 1991a; Bischoff and Ponstingl, 1991b).

TC4 was initially identified as a ras-related protein in teratocarcinoma cells (Drivas et al., 1990). Later work indicated that RCC1 was present as part of a complex, and the other component, Ran, was identified as TC4 by peptide sequencing and antibody studies (Bischoff and Ponstingl, 1991a; Bischoff and Ponstingl, 1991b). Ran/TC4 appears to be present in a 25-fold molar excess over RCC1. The RCC1-Ran/TC4 complex dissociates in the presence of guanine nucleotides. RCC1 has been shown to catalyze GDP/GTP nucleotide exchange on Ran/TC4. The complex appears to bind chromatin, but this binding is lost during mitosis. Recently Ran/TC4 has been implicated in protein import into the nucleus (Moore and Blobel, 1993). Biochemical purification of a cytosolic fraction that mediates protein

import into *Xenopus* oocytes identified a Ran/TC4 homolog as one of two essential proteins for this activity.

A number of differing models have been presented to explain these diverse data (for reviews see Dasso, 1993; Murray, 1992; Nishimoto et al., 1992). Most of the models postulate that RCC1 acts as a guanine nucleotide exchange factor for Ran/TC4, modulating its activity in some manner. The RCC1-Ran/TC4 complex may act to couple the state of DNA synthesis with the onset of mitosis. However, the nature of this signal is unclear. There is some evidence to support the idea that loss of RCC1-Ran/TC4 allows the M-phase specific kinase $p34^{cdc2}$ to activate prematurely (Seino et al., 1991). Which protein in the RCC1-Ran/TC4 complex is responsible for the generation of the inhibiting signal is also unclear. These models are further complicated by the recent data that implicates Ran/TC4 in protein import into the nucleus (Moore and Blobel, 1993).

Ats1p and RCC1 are similar throughout much of the coding region of the two proteins, with a number of residues in each repeat conserved between the two proteins (see figure 2-13). Pairwise alignments of each repeat in RCC1 indicate that the RCC1 repeats are approximately 47.7% similar, using the Genetics Computer Group program 'Bestfit'. A similar calculation for the repeats in the *ATS1* protein indicate that they are 47.5% similar. A pairwise alignment between the Ats1p repeats and RCC1 repeats yields an average similarity of 46.8%. It can be concluded that the repeats in the *ATS1* protein are as similar to the repeats in RCC1 as they are to themselves, and *vice versa* (see table 3b).

Table 3b:

Percentage similarity between *ATS1* repeats, RCC1 repeats, and *ATS1* and RCC1 repeats. Similarities were generated using the Genetics Computer Group program 'Bestfit'. Settings for the program were the standard default settings. Each *ATS1* repeat corresponds to the repeats given in Figure 2-12. RCC1 repeats are as given in figure 2-13, with the exception of repeat #4, from which the unique amino acid region shown in figure 2-13 was deleted. Bold percentages indicate the highest and lowest percentage within each comparison group.

Table 3b:

	ATS1 1	ATS1 2	ATS1 3	ATS1 4	ATS1 5	ATS1 6
ATS1 7	53.7	44.7	48.6	51.2	36.8	52.8
ATS1 6	**60.5**	50.0	36.6	57.5	52.8	
ATS1 5	**26.5**	47.4	44.4	41.7		
ATS1 4	50.0	46.0	48.6			
ATS1 3	40.5	48.7				
ATS1 2	50.0					

	RCC1 1	RCC1 2	RCC1 3	RCC1 4	RCC1 5	RCC1 6	RCC1 7
ATS1 7	56.4	44.2	45.0	55.8	35.7	45.2	39.5
ATS1 6	46.8	55.0	56.8	50.0	47.4	40.9	55.0
ATS1 5	46.9	35.0	42.1	38.9	44.4	**34.2**	47.4
ATS1 4	46.8	36.5	53.2	43.1	40.0	34.7	44.0
ATS1 3	41.5	48.5	44.7	46.3	51.4	43.6	36.8
ATS1 2	46.9	53.1	56.9	45.1	40.8	51.0	57.1
ATS1 1	50.0	**60.0**	52.9	53.8	41.2	57.1	52.9

	RCC1 1	RCC1 2	RCC1 3	RCC1 4	RCC1 5	RCC1 6
RCC1 7	49.0	45.8	44.0	44.0	50.9	48.9
RCC1 6	47.1	51.0	45.8	54.9	44.9	
RCC1 5	43.1	52.0	**28.0**	46.3		
RCC1 4	56.9	53.8	40.4			
RCC1 3	43.8	**60.0**				
RCC1 2	51.0					

-An *ATS1* homolog in *Schizosaccharomyces pombe*:

pim1, the *S. pombe* homolog of RCC1, exhibits many of the same characteristics as RCC1. A quantitative suppressor (*spi1*) of the *pim1* temperature sensitivity encodes a homolog of Ran/TC4 (Matsumoto and Beach, 1991). In addition to associating with a ras-like protein, the phenotypes of *pim1* temperature-sensitive mutations are reminiscent of the chromosome condensation phenotype of the RCC1 temperature-sensitive mutation. *pim1* was initially isolated in a screen for mutations that arrested with a high proportion of cells exhibiting chromosome condensation (Matsumoto and Beach, 1991). *pim1* mutants are capable of arresting with condensed chromosomes from any stage in the cell cycle, unlike RCC1. As in RCC1 mutants, the M-phase kinase becomes activated in *pim1* at the restrictive temperature, and is required for the aberrant *pim1*-induced mitosis. Recently an extragenic suppressor (*ppe1*) of a temperature sensitive allele of *pim1* (Matsumoto and Beach, 1993) was isolated. The *ppe1* gene product has extensive homology with type 2A protein phosphatases and genetic evidence indicates that it might act downstream of the *pim1-spi1* complex. The existence of a phosphatase as an interacting element was predicted by the comparison of Ran/TC4 function with the ras protein GTPase cycle. The ras protein interacts sequentially with a guanine nucleotide exchange factor, a GTPase activating factor, and a phosphatase to modulate ras activity (see Bourne et al., 1991 for an overview).

pim1 mutant strains exhibit some irregularities in microtubule regulation. Spindle microtubules initially are found in *pim1* mutants shifted to the restrictive temperature, when the cells arrest with condensed chromosomes as if in mitosis. These spindles eventually disappear and are replaced with interphase microtubule structures even though the

chromosomes still appear condensed. Thus, the microtubule state becomes dissociated from the cell cycle stage in strains containing the *pim1* mutation (Matsumoto and Beach, 1991).

-An *ATS1* homolog in *Saccharomyces cerevisiae*:

Mutations in *SRM1/PRP20* in *S. cerevisiae* have pleiotropic phenotypes. Mutants have been isolated as defective in RNA polyA tail processing and splicing (Aebi et al., 1990; Fleischmann et al., 1991), in addition to acting to allow mating in a *MATa* strain lacking the *STE3* receptor (Clark and Sprague, 1989). However, *SRM1/PRP20* mutants exhibit some phenotypes reminiscent of the RCC1 and *pim1* mutations. Chromosome condensation cannot be seen in *S. cerevisiae* for technical reasons, but alleles of *SRM1* exhibit chromosome instability and increased plasmid loss when transferred to restrictive temperatures (Clark et al., 1991). This result indicates that there is some defect at the level of the chromosome, possibly in replication, mitosis or the coordination of the two. The *SRM1/PRP20* protein is located in the nucleus, as is RCC1. *SRM1* and the *D. melanogaster* BJ1 gene are capable of suppressing the temperature sensitivity of *ts*BN2 cells (Ohtsubo et al., 1991). In a similar manner, RCC1 can complement a number of the independently isolated temperature-sensitive alleles of *SRM1* and *PRP20*, but it is incapable of complementing a complete deletion of the locus (Clark et al., 1991; Fleischmann et al., 1991). However, unlike *pim1* and RCC1, the M-phase kinase does not appear to activate in *SRM1/PRP20* mutants at the nonpermissive temperature (Clark et al., 1991). In *S. cerevisiae*, *GSP1* and *GSP2* were identified as high copy suppressors of *prp20-1* mutations, and encode Ran/TC4 homologs

(Belhumeur et al., 1993). *S. cerevisiae* is the first organism in which two homologs of RCC1 or Ran/TC4 have been identified.

Therefore, while there are a number of features in common between *SRM1/PRP20*, *pim1*, and RCC1, there are a number of differences in each case. These differences between homologs make it difficult to interpret to what extent the functions of the various proteins overlap. In *S. cerevisiae*, the presence of two homologs (*ATS1* and *SRM1/PRP20*) increases the difficulty in interpretation. *ATS1* and *SRM1/PRP20* encode similar proteins. Pairwise combinations of the Ats1p repeats yield an average similarity of 47.5%, while the same calculations on the Prp20p repeats indicates that they are 51.5% similar. Comparisons between the two proteins generates a 45.6% similarity (see table 3c).

-*PRP20* in Class 2 mutants:

Given the degree of similarity between *ATS1* and *PRP20*, the ability of *PRP20* to suppress the cold-sensitivity of Class 2 extra microtubule mutant strains was assayed. Introduction of pWF48, a 2-μm plasmid containing *PRP20*, into DBY2412 (*tub1-730*) allows colonies to form at nonpermissive temperatures (figure 2-24). Other Class 2 strains also are suppressed with excess *PRP20* (summarized in Table 3a) The large-budded arrest phenotype of DBY2412 is also restored to wildtype in *PRP20*-transformed cells (see figure 2-25).

-*ATS1* and *SRM1/PRP20* are not functionally interchangeable:

Although *SRM1/PRP20* overexpression is capable of suppressing the cold-sensitivity associated with the Class 2 *tub1* mutants in a manner similar

Table 3c:

Percentage similarity between *ATS1* repeats, *PRP20* repeats, and *ATS1* and *PRP20* repeats. Similarities were generated using the Genetics Computer Group program 'Bestfit'. Settings for the program were the standard default settings. Each *ATS1* repeat corresponds to the repeats given in Figure 2-12. Bold percentages indicate the highest and lowest percentage within each comparison group.

Table 3c:

	ATS1 1	ATS1 2	ATS1 3	ATS1 4	ATS1 5	ATS1 6
ATS1 7	53.7	44.7	48.6	51.2	36.8	52.8
ATS1 6	**60.5**	50.0	36.6	57.5	52.8	
ATS1 5	**26.5**	47.4	44.4	41.7		
ATS1 4	50.0	46.0	48.6			
ATS1 3	40.5	48.7				
ATS1 2	50.0					

	PRP20 1	PRP20 2	PRP20 3	PRP20 4	PRP20 5	PRP20 6	PRP20 7
ATS1 7	39.5	47.4	33.3	40.5	44.2	39.0	40.5
ATS1 6	50.0	29.8	**62.9**	47.7	54.1	48.7	39.5
ATS1 5	42.5	40.5	47.5	42.4	37.5	50.0	48.4
ATS1 4	47.1	55.1	49.0	38.5	43.1	**28.6**	42.0
ATS1 3	60.0	41.5	44.4	40.0	43.9	48.6	44.4
ATS1 2	44.9	43.1	48.9	47.7	39.2	39.2	44.2
ATS1 1	50.0	57.7	51.9	47.2	61.5	52.0	55.8

	PRP20 1	PRP20 2	PRP20 3	PRP20 4	PRP20 5	PRP20 6
PRP20 7	49.0	54.0	**39.0**	45.4	54.0	53.2
PRP20 6	58.2	47.6	59.6	45.8	**62.3**	
PRP20 5	56.4	58.9	45.1	52.9		
PRP20 4	52.0	48.1	41.2			
PRP20 3	55.1	49.1				
PRP20 2	54.4					

to *ATS1*, the two genes are not functionally interchangeable. Overexpression of *ATS1* in *prp20-1* temperature-sensitive strains at a nonpermissive temperature does not rescue the cells, while deletion of *ATS1* does not alter the phenotypes of the *prp20-1* mutant. The pleiotropy of phenotypes exhibited by various alleles at this locus makes it difficult to assess the extent to which *SRM1/PRP20* normally affects the same function as *ATS1*. Additionally, the pleiotropic terminal phenotypes associated with mutations in *SRM1/PRP20* may reflect downstream consequences of the mutations.

Possible Modes of Action of *ATS1*

-*ATS1* as a proximal microtubule destabilizer:

Is *ATS1* suppressing the effects of the Class 2 extra microtubule mutations by acting as a microtubule destabilizer? To address this question, a number of experiments were conducted. If the suppression seen in the extra microtubule mutants is due to *ATS1* acting as a destabilizer of microtubules, then overexpression of *ATS1* in wildtype cells might prove deleterious through reduction of normal microtubule structures. Growth rates for strains bearing excess *ATS1* were not altered as compared to control strains. In order to look for more subtle alterations, bud size distributions were also examined, with the same result. Finally, no alteration in sensitivity to benomyl was observed in any of the strains containing *tub1* mutations when excess *ATS1* was present.

Overexpression of a protein that down-regulates microtubule number or extent might exacerbate the no-microtubule phenotype of Class 1 mutations. To determine if overexpression of *ATS1* was actually deleterious,

the pDK33 plasmid, containing a galactose-inducible high level expression construct of *ATS1*, was introduced into the eleven Class 1 mutants. The permissive temperature range for each mutation did not change, and no alteration in the severity of the phenotypes was observed (figure 2-22). The weight of evidence indicates that *ATS1* is not functioning as a proximal microtubule destabilizer.

-*ATS1* as a checkpoint protein:

-Model for *ATS1* action:

A model of *ATS1* suppression that is consistent with the data generated in our study takes into account the data concerning RCC1 and related proteins. The mutant α-tubulin produced by the Class 2 *tub1* mutants could cause the cells to arrest at a point in the cell cycle near mitosis, leading to the large-budded phenotype. This cessation of the cell cycle is postulated to be the reason colonies fail to form at nonpermissive temperatures in the Class 2 mutants. Suppression of this block occurs when overproduction of *ATS1* overrides the signal being generated by the mutant *tub1* protein, either directly or indirectly, and so transit through the cell cycle resumes. By this model, the excess microtubule morphology observed is a consequence of the extended arrest at this point in the cell cycle.

This model explains why *ATS1* overexpression has no detectable phenotype: cells normally do not arrest at the Ats1p execution point and so are not affected by excess *ATS1* protein. The β-tubulin mutants and Class 1 no-microtubule mutants also are not suppressed by excess *ATS1* because they are not blocked at an appropriate stage. Because the excess microtubules are generated as a downstream consequence of the halt in the

cell cycle, proteins that negatively regulate microtubules would not be expected to suppress.

-Checkpoint proteins:

Many features of this model are held in common with a class of proteins postulated to exist by Hartwell and Weinert (Hartwell and Weinert, 1989). Called checkpoint proteins, they act to regulate transitions through the cell cycle, responding to signals generated by factors or events that interact with specific stages of the cycle. By monitoring to ensure that early events are completed before initiation of later events dependent upon those early events, the coordination of the cell cycle is achieved. These checkpoint proteins need not be essential, as the feedback control may not be required in every cell cycle due to the tendency of the cell cycle to continue unless perturbed. Therefore, checkpoint proteins may not serve an essential function (as reviewed in Murray, 1992).

A cell cycle arrest due to a failure to complete a specific step can be overcome by mutations in checkpoint control genes. Indeed, finding conditions or mutations that alleviate induced arrests is one way in which feedback controls have been identified. A number of such mutants have been identified in *S. cerevisiae*, including the *RAD9* gene (Weinert and Hartwell, 1988), and the set of *MAD* (Li and Murray, 1991) and *BUB* genes (Hoyt et al., 1991). For example, mutations in genes functioning in DNA replication normally cause an arrest during S phase. However, a second mutation in *RAD9* will allow these cells to continue through the cell cycle once again. Thus, the *rad9* mutation removes a checkpoint control that normally does not permit the cell cycle to continue in the presence of unreplicated DNA (Weinert and Hartwell, 1988). The suppression of the

Class 2 *tub1* mutations by *ATS1* and *SRM1/PRP20* can be thought of in a similar manner. However, in the case of *ATS1* and *SRM1/PRP20*, it is not a genetic mutation that is allowing the checkpoint to be overcome, but excess copies of a wildtype gene.

-*ATS1* and *PRP20* - Similar to bacterial two-component systems?

The suppression of Class 2 mutants by both *ATS1* and *SRM1/PRP20* may be conceptually analogous to interactions seen between diverse bacterial two-component regulatory systems (reviewed in Albright et al., 1989 and Ronson et al., 1987). Each system consists of two proteins that interact, affecting a specific regulatory system, such as nitrogen utilization or chemotaxis. One protein, the modulator or sensor protein, is a protein kinase that phosphorylates the effector or regulator protein, which then performs some action, such as activation of transcription. The nitrogen regulation system, for example, consists of a modulator protein NtrB (NR_{II}) and a regulator protein, NtrC (NR_I). Phosphorylation of NtrC by NtrB allows NtrC to activate transcription at promoters that are nitrogen-regulated. The chemotaxis system has a single modulator, CheA, but two effector proteins, CheY and CheB. CheY, when activated by CheA, influences the action of the flagellar motor, while activated CheB affects the chemotactic receptor system. NtrB and CheA are homologous in their carboxy termini, while NtrC, CheY and CheB are homologous in their amino termini (Stock et al., 1988). *In vitro* CheA can phosphorylate NtrC, while a mutant form of NtrB that has a very high activity is capable of suppressing a cheA mutation *in vivo* (Ninfa et al., 1988). Thus, one component of a system is capable of affecting the activity of a second component of a totally independent system when the second component's partner is eliminated (see also Nixon et al.,

1986). Because of the homology between the effectors and modulators of the two systems, function can be restored by an aberrant interaction with another system's effector or modulator.

The functional overlap seen with *ATS1* and *SRM1/PRP20* may be a parallel to this type of interaction. The structural similarity between the two proteins and their ability to suppress the Class 2 *tub1* mutations may indicate that they are functioning in a similar manner. However, the two proteins may be acting on different systems, as suggested by the inability of *ATS1* to complement the *prp20-1* temperature sensitivity. The pleiotropy of mutations at the *SRM1/PRP20* locus makes it difficult to determine its exact function, complicating the comparison between *ATS1* and *SRM1/PRP20*, including to what extent their functions overlap. Mutations in the modulator proteins of a number of two-component systems often lead to complex phenotypes. These phenotypes have been explained by saying that low-level activity is still possible due to 'cross-talk' between effectors and modulators of differing systems (Ninfa et al., 1988). Perhaps in *S. cerevisiae* a similar mechanism is responsible for the pleiotropy of *SRM1/PRP20* phenotypes.

In Conclusion

I have identified suppressors of the Class 2 extra microtubule *tub1* mutants. The proteins encoded by these suppressors, *ATS1* and *SRM1/PRP20*, have similar structures. Analysis of the *ATS1* suppression indicates that it is not functioning to directly alter the extent of microtubule polymerization in the extra microtubule mutant strains. Both *ATS1* and *SRM1/PRP20* are structurally similar to a class of proteins whose members

have been implicated in cell cycle control via feedback mechanisms. Suppression of the *tub1* mutations may also be occurring through modulation of a feedback control mechanism.

It is intriguing that suppression of mutant *tub1* alleles by overexpression of wildtype genes has, in two separate cases, pointed to links between the microtubule and regulation of the cell cycle. In addition to this report, suppression of Class 1 no-microtubule *tub1* mutants has led to the isolation of *BUB3*, a previously identified gene thought to encode a checkpoint protein in *S. cerevisiae* (Hoyt et al., 1991) (see Introduction). Overexpression of *BUB3* in a subset of the Class 1 mutants, those that have an alanine to valine substitution at position 422, rescues the cold-sensitivity associated with the mutation (S. Guénette et al. submitted). It appears that mutations in *TUB1* can lead to cell cycle arrest at a number of discrete points, each under the control of different checkpoint proteins. As the state of the cell cycle and the control of the action of microtubules must by necessity be tightly coordinated, more interactions of this nature may very well be uncovered.

REFERENCES

Aebi, M., M. W. Clark, U. Vijayraghavan, and J. Abelson. 1990. A Yeast Mutant, *PRP20*, Altered in mRNA Metabolism and Maintenance of the Nuclear Structure, is Defective in a Gene Homologous to the Human Gene RCC1 Which is Involved in the Control of Chromosome Condensation. *Mol. Gen. Genet.* 224: 72-80.

Albright, L. M., E. Huala, and F. M. Ausubel. 1989. Prokaryotic Signal Transduction Mediated by Sensor and Regulator Protein Pairs. In *Annual Review of Genetics*. 311-336. Annual Reviews, Inc.

Baum, P., C. Yip, L. Goetsch, and B. Byers. 1988. A Yeast Gene Essential for Regulation of Spindle Pole Duplication. *Mol. Cell. Biol.* 8: 5386-5397.

Belhumeur, P., A. Lee, R. Tam, T. DiPaolo, N. Fortin, and M. W. Clark. 1993. *GSP1* and *GSP2*, Genetic Suppressors of the *prp20-1* Mutant in *Saccharomyces cerevisiae*: GTP-Binding Proteins Involved in the Maintenance of Nuclear Organization. *Mol. Cell. Biol.* 13: 2152-2161.

Berlin, V., C. A. Styles, and G. R. Fink. 1990. *BIK1*, a Protein Required for Microtubule Function during Mating and Mitosis in *Saccharomyces cerevisiae*, Colocalizes with Tubulin. *J. Cell Biol.* 111: 2573-2586.

Bischoff, F. R., G. Maier, G. Tilz, and H. Ponstingl. 1990. A 47-kDa Human Nuclear Protein Recognized by Antikinetochore Autoimmune Sera is Homologous with the Protein Encoded by RCC1, a Gene Implicated in Onset of Chromosome Condensation. *Proc. Natl. Acad. Sci. USA* 87: 8617-8621.

Bischoff, F. R., and H. Ponstingl. 1991a. Catalysis of Guanine Nucleotide Exchange on Ran by the Mitotic Regulator RCC1. *Nature* 354: 80-82.

Bischoff, F. R., and H. Ponstingl. 1991b. Mitotic Regulator Protein RCC1 is Complexed with a Nuclear ras-related Polypeptide. *Proc. Natl. Acad. Sci. USA* 88: 10830-10834.

Bond, J. F., J. L. Fridovich-Keil, L. Pillus, R. C. Mulligan, and F. Solomon. 1986. A Chicken-Yeast Chimeric β-tubulin Protein is Incorporated into Mouse Microtubules In Vivo. *Cell* 44: 461-468.

Bourne, H. R., D. A. Sanders, and F. McCormick. 1991. The GTPase Superfamily: Conserved Structure and Molecular Mechanism. *Nature* 349: 117-127.

Clark, K. L., M. Ohtsubo, T. Nishimoto, M. Goebl, and G. F. Sprague. 1991. The yeast *SRM1* Protein and Human RCC1 Protein Share Analogous Functions. *Cell Regulation* 2: 781-792.

Clark, K. L., and G. F. Sprague. 1989. Yeast Pheromone Response Pathway: Characterization of a Suppressor That Restores Mating to Receptorless Mutants. *Mol. Cell. Biol.* 9: 2682-2694.

Clark, M. W., W. W. Zhong, T. Keng, R. K. Storms, A. Barton, D. B. Kaback, and H. Bussey. 1992. Identification of a *Saccharomyces cerevisiae* Homolog of the *SNF2* Transcriptional Regulator in the DNA Sequence of an 8.6 kb Region in the *LTE-CYS1* Interval on the Left Arm of Chromosome I. *Yeast* 8: 133-145.

Cleveland, D. W., and K. F. Sullivan. 1985. Molecular Biology and Genetics of Tubulin. In *Annual Reviews of Biochemistry*. 331-365.

Conde, J., and G. R. Fink. 1976. A mutant of *Saccharomyces cerevisiae* defective for nuclear fusion. *Proc. Natl. Acad. Sci. USA* 73: 3651-3655.

Dasso, M. 1993. RCC1 in the Cell Cycle: the Regulator of Chromosome Condensation Takes on New Roles. *Trends in Biochemical Sciences* 18: 96-101.

Doheny, K. F., P. K. Sorger, A. A. Hyman, S. Tugendreich, F. Spencer, and P. Hieter. 1993. Identification of Essential Components of the *S. cerevisiae* Kinetochore. *Cell* 73: 761-774.

Drivas, G. T., A. Shih, E. Coutavas, M. G. Rush, and P. D'Eustachio. 1990. Characterization of Four Novel *ras*-Like Genes Expressed in a Human Teratocarcinoma Cell Line. *Mol. Cell. Biol.* 10: 1793-1798.

Drubin, D. G. 1990. Actin and Actin-Binding Proteins in Yeast. *Cell Motility and the Cytoskeleton* 15: 7-11.

Elble, R. 1992. A Simple and Efficient Procedure for Transformation of Yeasts. *BioTechniques* 13: 18-20.

Feinberg, A., and B. Vogelstein. 1983. A Technique for Radiolabelling DNA Restriction Endonuclease Fragments to High Specific Activity. *Analytical Biochemistry* 132: 6-13.

Fleischmann, M., M. W. Clark, W. Forrester, M. Wickens, T. Nishimoto, and M. Aebi. 1991. Analysis of Yeast *prp20* Mutations and Functional Complementation of the Human Homologue RCC1, a Protein Involved In the Control of Chromosome Condensation. *Mol. Gen. Genet.* 227: 417-423.

Frasch, M. 1991. The Maternally Expressed *Drosophila* Gene Encoding the Chromating-binding Protein BJ1 is a Homolog of the Vertebrate Gene Regulator of Chromatin Condensation, RCC1. *EMBO Journal* 10: 1225-1236.

Goh, P.-Y., and J. Kilmartin. 1993. *NDC10:* a gene involved in chromosome segregation in *S. cerevisiae*. *J. Cell Biol.* 121: 503-512.

Guarente, L., R. R. Yocum, and P. Gifford. 1982. A *GAL10-CYC1* Hybrid Yeast Promoter Identifies the *GAL4* Regulatory Region as an Upstream Site. *Proc. Natl. Acad. Sci. USA* 79: 7410-7414.

Guthrie, C., and G. R. Fink. 1991. Guide to Yeast Genetics and Molecular Biology. New York: Academic Press, Inc.

Hartwell, L. H., and T. A. Weinert. 1989. Checkpoints: Controls that Ensure the Order of Cell Cycle Events. *Science* 246: 629-634.

Hayles, J., D. Beach, B. Durkacz, and P. Nurse. 1986. The Fission Yeast Cell Cycle Control Gene *cdc2*: Isolation of a Sequence *suc1* that Suppresses *cdc2* Mutant Function. *Mol. Gen. Genet.* 202: 291-293.

Holm, C., D. W. Meeks-Wagner, W. L. Fangman, and D. Botstein. 1986. A Rapid, Efficient Method for Isolating DNA from Yeast. *Gene* 42: 169-173.

Hoyt, M. A., T. Stearns, and D. Botstein. 1990. Chromosome Instability Mutants of *Saccharomyces cerevisiae* That Are Defective in Microtubule-Mediated Processes. *Mol. Cell. Biol.* 10: 223-234.

Hoyt, M. A., L. Totis, and B. T. Roberts. 1991. *S. cerevisiae* Genes Required for Cell Cycle Arrest in Response to Loss of Microtubule Function. *Cell* 66: 507-517.

Ito, H., Y. Fukuda, K. Murata, and A. Kimura. 1983. Transformation of Intact Yeast Cells Treated with Alkali Cations. *J. Bacteriol.* 153: 163-168.

Jarvik, J., and D. Botstein. 1975. Conditional-lethal Mutations that Suppress Genetic Defects in Morphogenesis by Altering Structural Proteins. *Proc. Natl. Acad. Sci. USA* 72: 2738-2742.

Katz, W., B. Weinstein, and F. Solomon. 1990. Regulation of Tubulin Levels and Microtubule Assembly in *Saccharomyces cerevisiae*: Consequences of Altered Tubulin Gene Copy Number. *Mol. Cell. Biol.* 10: 5286-5294.

Katz, W. S., and F. Solomon. 1988. Diversity among β-Tubulins: A Carboxy-Terminal Domain of Yeast β-Tubulin Is Not Essential *In Vivo*. *Mol. Cell. Biol.* 8: 2730-2736.

Kim, S., M. Magendantz, W. Katz, and F. Solomon. 1987. Development of a Differentiated Microtubule Structure: Formation of the Chicken Erythrocyte Marginal Band In Vivo. *J. Cell Biol.* 104: 51-59.

Kitada, K., A. L. Johnson, L. H. Johnston, and A. Sugino. 1993. A Multicopy Suppressor Gene of the *Saccharomyces cerevisiae* G_1 Cell Cycle Mutant Gene *dbf4* Encodes a Protein Kinase and is Identified as *CDC5*. *Mol. Cell. Biol.* 13: 4445-4457.

Koshland, Douglas, John C. Kent, and Leland H. Hartwell. 1985. Genetic Analysis of the Mitotic Transmission of Minichromosomes. *Cell* 40: 393-403.

Kouprina, N., A. Tsouladze, M. Koryabin, P. Hieter, F. Spencer, and V. Larionov. 1993. Identification and Genetic Mapping of *CHL* Genes Controlling Mitotic Chromosome Transmission in Yeast. *Yeast* 9: 11-19.

Lechner, J., and J. Carbon. 1991. A 240 kd multisubunit protein complex, CBF3, is a major component of the budding yeast centromere. *Cell* 717-725.

Li, R., and A. W. Murray. 1991. Feedback Control of Mitosis in Budding Yeast. *Cell* 66: 519-531.

Li, Y.-Y., E. Yeh, T. Hays, and K. Bloom. 1993. Disruption of mitotic spindle orientation in a yeast dynein mutant. *Proc. Natl. Acad. Sci. USA* 90: 10096-10100.

Link, A. J., and M. V. Olson. 1991. Physical Map of *Saccharomyces cerevisiae* genome at 110-kilobase resolution. *Genetics* 127: 681-698.

Matsumoto, T., and D. Beach. 1991. Premature Initiation of Mitosis in Yeast Lacking RCC1 or an Interacting GTPase. *Cell* 66: 347-360.

Matsumoto, T., and D. Beach. 1993. Interaction of the *pim1/spi1* Mitotic Checkpoint With a Protein Phosphatase. *Molecular Biology of the Cell* 4: 337-345.

Meluh, P. B., and M. D. Rose. 1990. *KAR3*, a Kinesin-Related Gene Required for Yeast Nuclear Fusion. *Cell* 60: 1029-1041.

Moore, M. S., and G. Blobel. 1993. The GTP-Binding Protein Ran/TC4 is Required for Protein Import into the Nucleus. *Nature* 365: 661-663.

Murray, A. W. 1992. Creative blocks: cell-cycle checkpoints and feedback control. *Nature* 359: 599-604.

Nasmyth, K. A., and S. I. Reed. 1980. Isolation of Genes by Complementation in Yeast: Molecular Cloning of a Cell-Cycle Gene. *Proc. Natl. Acad. Sci. USA* 77: 2119-2123.

Natsoulis, G., F. Hilger, and G. R. Fink. 1986. The *HTS1* Gene Encodes Both the Cytoplasmic and Mitochondrial Histidine tRNA Synthetases of *S. cerevisiae*. *Cell* 46: 235-243.

Neff, N. F., J. H. Thomas, P. Grisafi, and D. Botstein. 1983. Isolation of the β-Tubulin Gene from Yeast and Demonstration of Its Essential Function *In Vivo*. *Cell* 33: 211-219.

Ninfa, A. J., E. G. Ninfa, A. N. Lupas, A. Stock, B. Magasanik, and J. Stock. 1988. Crosstalk Between Bacterial Chemotaxis Signal Transduction Proteins and Regulators of Transcription of the Ntr Regulon: Evidence that Nitrogen Assimilation and Chemotaxis are Controlled by a Common Phosphotransfer Mechanism. *Proc. Natl. Acad. Sci. USA* 85: 5492-5496.

Nishimoto, T., E. Eilen, and C. Basilico. 1978. Premature Chromosome Condensation in a ts DNA- Mutant of BHK Cells. *Cell* 15: 475-483.

Nishimoto, T., S. Uzawa, and R. Schlegel. 1992. Mitotic Checkpoints. *Current Opinion in Cell Biology* 4: 174-179.

Nishitani, H., H. Kobayashi, M. Ohtsubo, and T. Nishimoto. 1990. Cloning of *Xenopus* RCC1 cDNA, a Homolog of the Human RCC1 Gene: Complementation of tsBN2 Mutation and Identification of the Product. *Journal of Biochemistry* 107: 228-235.

Nixon, B. T., C. W. Ronson, and F. M. Ausubel. 1986. Two-component regulatory systems responsive to environmental stimuli share strongly conserved domains with the nitrogen assimilation regulatory genes *ntrB* and *ntrC*. *Proc. Natl. Acad. Sci. USA* 83: 7850-7895.

Oakley, B. R. 1992. γ-Tubulin: the Microtubule Organizer? *Trends in Cell Biology* 2: 1-5.

Ohtsubo, M., R. Kai, N. Furuno, T. Sekiguchi, M. Sekiguchi, H. Hayashida, K.-i. Kuma, T. Miyata, S. Fukushige, T. Murotsu, K. Matsubara, and T. Nishimoto. 1987. Isolation and Characterization of the Active cDNA of the Human Cell Cycle Gene (RCC1) Involved in the Regulation of Onset of Chromosome Condensation. *Genes & Development* 1: 585-593.

Ohtsubo, M., H. Okazaki, and T. Nishimoto. 1989. The RCC1 Protein, A Regulator for the Onset of Chromosome Condensation Locates in the Nucleus and Binds to DNA. *J. Cell Biol.* 109: 1389-1397.

Ohtsubo, M., T. Yoshida, H. Seino, H. Nishitani, K. L. Clark, G. F. Sprague, M. Frasch, and T. Nishimoto. 1991. Mutation of the Hamster Cell Cycle Gene RCC1 is Complemented by the Homologous Genes of *Drosophila* and *S. cerevisiae*. *EMBO Journal* 10: 1265-1273.

Ouellette, B. F., M. W. Clark, T. Keng, R. K. Storms, W. Zhong, B. Zeng, N. Fortin, S. Delaney, A. Barton, D. B. Kaback, and H. Bussey. 1993. Sequencing of chromosome I from *Saccharomyces cerevisiae*: analysis of a 32 kb region between the *LTE1* and *SPO7* genes. *Genome* 36: 32-42.

Page, B. D., and M. Snyder. 1992. *CIK1*: a developmentally regulated spindle pole body-associated protein important for microtubule functions in *Saccharomyces cerevisiae*. *Genes & Development* 6: 1414-1429.

Pringle, J. R., and L. H. Hartwell. 1981. The *Saccharomyces cerevisiae* cell cycle. In *The Molecular Biology of the Yeast Saccharomyces cerevisiae.* Edited by J. N. Strathern, E. W. Jones and J. R. Broach. 97-142. Cold Spring Harbor Laboratory Press.

Raff, E. C., and M. T. Fuller. 1984. Genetic analysis of microtubule function in *Drosophila.* In *Molecular Biology of the Cytoskeleton.* Edited by G. G. Borisy, D. W. Cleveland and D. B. Murphy. 293-304. Cold Spring Harbor Laboratory Press.

Ronson, C. W., B. T. Nixon, and F. M. Ausubel. 1987. Conserved Domains in Bacterial Regulatory Proteins That Respond to Environmental Stimuli. *Cell* 49: 579-581.

Rose, M. D., P. Novick, J. H. Thomas, D. Botstein, and G. R. Fink. 1987. A *Saccharomyces cerevisiae* genomic plasmid bank based on a centromere-containing shuttle vector. *Gene* 60: 237-243.

Rose, M. D., and G. R. Fink. 1987. *KAR1*, A Gene Required for Function of Both Intranuclear and Extranuclear Microtubules in Yeast. *Cell* 48: 1047-1060.

Sambrook, J., E. F. Fritsch, and T. Maniatis. 1989. *Molecular Cloning: A Laboratory Manual.* 2 ed. Cold Spring Harbor Laboratory Press.

Saunders, W. S., and M. A. Hoyt. 1992. Kinesin-Related Proteins Required for Structural Integrity of the Mitotic Spindle. *Cell* 70: 451-458.

Schatz, P. J., L. Pillus, P. Grisafi, F. Solomon, and D. Botstein. 1986a. Two Functional α-Tubulin Genes of the Yeast *Saccharomyces cerevisiae* Encode Divergent Proteins. *Mol. Cell. Biol.* 6: 3711-3721.

Schatz, P. J., F. Solomon, and D. Botstein. 1986b. Genetically Essential and Nonessential α-Tubulin Genes Specify Functionally Interchangeable Proteins. *Mol. Cell. Biol.* 6: 3722-3733.

Schatz, P. J., F. Solomon, and D. Botstein. 1988. Isolation and Characterization of Conditional-Lethal Mutations in the *TUB1* α-Tubulin Gene of the Yeast *Saccharomyces cerevisiae. Genetics* 120: 681-695.

Seino, H., H. Nishitani, T. Seki, N. Hisamoto, T. Tazunoki, N. Shiraki, M. Ohtsubo, K. Yamashita, T. Sekiguchi, and T. Nishimoto. 1991. RCC1 is

a Nuclear Protein Required for Coupling Activation of cdc2 Kinase with DNA Synthesis and for Start of the Cell Cycle. In *Cold Spring Harbor Symposia on Quantitative Biology*. 367-375. Cold Spring Harbor Laboratory Press.

Seki, T., K. Yamashita, H. Nishitani, T. Takagi, P. Russell, and T. Nishimoto. 1992. Chromosome Condensation Caused by Loss of RCC1 Function Requires the cdc25C Protein That is Located in the Cytoplasm. *Molecular Biology of the Cell* 3: 1373-1388.

Sherman, F., G. R. Fink, and J. B. Hicks. 1986. *Laboratory Course Manual for Methods in Yeast Genetics*. Cold Spring Harbor Laboratory.

Solomon, F., L. Connell, D. Kirkpatrick, V. Praitis, and B. Weinstein. 1992. Methods for Studying the Cytoskeleton in Yeast. In *The Cytoskeleton: A Practical Approach*. Edited by K. L. Carraway and C. A. C. Carraway. 197-221. Oxford University Press.

Spang, A., I. Courtney, U. Fackler, M. Matzner, and E. Schiebel. 1993. The Calcium-binding Protein Cell Division Cycle 31 of *Saccharomyces cerevisiae* Is a Component of the Half Bridge of the Spindle Pole Body. *J. Cell Biol.* 123: 405-416.

Stearns, T., and D. Botstein. 1988. Unlinked Noncomplementation: Isolation of New Conditional-Lethal Mutations in Each of the Tubulin Genes of Saccharomyces cerevisiae. *Genetics* 119: 249-260.

Stearns, T., L. Evans, and M. Kirschner. 1991. γ-Tubulin is a Highly Conserved Component of the Centrosome. *Cell* 65: 825-836.

Stearns, T., M. A. Hoyt, and D. Botstein. 1990. Yeast Mutants Sensitive to Antimicrotubule Drugs Define Three Genes that Affect Microtubule Function. *Genetics* 124: 251-262.

Stock, A., T. Chen, D. Welsh, and J. Stock. 1988. CheA Protein, a Central Regulator of Bacterial Chemotaxis, Belongs to a Family of Proteins that Control Gene Expression in Response to Changing Environmental Conditions. *Proc. Natl. Acad. Sci. USA* 85: 1403-1407.

Sun, G.-H., A. Hirata, Y. Ohya, and Y. Anraku. 1992. Mutations in yeast calmodulin cause defects in spindle pole body functions and nuclear integrity. *J. Cell Biol.* 119: 1625-1639.

Thomas, J. H., and D. Botstein. 1986. A gene required for the separation of chromosomes on the spindle apparatus in yeast. *Cell* 44: 65-76.

Uchida, S., T. Sekiguchi, H. Nishitani, K. Miyauchi, M. Ohtsubo, and T. Nishimoto. 1990. Premature Chromosome Condensation is Induced by a Point Mutation in the Hamster RCC1 Gene. *Mol. Cell. Biol.* 10: 577-584.

Vallen, E. A., T. Y. Scherson, T. Roberts, K. v. Zee, and M. D. Rose. 1992. Asymmetric Mitotic Segregation of the Yeast Spindle Pole Body. *Cell* 69: 505-515.

Weinert, T. A., and L. H. Hartwell. 1988. The *RAD9* Gene Controls the Cell Cycle Response to DNA Damage in *Saccharomyces cerevisiae*. *Science* 241: 317-322.

Weinstein, Brant, and Frank Solomon. 1990. Phenotypic Consequences of Tubulin Overproduction in *Saccharomyces cerevisiae*: Differences between α-Tubulin and β-Tubulin. *Molecular and Cellular Biology* 10: 5295-5304.

Winey, M., L. Goetsch, P. Baum, and B. Byers. 1991. *MPS1* and *MPS2*: Novel Yeast Genes Defining Distinct Steps of Spindle Pole Body Duplication. *J. Cell Biol.* 114: 745-754.

Xiao, Z., J. T. McGrew, A. J. Schroeder, and M. Fitzgerald-Hayes. 1993. *CSE1* and *CSE2*, Two New Genes Required for Accurate Mitotic Chromosome Segregation in *Saccharomyces cerevisiae*. *Mol. Cell. Biol.* 13: 4691-4702.

Yeh, E., R. Driscoll, M. Coltrera, A. Olins, and K. Bloom. 1991. A dynamin-like protein encoded by the yeast sporulation gene *SPO15*. *Nature* 349: 713-715.